APSORC '97 LIST OF ABSTRACTS

POSTER SESSIONS

P100s & P200s

Tuesday afternoon, 7 October 1997

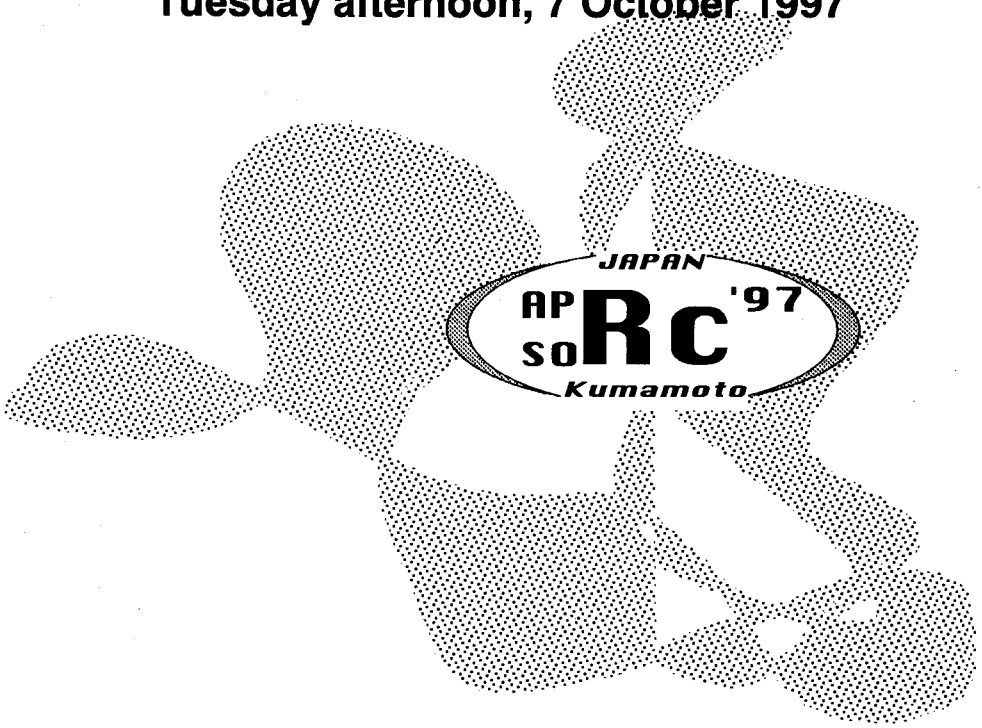

- KEYNOTE THEME -

EVER ONWARD TOWARDS THE FRONTIERS OF RADIOCHEMISTRY IN THE SECOND CENTURY OF RADIOACTIVITY DISCOVERY

P101
s.01

ISOMERIC YIELD RATIOS OF FISSION PRODUCTS IN PROTON-INDUCED FISSION OF ^{232}Th

S. Goto, D. Kaji, H. Kudo*, M. Fujioka[1], T. Shinozuka[1] and M. Fujita[1]

Department of Chemistry, Faculty of Science, Niigata University,
8050 Ikarashi 2-no-Cho, Niigata, 950-21, Japan
[1]*Cyclotron and Radioisotope Center, Tohoku University, Miyagi, Japan*

Summary: The isomeric yield ratios of fission products in ^{232}Th+p (13–26 MeV) system were measured by the use of IGISOL. It was found that the obtained isomeric yield ratios increased with proton energies.

Key words: ^{232}Th(p, f), fission products, isomeric yield ratio, fragment angular momenta

In nuclear fission process, the angular momentum of fission fragments provides much information for understanding of fission mechanism. Because an isomeric yield ratio reflects directly the angular momentum, the isomeric yield ratio has been examined precisely in the present work.

Until now, isomeric yield ratios have been measured in a wide mass range for the system of 24 MeV proton-induced fission of ^{238}U[1)] and ^{232}Th. In the present work, the isomeric yield ratio of fission products in proton-induced fission of ^{232}Th was measured by the use of IGISOL in a proton energy range of 13 to 26 MeV. The determination of fission products was made by a gamma-ray spectrometry. The obtained radioactvities were converted to independent yields by correcting the amount from precursors.

The obtained isomeric yield ratios generally increase with a proton energy. As an example, the isomeric yield ratio of ^{135}Xe is shown in Fig. (a). The same tendency has been found in other fragment masses and in other systems. In order to see the correlation of the isomeric yield ratio with the charge dispersion, the fractional yield is determined. In the case of ^{135}Xe, Fig. (b), it is found that the fractional yield increases with the proton energy except in E_p=13 MeV. This indicates that the charge dispersion of fission fragments relates to the isomeric yield ratios. The detailed analysis is now in progress. Comparison with isomeric yield ratios of other nuclides will be shown.

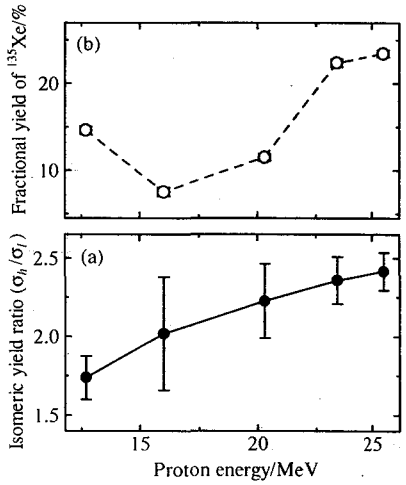

Fig. A plot of (a) isomeric yield ratios and (b) fractional yield of ^{135}Xe against the proton energy in system of proton-induced fission of ^{232}Th.

References

1) M. Tanikawa, et al., Z. Phys. **A347**, (1993) 53

Fax: +81-25-262-6116, E-mail: hkudo@sc.niigata-u.ac.jp

P102
s.01

NUCLEAR CHARGE DISTRIBUTION OF FISSION PRODUCTS IN THE SYSYTEM OF PROTON-INDUCED FISSION OF ^{232}Th.

D.Kaji, S.Goto, H.Kudo*, M.Fujioka[1], T.Shinozuka[1], and M.Fujita [1]

Department of Chemistry, Faculty of Science, Niigata University, Niigata, Japan
8050 Ikarashi 2-no-Cho, Niigata, 950-21, Japan
[1]*Cyclotron and Radioisotope Center, Tohoku University, Miyagi, Japan*

Summary: The charge distributions of fission products have been measured in a wide mass range for the system of proton-induced fission of ^{232}Th by the use of IGISOL. The obtained results were discussed in various view points.

Key words: ^{232}Th(p, f) E_P=13-26MeV, fission products, IGISOL, charge distribution

In nuclear fission process, the way of the nuclear charge division of fissioning nucleus between two fragments is directly related to the mass splitting. Accordingly, the study of the charge distribution of fission products provides an important information about nuclear fission mechanism.

In present work the charge distributions of fission products have been measured in a wide mass range for the system of proton-induced fission of ^{232}Th by the use of Ion Guide Isotope Separator On-Line (IGISOL).The determination of fission products was made by a gamma-ray spectrometry.

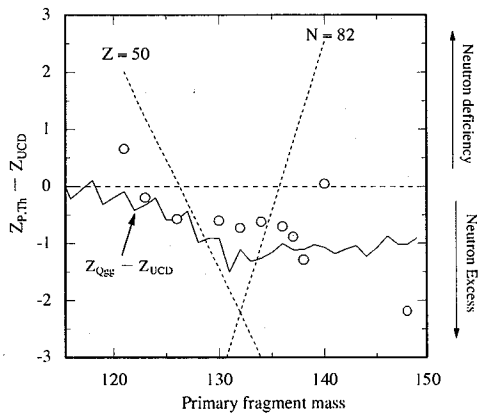

Fig.1 Deviation of the Zp from Z $_{UCD}$ distribution plotted versus the primary mass for ^{232}Th+p, 24MeV.

It is found that the obtained most probable charge Z_P does not constantly increase with a mass number. This tendency is different from UCD model. In order to consider the charge polarization in fission, the deviation of the Z_P from the Z_{UCD} expected from the UCD model is plotted against primary heavy fragment masses. The results are shown in Fig.1 for E_P = 24MeV. The Z_P lies in a neutron excess region for an asymmetric mass division. In general it is known that the proton-to-neutron ratio of stable nuclei decreases with increasing mass number. Therefore the nuclear stability may reflect the charge polarization in fission. This can be ascertained by the consideration of production Q-values. The result is shown in Fig.1as a solid curve. The deviation of the Z_P from the Z_{UCD} was found to fairly agree with the expectation Z_{Qgg} from production Q-values.

Additionally the mass, energy and target dependencies on the parameters which define the shape of the nuclear charge distribution will be presented and discussed in detail.

Fax : +81-25262-6116 , E-mail : hkudo@ curie.sc.niigata-u.ac.jp

P103 s.01 CHARACTERISTICS OF SHELL-GOVERNED SCISSION STATE IN PROTON INDUCED FISSION OF ^{244}Pu

Y. L. Zhao[1,2], I. Nishinaka[2], Y. Nagame[2], K.Tsukada[2], M. Tanikawa[3], Z. Qin[2], S. Ichikawa[2], H. Nakahara[1], Y. Hatsukawa[2], K. Hata[2], H. Ikezoe[2], Y. Oura[1], K. Sueki[1], T. Ohtsuki[4], S. Goto[5] and H. Kudo[5]

[1]*Tokyo Metropolitan University, Hachioji, Tokyo 192-03, Japan*
[2]*Japan Atomic Energy Research Institute, Tokai-mura, Ibaraki 319-11, Japan*
[3]*University of Tokyo, Bunkyo-ku, Tokyo 113, Japan*
[4]*Tohoku University, Sendai 982, Japan*
[5]*Niigata University, Niigata 950-21, Japan*

Summary: The properties of nuclear scission states are investigated via on- line measurements of mass and velocities of fission fragments produced from low energy p+^{244}Pu using a time-of-flight spectrometer.

Key words: Nuclear scission states, TKE, fragment mass, time-of-flight.

The properties of nuclear scission states were investigated via on-line measurements of the velocities of fragments produced by p+^{244}Pu using a double velocity time-of-flight spectrometer. A binary structure was observed in total kinetic energy (TKE) distributions of the fragment mass around A=130, and it was then decomposed based on an assumption of two Gaussian components. As a sample, the TKE distribution and its decomposed results for A=130 are plotted in fig. 1. It indicates that there exists at least two kinds of scission configurations for a certain mass split. From the results and their analyses, some features for these two categories of scissions have been understood. The mean value of the high TKE component associated with compact scission configuration shows a large fragment mass split dependence while that of the low TKE one with elongated scission is rather weak. The intensity corresponding to each TKE component is used to decompose the fragment mass yield into symmetric and asymmetric distributions. The asymmetric one follows shell-directed deformation terminated in the scission with its center length between the two fragments in the order of about 17 fm, whereas the symmetric deformation path terminated in the scission with center length being approximately 2.5 fm longer than the former. The fragment elongation variance stemmed from the low TKE scission is about 125% of that from the high TKE one. This is just similar with the width ratio of the symmetric to asymmetric mass distributions of 124%. In the symposium, the details of varying properties of shell-governed scission states along the mass split axis will be discussed.

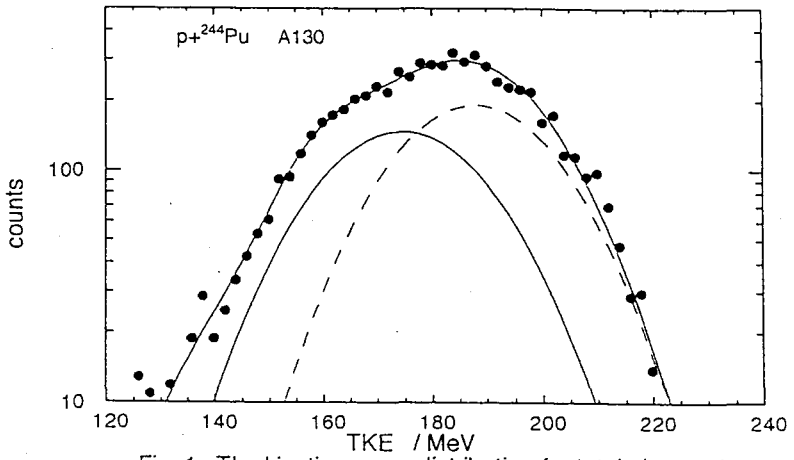

Fig. 1. The kinetic energy distribution for total , low and high TKE components in mass split of fragment A=130.

zhao-yuliang@c.metro-u.ac.jp, or zhao@popsvr.tokai.jaeri.go.jp.

P104 s.01 MASS YIELD DISTRIBUTIONS IN PROTON-INDUCED FISSION OF ^{248}Cm

Z.Qin[1,2], K.Tsukada[1], N.Shinohara[1], Y.L.Zhao[1,3], Y.Hatsukawa[1], I.Nishinaka[1], S.Ichikawa[1], K.Hata[1] and Y.Nagame[1]

[1]*Japan Atomic Energy Research Institute, Tokai-mura, Ibaraki 319-11, Japan*

[2] *Institute of Modern Physics, Academia Sinica, Lanzhou 730000, China*

[3]*Tokyo Metropolitan University, Hachioji, Tokyo 192-03, Japan*

Summary: Mass yield distributions in the fission of ^{248}Cm induced by low energy proton had been studied using a radiochemical method. The asymmetric mass yield peaks were to be 17± 2 u.
Key words: fission, mass yield distribution, width of asymmetric mass yield peak

The experiment was performed at the JAERI tandem accelerator. Mass yield distributions in the 10.5 ~ 20 MeV proton induced fission of ^{248}Cm were constructed from the cross section of fission products using the conventional stack-target method. The distributions were typically asymmetric, and FWHMs of the asymmetric mass yield peaks were to be 17± 2 u under the energy region of this study. The dependence of FWHM as a function of fissioning mass number for the proton-induced fission is shown in Fig.1 together with those of the thermal-neutron induced and spontaneous fissions[1]. It is found that FWHM for proton-induced fission also has a minimum around Af=240~245. The yield of the asymmetric mass yield peak of the heavier wing in this work was larger than those of the thermal-neutron induced fission of ^{235}U and the proton-induced fission of ^{238}U, which suggests that this target-projectile combination would be a candidate to produce more neutron-rich lanthanide with mass number larger than 150. The excitation functions of the typical products will be also presented in this report.

This work was supported by JAERI under the STA scientists exchange program.

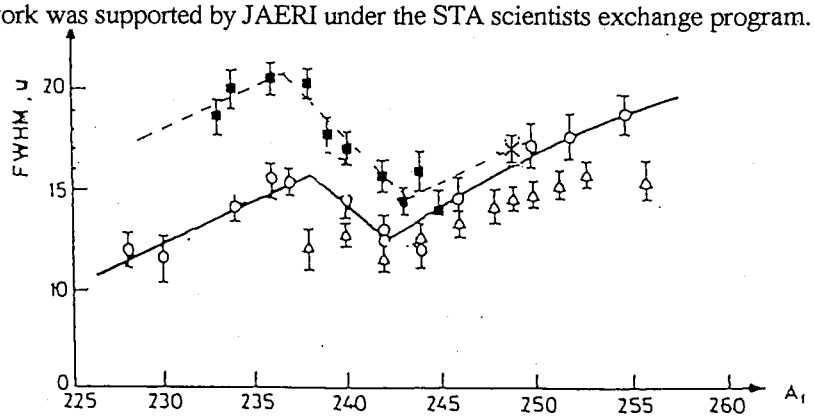

Fig.1. The dependence of full width at half maximum height (FWHM) of heavy asymmetric mass yield peak as a function of fissioning mass number. Open triangles are for spontaneous fission, open circles for thermal-neutron induced fissions, filled squares are for proton-induced fission, taken from Ref.[1], the cross symbol represents the present result. .

Reference

[1] T. Ohtsuki et al., Phys.Rev.C40(1989)2144.

Fax: 029-282-5963

P105
s.01

CORRELATION BETWEEN MASS DIVISION MODES AND NEUTRON MULTIPLICITY IN FISSION OF ACTINIDES

I. Nishinaka[1], Y.L. Zhao[1,3], Y. Nagame[1], K. Tsukada[1], S. Ichikawa[1], H. Ikezoe[1], M. Tanikawa[2], and H. Nakahara[3]

[1] *Japan Atomic Energy Research Institute, Tokai-mura, Ibaraki 319-11, Japan*
[2] *University of Tokyo, Bunkyo-ku, Tokyo 113, Japan*
[3] *Tokyo Metropolitan University, Hachioji, Tokyo 192-03, Japan*

Summary: The correlation between the mass division modes and the neutron multiplicity in the p + ^{232}Th, ^{238}U fission at E_p = 10 – 16 MeV has been investigated by a double time-of-flight technique.

Key words: nuclear fission, mass yield, TKE, neutron multiplicity, mass division mode

Two mass division modes in fission have been revealed by the accurate measurement of fragment mass and total kinetic energy (TKE) in the proton induced fission of ^{232}Th. The TKE of fragments in the asymmetric mass division mode was found to be higher than that in the symmetric one. It indicated that the effective distance of fragment centers at scission in the asymmetric mass division mode is shorter than that in the symmetric one.

In order to understand how the deformability of fragments is related to the mass division modes, we have measured TKE and neutron multiplicty (ν) as a function of fragment mass number in the p + ^{232}Th, ^{238}U fission using a double-TOF technique. The correlation between fragment mass, TKE, and ν has been investigated.

Proton beams at E_p = 11 – 16 MeV were supplied from the JAERI tandem accelerator to bombard the ^{232}Th and ^{238}U targets (70 μg/cm^2) evaporated on carbon backing foils (30 μg/cm^2). Two microchannel plate detectors (MCPDs) and an SSD were placed at Θ_{lab} = 50° to measure the velocity and energy of a fission fragment. An MCPD and a two-dimensional position sensitive (10 cm × 10 cm) parallel plate avalanche counter were set at Θ_{lab} = 129° at the opposite side of the beam direction to detect the complementaly fragment. The flight path and solid angle of the former detector was 55 cm and 0.17 msr, and that of the latter was 50 cm and 32 msr.

The number of neutrons emitted from the fragment is obtained from the defference between the primary fragment mass number and the secondary one. The shapes of the neutron multiplicity as a function of fragment mass number in both the reactions show the "saw-tooth" structure, in which the multiplicity increases with fragment mass and a large dip is observed in the region of the mass number A ~ 130. In the p + ^{232}Th reaction, another dip is clearly observed around A ~ 100. These dips are correlated to the peaks of the asymmetric mass distribution where the average TKEs of fragments show maxima.

In this report, we will discuss the correlation between the mass division modes and the neutron multiplicity in view of the energy balance in the fission process.

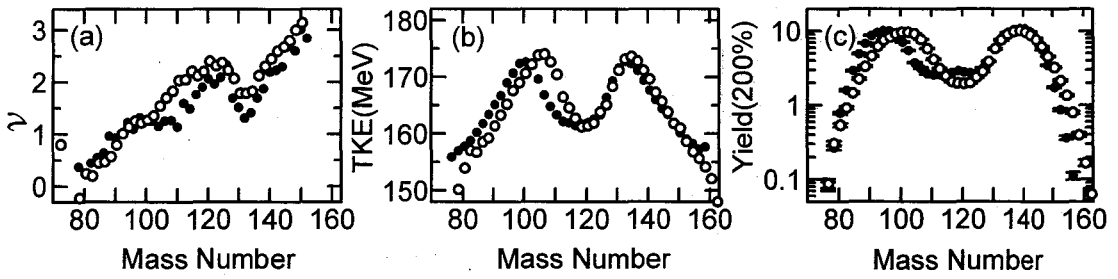

Figure:(a) Average number of neutrons emitted per fragments, (b) average total kinetic energies, and (c) mass distribution of primary fragments as functions of primary fragment mass in the 13.2 MeV p + ^{232}Th (solid symbols) and the 12.8 MeV p + ^{238}U (open symbols) reactions.

FAX: +81-29-282-5796, E-mail: ichiro@popsvr.tokai.jaeri.go.jp

P106 s.01 FISSION FRAGMENT CONFIGURATIONS AT SCISSION POINT OF ^{233}U, ^{235}U AND $^{239}Pu(n_{th},f)$

K. Takamiya[1], T. Inoue[1], K. Nakanishi[1], A. Yokoyama[1], N. Takahashi[1], T. Saito[1], H. Baba[1] and Y. Nakagome[2]

1) *Department of Chemistry, Graduate School of Science, Osaka University; Machikaneyama 1-1, Toyonaka, Osaka 560, Japan*

2) *Kyoto University Research Reactor Institute; Noda, Kumatori, Sen-nan, Osaka 590-04, Japan*

Summary: The scission point configurations were calculated event by event for thermal neutron induced fission of $^{233,235}U$ and ^{239}Pu. There were two types of scission configurations distinguished by means of the heavy fragment shape.

Key words: scission configuration, thermal neutron fission, ^{233}U, ^{235}U, ^{239}Pu

The double-velocity and double-energy measurements of the $^{233,235}U$ and $^{239}Pu(n_{th},f)$ reactions were carried out at Kyoto University Reactor. The numbers of measured fission events were about 18,600, 16,200 and 8,500, respectively, for the three systems. The primary fragment masses, kinetic energies, and the numbers of prompt neutrons were obtained event by event.

In the subsequent data analysis, the configuration at scission point was evaluated event by event. The correlation between the mass and the deformation rate of fission fragments revealed that all light fragments are highly deformed while heavy fragments are classified into two groups, one is highly deformed as light fragments and the other is practically spherical. The situation was quite analogous for $^{233, 235}U$ and $^{239}Pu(n_{th},f)$. The mass and total kinetic energy distributions were parted into two groups depending on the deformation rate of heavy fragments. The peak positions of mass distributions (shown in Figure) are 141 and 136, respectively, for deformed and spherical heavy fragments in case of $^{235}U(n_{th},f)$. The proton shell (Z=50) locates around the mass number 128 if one applies the UCD approximation, while the yield at the mass number 128 is very scarce. Therefore, the contribution of the proton shell should be negligible. On the other hand, the neutron shell (N=82) locates around A=134, which is close to the peak of the mass distribution of the spherical heavy fragment.

The total kinetic energy distribution sorted to each of the two groups resulted in a difference by about 10MeV between the two groups. The difference may be partly attributed to the difference in the distance between the centers of fission fragments at the moment of scission.

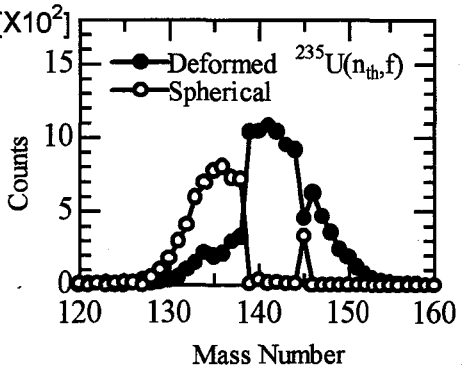

Fig : Two sorted mass distributions.

e-mail : takamiya@chem.sci.osaka-u.ac.jp

P107 s.02 PRODUCTION OF LIGHT NUCLEI FROM VARIOUS TARGETS WITH INTERMEDIATE-ENERGY BREMSSTRAHLUNG

H. Matsumura[1], K. Washiyama[1], H. Haba[1], Y. Miyamoto[1], K. Sakamoto[2], Y. Oura[3], S. Shibata[4], M. Furukawa[5] and I. Fujiwara[6]

[1]*Division of Physical Sciences, Graduate School of Natural Science and Technology, Kanazawa University, Kanazawa, Ishikawa 920-11, Japan*

[2]*Department of Chemistry, Faculty of Science, Kanazawa University, Kanazawa, Ishikawa 920-11, Japan*

[3]*Department of Chemistry, Faculty of Science, Tokyo Metropolitan University, Hachioji-shi, Tokyo 192-03, Japan*

[4]*Research Reactor Institute, Kyoto University, Sennan-gun, Osaka 590-04, Japan*

[5]*Faculty of Environmental and Information Science, Yokkaichi University, Yokkaichi-shi, Mie 470-01, Japan*

[6]*School of Economics, Ottemongakuin University, Ibaragi, Osaka 567, Japan*

Summary: Yields of ^{7}Be, ^{10}Be, ^{22}Na, ^{24}Na and other heavier nuclei from various targets over the periodic table in irradiations with bremsstrahlung having maximum end-point energies (E_0) up to 1200 MeV have been determined, and compared with the proton cross sections.

Key words: fragmentation, photonuclear reaction, bremsstrahlung, ^{7}Be, ^{10}Be, ^{22}Na, ^{24}Na

The present work concerns the radiochemical measurements of the photonuclear reaction yields of light nuclei (^{7}Be, ^{10}Be, ^{22}Na, ^{24}Na and other heavier nuclei) from various targets over the periodic table in irradiations with bremsstrahlung beams having maximum end-point energies (E_0) up to 1200 MeV. The results were compared with the proton cross sections for formation of these nuclides because it is expected that the difference of their initial steps might be reflected in the yield profiles of the fragmentation products. It would also be interesting to find some clues for distinctions whether a heavy nuclear cluster is formed as a result of emission with a certain kinetic energy (fragmentation) or as a result of many nucleon-emission (spallation residue), from an excited nucleus.

It was found that there exists direct emissions of ^{7}Be and ^{24}Na, as indicated by their reaction thresholds for several targets. And the present results show that target mass (A_t) -dependence of the yields at E_0 = 1000 MeV have two components. The first component could be explained by spallation, and the second one could be explained by fragmentation. However, the extents of the relative contributions are different in different targets. This could be also confirmed by the relation between the yields of light nuclei and those estimated by the Rudstam's empirical formula for spallation. The profile of the A_t-dependence of the ^{7}Be and ^{10}Be yields was found to be quite different, reflecting the difference of (N/Z), neutron to proton ratios, both the products and targets. Furthermore, the A_t-dependence of the yields at E_0 = 1000 MeV was found to be comparable in shape with the A_t-dependence of the proton cross sections at E_p = 400 to 600 MeV.

FAX: +81-76-264-5742, E-mail: matsu@kenroku.ipc.kanazawa-u.ac.jp

P108 s.02 REACTION MECHANISM FOR THE TARGET-LIKE PRODUCTS FROM THE ^{197}Au TARGET BOMBARDED WITH ^{12}C IONS OF ENERGIES ABOVE 100 MeV/u

A. Yokoyama[1], S. Morimoto[1], T. Inoue[1], J. Sanada[1], H. Araki[1], T. Saito[1], H. Baba[1], S. Shibata[2], A. Shinohara[3], T. Muroyama[3], and Y. Ohkubo[4]

1 Department of Chemistry, Graduate School of Science, Osaka University, 1-1 Machikaneyama, Toyonaka, Osaka 560, Japan

2 National Institute of Radiological Sciences, 4-9-1 Anagawa, Inage, Chiba 263, Japan

3 Department of Chemistry, Faculty of Science, Nagoya University, Chikusa, Nagoya 464-01, Japan

4 Research Reactor Institute, Kyoto University, Kumatori, Sen-nan, Osaka 590-04, Japan

Summary: Target-like products from the ^{197}Au target bombarded with ^{12}C ions of energies above 100 MeV/u were measured by using off-line γ-ray spectrometry. The reaction mechanism correlated with the products was investigated.

Key words: heavy ion reaction, γ-ray spectrometry, carbon-12, gold-197, mass distribution

Heavy-ion reactions of heavy targets in the energy range around 100 MeV/u are of much interest in view of a variety of reaction products covering a wide range of mass and charge. In this study, we concentrate on the target-like products from a target nucleus of ^{197}Au in the heavy-ion reaction with ^{12}C projectiles of energies above 100 MeV/u and investigate the reaction mechanism correlated with the products.

We had a stack of a gold foil of 0.01 mm in thickness and aluminum foils of 0.05 mm in thickness as catchers for the products bombarded with carbon ions from the HIMAC facility of the National Institute of Radiological Sciences. Target-like products for the reaction with ^{12}C ions at incident energies of 180, 230, and 400 MeV/u were radiochemically studied. The irradiated samples were subjected to chemical separation to isolate nuclides of gold, platinum and iridium as precipitates from the other products. And the prepared samples were assayed by γ-ray spectrometry for identification of the product nuclides and measurement of their yields.

Examples of the distributions of gold are exhibited in Fig. 1. We found that there are some nuclides which are enhanced with the increase of the incident energy in the range studied while the yields of most of the products attain the limiting values at the high energy region. The enhancement of the near target nuclides was prominent in comparison with a proton-induced reaction of gold at a similar incident energy in the literature as demonstrated in the figure. In conclusion, we would suggest that the near target nuclides may be produced via the Coulomb excitation which is prominent in the interplay of heavy nuclei.

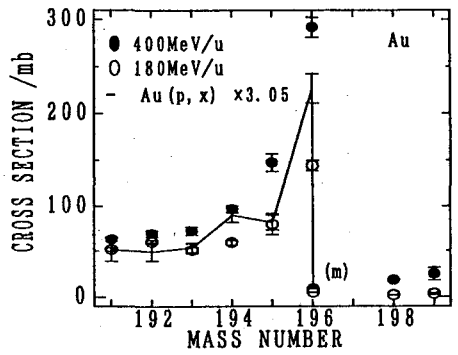

Fig.1. Mass distributions of Au isotopes for the systems with 400 and 180 MeV/u ^{12}C projectiles. Present data are compared to those for the proton-induced reaction of gold at the total energy of 2.6 GeV.

P109
s.02

Reinvestigation of Low-Lying Levels of ^{231}Th

T. Ohtsuki[1], H. Yuki[1], K. Nakazawa[1], T. Satoh[1], H. Yamazaki[1], J. Kasagi[1]
T. Mitsugashira[2]

[1]*Laboratory of Nuclear Science, Tohoku University*
[2]*The Oh-arai Branch, IMR, Tohoku University*

Summary: Excited levels of ^{231}Th were reinvestigated with γ single, α-γ and γ-γ coincidence measurements. From the analysis of the energy levels and transition intensities, 19.6 keV γ-ray of [631]7/2$^-$ 205.3 keV $\rightarrow$ [631]5/2$^-$ 185.7 keV was estimated to be larger than 90 %, though it was mostly converted to the Internal Conversion(IC) process.
Key word: α-decay of ^{235}U, Excited levels of ^{231}Th

Excited levels of ^{231}Th are fed by ^{235}U α-decay with $T_{(1/2)}=7\times10^8$ years. The structure of energy levels have permitted information to be obtained only on the low-lying levels and have been the object of many studies and surmmarized in ref.[1], however, the accuracy in determination of the level intensity in these studies is still less. From ref.[1], the intensity of [631]7/2$^-$ 205.3 keV $\rightarrow$ [631]5/2$^-$ 185.7 keV transition seems to be imbalance in respect of some branching ratios: the transition can be more favored due to the magnitude of α branching ratios of each level. The purpose of present study is to reinvestigate such intensities of the level transition and to reconstruct the more balancing level scheme accompanying with the α-decay from ^{235}U.

Experiments were separately done in γ single, α-γ and γ-γ coincidence measurements using highly purified ^{235}U. 1) the γ single measurement was done in a normal way using a Ge-detector. 2) α-γ coincidence measurement; the source was mounted inside a vacuum chamber of 60 mm$\times$30 mm$\times$2.5 mm. A transmission type Si(Au) surface barrier detector(SBD) of 200 mm^2 was set at about 5 mm distance from the ^{235}U source. Two 35 % Ge detectors which are equipped with Be window for measurement of X- and γ-ray was placed on 0° and 180° with respect to the ^{235}U source and the SBD direction. To avoid an absorption of low energy photons, a thin window of mailor foil was set in the vacuum chamber. The α-γ coincidence measurement was performed using a fast-slow coincidence system to record γ-ray spectra with selected α-rays. 3) γ-γ coincidence measurement; the ^{235}U source was set between two Ge-detectors in air. The measurement procedure was the same way as the α-γ coincidence measurement.

Here, the main three branches, namely [743]7/2$^-$ 387.8 keV, [631]7/2$^-$ 205.3 keV and [631]5/2$^-$ 185.7 keV states, were used to construct the level scheme. From the analysis, it seems that the [631]7/2$^-$ 205.3 keV $\rightarrow$ [631]5/2$^-$ 185.7 keV is not so weak transition since the strong intensities in the [743]7/2$^-$ 387.8 keV $\rightarrow$ [631]7/2$^-$ 205.3 keV were observed in the γ-γ coincidence spectra gated in the [631]5/2$^-$ 185.7 keV $\rightarrow$ [633]7/2$^+$ 41.9 keV and also in the [631]5/2$^-$ 185.7 keV $\rightarrow$ [633]g.s. transitions. Finaly, we found that the 19.6 keV transition intensity in the transition of [631]7/2$^-$ 205.3 keV $\rightarrow$ [631]5/2$^-$ 185.7 keV is estimated to be about 90%. This fact indicates that the 19.6 keV γ-ray can not be observed since the most of γ-rays are converted to the Internal Conversion(IC) process.

[1]R.B. Firestone, V.S. Shirley, Eds. *Table of Isotopes,* 8th ed. (J. W. & Sons, Inc., NY, 1996).

1)Mikamine, Taihaku, Sendai 982, Japan, E-mail: Ohtsuki@LNS.tohoku.ac.jp, and Kasagi@
2)Oh-arai, Higashi-Ibaraki 311-13, Japan, E-mail: mitsug@ob.imr.tohoku.ac.jp

P110
s.62

MEASUREMENTS OF NUCLEAR DATA OF MINOR ACTINIDES FOR TRANSMUTATION OF HIGH-LEVEL WASTE

N. Shinohara, Y. Hatsukawa, K. Hata, N. Kohno, M. Andoh, H. H. Saleh[1], W. S. Charlton[1], T. A. Parish[1], and S. Raman[2]
Japan Atomic Energy Research Institute, Tokai-mura, Naka-gun, Ibaraki-ken 319-11, Japan
[1]*Texas A & M University, College Station, TX 77843-3133, USA*
[2]*Oak Ridge National Laboratory, P. O. Box 2008, Oak Ridge, TN 37831-6354, USA*

Summary: For nuclear transmutation of minor actinides, the neutron capture cross sections of ^{241}Am were measured radiochemically. Delayed neutron emission measurements for ^{235}U, ^{237}Np, ^{241}Am and ^{243}Am were also carried out in thermal and fast neutron irradiation locations.
Key words: minor actinides, waste, transmutation, cross sections, delayed neutron yields

Minor actinides are produced from successive neutron capture reactions in nuclear fuel starting from ^{238}U and accumulate together with fission products in high burnup reactors. The minor actinides pose a unique problem in waste management because of their long half-lives that cause them to dominate the long term toxicity of high level waste and it is difficult to "prove" the integrity of their disposal for 1000s of years. The present work concerns both the processes of their formation and transmutation. In order to quantitatively understand the formation of minor actinides in reactors, it is essential to obtain precise nuclear data for their neutron capture cross sections. In this study, the thermal neutron capture cross sections and the neutron capture resonance integrals of ^{241}Am leading to the production of the isomer ^{242m}Am and the ground-state ^{242g}Am were measured radiochemically by the Cd-ratio technique using neutron flux monitors of Co/Al and Au/Al alloy. Highly-purified ^{241}Am targets were irradiated in an aluminum capsule by using the JAERI JMTR reactor. The thermal neutron fluxes and the epithermal neutron fractions were determined by measuring gamma rays of ^{60}Co and ^{198}Au. The yields of ^{242m}Am and ^{242g}Am were determined by analyzing the growth and decay curves of the alpha activity ratios of ^{242}Cm/^{241}Am. From the measured data, it was possible to understand more quantitatively the nuclear transmutation process due to the neutron capture reaction on ^{241}Am.

One of the options for high-level radioactive waste management is to transmute the actinide wastes into short-lived fission fragments by fast neutron induced fission. Reactors designed to achieve high transmutation rates are called actinide burners. The neutronic properties of the minor actinide isotopes are important in determining the criticality and kinetic characteristics of such reactors. In order to improve the basic nuclear data needed for actinide burner design studies, delayed neutron emission measurements for ^{235}U, ^{237}Np, ^{241}Am and ^{243}Am were carried out in a standard thermal neutron irradiation location at the Texas A & M University TRIGA reactor using a quick pneumatic transfer system. Absolute delayed neutron yields, six group relative yields and decay constants were determined for each isotope. In a second set of experiments, delayed neutron emission measurements for ^{235}U and ^{237}Np have been carried out at the Texas A&M reactor in a fast neutron irradiation location that includes a boron carbide liner to decrease the number of thermal neutrons irradiating the actinide samples. It is expected that these newly measured data for the delayed neutron parameters will be adopted for inclusion in basic nuclear data libraries.

In the symposium, the experimental results will be discussed from the viewpoint of nuclear waste management. The accelerator driven transmutation of minor actinides by high-energy neutrons from spallation reactions will be also presented.

Fax: +81-29-282-5525, E-mail: shino@popsvr.tokai.jaeri.go.jp

P111
s.02

IDENTIFICATION OF NEW NEUTRON-RICH RARE-EARTH ISOTOPES PRODUCED IN PROTON-INDUCED FISSION OF ^{238}U

S. Ichikawa*[1], K. Tsukada[1], M. Asai[2], A. Osa[3], Y. Oura[4], H. Iimura[1], Y. Kojima[2], T. Hirose[2], M. Shibata[2], I. Nishinaka[1], Y. Hatsukawa[1], Y. Nagame[1] and K. Kawade[2]

[1] *Japan Atomic Energy Research Institute, Tokai-mura, Ibaraki 319-11, Japan*
[2] *Nagoya University, Nagoya 464-01, Japan*
[3] *Japan Atomic Energy Research Institute,1233 Watanuki-cho, Takasaki, Gunma 370-12, Japan*
[4] *Tokyo Metropolitan University, Hachioji, Tokyo 192-03, Japan*

Summary: Three new isotopes ^{161}Sm, ^{165}Gd and ^{166}Tb produced in the proton-induced fission of ^{238}U were identified using the JAERI on-line isotope separator (JAERI-ISOL). Their half-lives were determined to be 4.8 ± 0.8 s for ^{161}Sm, 10.3 ± 1.6 s for ^{165}Gd and 21 ± 6 s for ^{166}Tb.

Key words: Radioactivity, ^{161}Sm, ^{165}Gd, ^{166}Tb, measured $T_{1/2}$, mass separation, gas-jet

To study the decay properties of neutron-rich rare-earth isotopes, a gas-jet coupled thermal ion source was developed for the JAERI-ISOL. The gas-jet transport system connected to the target chamber was designed to efficiently collect fission fragments recoiling out of the target and quickly transport into the thermal ion source. The thermal ion source was used to ionize efficiently rare-earth elements. The performance of the gas-jet coupled thermal ion source was tested using short-lived isotopes produced via the proton-induced fission of ^{238}U. The separation efficiency of the whole system was measured to be a few percent for La, Pr, Pm and Eu, and the delay time between production of atoms and extraction of the ion was evaluated to be 2 ∼ 3 s.

With this system, search for unknown neutron-rich rare-earth isotopes produced in the proton-induced fission of ^{238}U was carried out. The atom of interest was ionized as its monoxide ion in the thermal ion source, then mass-separated at the mass-A+16 fraction. In X/γ-ray spectra observed at the mass-A+16 fraction, KX-rays associated with the β^--decay of the isotope of interest was clearly identified and contamination from other molecular beams was almost negligible. The half-life values measured for the three new isotopes are listed in Table 1 together with the two theoretical predictions.

Table 1: The measured half-life of ^{161}Sm, ^{165}Gd and ^{166}Tb compared with the results of two theoretical predictions.

Nuclide	Present experiment	Theoretical predictions			
		Gross theory		pn-QRPA model	
	half-life(s)	half-life(s)	Q_β (MeV)	half-life(s)	Q_β(MeV)
^{161}Sm	4.8 ± 0.8	6.72	7.987	12.6	4.98
^{165}Gd	10.3 ± 1.6	16.0	4.18	18.4	4.14
^{166}Tb	21 ± 6	51.7	5.01	82.8	4.81

e-mail address: sichi@popsvr.tokai.jaeri.go.jp

P112
s.02

MASS SEPARATION OF NEUTRON DEFICIENT AMERICIUM ISOTOPES USING THE GAS-JET COUPLED JAERI-ISOL

K. Tsukada[1], Y. Oura[2], S. Ichikawa[1], Y. Nagame[1], I. Nishinaka[1], K. Hata[1], Y. Hatsukawa[1], N. Shinohara[1], Z. Qin[1], Y. L. Zhao[2], K. Sueki[2], T. Ohyama[2], H. Nakahara[2], M. Asai[3], T. Hirose[3], Y. Kojima[3], H. Yamamoto[3], K. Kawade[3]

[1] *Japan Atomic Energy Research Institute, Tokai-mura, Ibaraki 319-11, Japan*
[2] *Tokyo Metropolitan University, Hachioji, Tokyo 192-03, Japan*
[3] *Nagoya University, Nagoya 464-01, Japan*

Summary: Using the gas-jet coupled JAERI-ISOL, nuclear properties of neutron deficient actinide isotopes are being studied. ^{236,237}Am produced in the ^{235}U(^{6}Li, xn) reactions have been successfully measured, and the half-life of ^{236}Am has been determined to be 4.4 ± 0.8 min.
Key words: Am isotopes, ^{235}U(^{6}Li, xn) reaction, Mass separation, Gas-jet apparatus

There has been great progress in the frontiers of short-lived isotopes far from the β stability line by means of in-flight and on-line mass separations. In the region of neutron-deficient Am, Cm and Bk isotopes, many unknown isotopes are expected to decay mainly via orbital electron capture (EC), which enables us to identify them with a radiochemical method or an isotope separator on-line (ISOL). In fact, by improving a rapid chemical separation method, the new isotopes ^{238}Bk and ^{235}Am have been identified recently [1,2].

To study nuclear properties of unknown neutron deficient americium isotopes produced in heavy ion fusion reactions, we have developed a composite system consisting of a gas-jet transport apparatus including a multiple target system, and a thermal ion-source in the JAERI-ISOL. The multiple target system is designed to increase the effective target thickness and collect efficiently reaction products recoiling out from each target. The performance of the system has been tested using the ^{143m}Sm isotope produced in the ^{141}Pr(^{6}Li, 4n) reaction and ^{237}Am in the ^{235}U(^{6}Li, 4n) reaction. The separation efficiencies of the whole system have been evaluated to be 0.14% for ^{143m}Sm and ~0.1% for ^{237}Am.

With this system, search for the unknown isotope ^{236}Am produced in the ^{235}U(^{6}Li, 5n) reaction has been performed. Pu KX-rays associated with the EC decay of ^{236}Am were observed at the mass-236 fraction. The half-life of ^{236}Am is determined to be 4.4 ± 0.8 min, and the production cross section is estimated to be about 30 μb. The experimental and theoretical half-life values are listed in Table 1.

In this symposium, we will report the performance of the gas-jet transport apparatus coupled with the JAERI-ISOL and the recent results of search for unknown americium isotopes.

[1]. S. A. Kreek *et al.*, Phys. Rev. C **49**, 1859 (1994).
[2]. J. Guo *et al.*, Z. Phys. A **255**, 111 (1996).
[3]. H. L. Hall *et al.*, LBL-27878 (1989).

Table 1: The experimental half-life together with reported value of ^{236}Am compared with the theoretical predictions.

Present result	Hall *et al.*[3]	Gross theory	pn-QRPA model
4.4 ± 0.8 min	3.73 ± 0.28 min	11.1 min	8.87 min

E-mail: ktsuka@popsvr.tokai.jaeri.go.jp

P113
s.02

RECENT RESULTS FROM THE JAERI RECOIL MASS SEPARATOR

S. Mitsuoka, H. Ikezoe, T. Ikuta, S. Hamada, Y. Nagame, K. Tsukada, I. Nishinaka, and T. Ohtsuki[1]

Japan Atomic Energy Research Institute, Tokai, Ibaraki 319-11, Japan
[1] *Tohoku University, Sendai 982, Japan*

Summary: The JAERI Recoil Mass Separator (JAERI-RMS) at the JAERI tandem-booster facility has been operational. Some test runs and experiments have been carried out. A brief facility description is followed by resent experimental results.
Key words: Recoil mass separator, Fusion evaporation residue, New isotope, ^{209}Th, ^{212}Pa

In order to separate rare fusion evaporation residues from the primary beam in flight, the JAERI Recoil Mass Separator (JAERI-RMS) has been constructed at the JAERI tandem-booster facility [1]. As shown in Fig. 1, the JAERI-RMS has a symmetric configuration of Q_1Q_2-ED_1-MD- ED_2-Q_3Q_4-O, 9.4 m in length. Two 25° electric dipoles ED_1 and ED_2 and one −50° magnetic dipole MD are used to spatially disperse reaction products by their mass/charge (m/q) ratio and to focus irrespective of their energies. Two quadrupole doublets Q_1Q_2 and Q_3Q_4 are used for angular focusing. The octupole magnet O is used to correct a non- linearity of the m/q dispersion. The m/q and energy acceptances are designed to be ±4% and ±12%, respectively, and the solid angle is 15 msr. In order to reduce a background originating from beams scattered from the ED_1 anode, the anode is vertically split into two parts separated by 1 cm, so that the primary beam can pass through without hitting the anode surface.
The performance of the recoil mass separator has been tested by using the ^{28}Si and ^{127}I beams from the JAERI tandem accelerator. The capability of the background suppression at the beam direction is 2×10^{12} for ^{nat}In target and the obtained mass resolution is $A/\Delta A \simeq 300$ which is nearly equal to the calculated value.
To study decay of short-lived α-emitting isotopes near the proton drip line in the light actinide region, new neutron deficient isotopes ^{209}Th [2] and ^{212}Pa [3] have been produced in the ^{182}W(^{32}S,5n) and ^{182}W(^{35}Cl,5n) at beam energies of 171 MeV and 183 MeV, respectively. The evaporation residues have been separated with the JAERI-RMS and identified on the basis of time- and position-correlated α-decay chains. The α-decay energies and half-lives of ^{209}Th and ^{212}Pa have been determined to be 8.080(50) MeV and $3.8^{+6.9}_{-1.5}$ ms, 8.270(30) MeV and $5.1^{+6.1}_{-1.9}$ ms, respectively. The reduced width W_α obtained from the present data by assuming s-wave α decay is consist with neighboring nuclei within experimental error.

[1] H. Ikezoe *et al.*, Nucl. Instr. and Meth. **A376**, 420 (1996).
[2] H. Ikezoe *et al.*, Phys. Rev. C **54**, 2043 (1996).
[3] S. Mitsuoka *et al.*, Phys. Rev. C **55**, 1555 (1997).

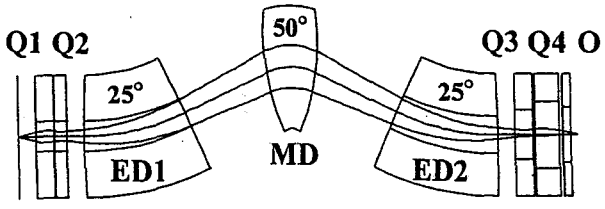

Fig. 1. Configuration of electric and magnetic components of the JAERI-RMS.

Fax: +81-29-282-5939, E-mail:mitsuoka@tdmalph1.tokai.jaeri.go.jp

P114 s.00/20 PREPARATION OF ^{18}F SOURCE FOR SLOW POSITRON BEAM BY PROTON BOMBARDMENT OF ^{18}O-WATER

T. Nozaki,[1] Y. Itoh,[1] Z.L. Peng,[1] Y. Ito,[2] N. Nakanishi,[1] H. Yoshida,[3] and A. Goto[1]

1: The Institute of Physical and Chemical Research (RIKEN), Hirosawa 2-1, Wako, Saitama 351-01, Japan

2: RCNST, The University of Tokyo, Tokai, Ibaraki, 319-11, Japan

3: Research and Develpment Dept, The Japan Steel Works Ltd, 4, Chatsumachi, Muroran 051, Japan

Summary: An automatic apparatus has been set up for preparing a source of slow positron beam from carriier-free ^{18}F produced by the $^{18}O(p,n)^{18}F$ reaction on ^{18}O-water, The ^{18}F is collcted on a small spot by adsorption or evaporation and placed close to a tungsten moderator foil.
Key Words: ^{18}F, Positron Source, Slow Positron Beam, Liquid Target.

For elevating the intensity of slow positron beam, we have thought it is highly effective to utilize short-lived positron emitter sources, which are produced routinely by ultra-compact cyclotrons in hospitals for positron emission tomography. The nuclides, after being sent to the room of slow positron generation, should be fixed on a small spot and placed just in front of the positron moderator by an automatic operation. We can use the techniques developed in nuclear medicine, with slight modifications. As the positron emitter, we selected ^{18}F (110 m) produced by the $^{18}O(p,n)^{18}F$ reaction on ^{18}O-water. The practical maximum yield is as high as 70 GBq (2 Ci), though 1 GBq is usually sufficient in preriminary works.

For fixing the ^{18}F in ^{18}O-water which shoud be recovered,we tried two methods: adsorption and evaporation. Figure 1 shows the automated apparatus we designed and set up. It consists of a turntable, T, source holder, S, and target-water receiver, R, the last two being of different structures according to the source prepartion method. The source holder can be moved up and down and, at the downside position, can be rotated. At the upside position, it is either in water-tight contact with the receiver or placed close to the moderator foil. The bombarded target water is once transferred into the receiver by a helium gas pressure. As the adsorbent, strongly basic anion exchange resin (100-200 mesh, OH-form) was found to be suitable. The target water ia passed slowly from the receiver through the resin bed with the aid of a peristaltic pump. In the evaporation method, a minute amount (0.1 mg) of K_2CO_3 is first placed on the holder, and the target water then transferred is evaporated by heating from outside, leaving the ^{18}F on a small area (usually 3-4 mm diameter). It takes about 10 min for the addition of newly prepared ^{18}F.

The evaporation method is thought to be superior, now giving 10^6 s^{-1} slow positrons. The use of gas or liquid targets possesses several advantages over on-site use of solid targets. Of all the reactions induced by an ultra-compact cyclotron, the $^{18}O(p,n)^{18}F$ reaction gives the highest yield. The life of ^{18}F is also suitable for the off-lne source preparation and use. By small improvements, we shall be able to obtain 10^7 s^{-1} slow positrons in near future.

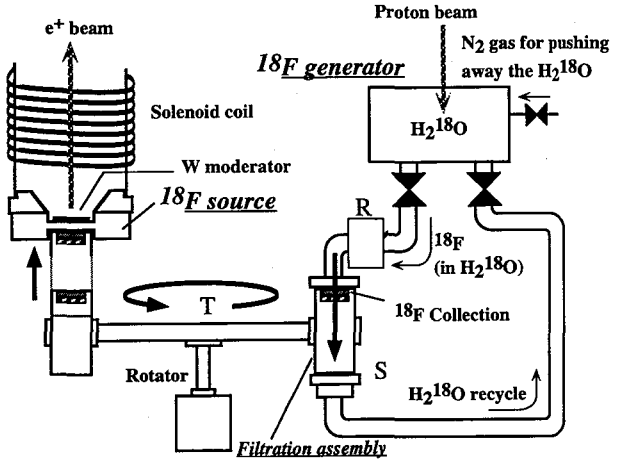

Fig. 1. Automated apparatus for preparing the ^{18}F source

Fax: 048-461-5301

P115 s.04 NEGATIVE PION TRANSFER PROCESS IN HYDROGEN-CONTAINING GAS MIXTURES

T. Muroyama, A. Shinohara[1], T. Saito[2], A, Yokoyama[2], K. Takamiya[2], S. Morimoto[2], K. Nakanishi[2], H. Baba[2], T. Miura[3], Y. Hamajima[4], T. Kaneko[5], H. Muramatsu[6], S. Kojima[7], M. Furukawa[8]

Low Level Radioisotope Laboratory, Kanazawa University, Tatsunokuchi, nobi-gun, Ishikawa 923-12, Japan,

[1] Graduate School of Science, Nagoya University, [2]Graduate School of Science, Osaka University,

[3]Radiation Science Center, KEK, [4]Faculty of Science, Kanazawa University,

[5]Faculty of Science, Niigata University, [6]Faculty of Education, Shinshu University,

[7]Radioisotope Research Center, Aichi Medical University,

[8]Faculty of Environmental and Information Sciences, Yokkaichi University

Summary: We measured the pion capture probabilities of hydrogen and rare gas in gas mixtures of H_2 + Z and CH_4 + Z systems (Z=He, Ne, Ar and Kr). We obtained the transfer rate Λ_Z used empirical formula and discussed the chemical effect of transfer process.

Keywords: pionic hydrogen atom, external transfer process

The capture process of a negative pion in a molecule is influenced by the chemical environments such as the molecular structure and the electron density distribution. Especially, in the molecule containing hydrogen atoms, a pion captured in a hydrogen atom is often transferred to one of the neighboring higher Z atoms. In the previous experiments, we studied the behavior of pionic hydrogen atom in liquid phase. Our understanding of capture process, however, is prevented by many inter-molecular interactions. Therefore, we choose gas samples to more clearly discuss the capture mechanism.

Experiments were carried out at a $\pi\mu$ channel of the 12-GeV proton synchrotron in the National Laboratory for High Energy Physics(KEK). We developed a measuring chamber made of beryllium for high pressure gas to measure the pionic X rays of carbon (18keV). The capture probabilities in any atoms except hydrogen atoms were obtained from pionic X rays. The capture probability of hydrogen atom was obtained from annihilation γ rays of π^0 from charge exchange reaction ($p + \pi^- \rightarrow n + \pi^0$). The pionic X rays were measured with two Ge low-energy photon spectrometers, and the annihilation γ rays were measured with two lead-glass Cherenkov counters mounted on the both sides of target. The simultaneous measurements of pionic X rays and annihilation γ rays are necessary to explain the capture process of a pion.

Samples were gas mixtures of H_2 + Z and CH_4 + Z systems, where Z were the gases, He, Ne, Ar and Kr. The compositions of Z atoms were 10, 20, 30, 40 and 60% in the samples. Figure 1 shows the results of H_2+ Ne system. The straight line shows the theoretical results without transfer process. The experimental data are not agreement with the line. This fact indicates that the external transfer process occurred in our experimental systems.

We will compare the systematical change of capture probabilities of hydrogen atoms in H_2 + Z systems with that in CH_4 + Z systems in order to discuss the chemical effects of the different chemical state of $p\pi^-$ atoms isolated from H_2 and CH_4. The pion transfer rate Λ_Z of hydrogen atom to Z atom are obtained using the new large mesomolecular model combined with an external transfer process. We will also compare these values Λ_Z with the formula by Russian group or our previous results in liquid phase.

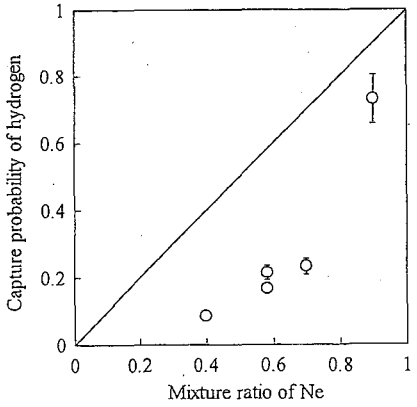

Fig. 1: The relationship between the capture probabilities of hydrogen atoms and those of neon atoms in H_2+ Ne system.

81-761-51-5528/f43595a@nucc.cc.nagoya-u.ac.jp

P116
s.04

CHEMICAL BEHAVIOR OF POSITIVE MUONS IN DIAMAGNETIC METAL ACETYLACETONATE SOLID SOLUTIONS

Michael K. KUBO[1*], Kusuo NISHIYAMA[2]

[1]*Department of Chemistry, School of Science, The University of Tokyo, Hongo, Tokyo 113, Japan.*

[2]*Meson Science Laboratory, Institute of Materials Structure Science, Oho, Tsukuba 305, Japan*

Summary: In $(Al_xCo_{1-x})(acac)_3$ and $(Ga_xCo_{1-x})(acac)_3$ systems, $Co(acac)_3$ was more influential on diamagnetic muon yield than $Al(acac)_3$ and $Ga(acac)_3$. Zerofield muon spin relaxation rate suggested the diamagnetic muon resides in the vicinity of $Co(acac)_3$ molecules.
Keywords: Positive muon, diamagnetic muon yield, metal acetylacetonate solid solution

Our previous μSR study on a variety of metal acetylacetonates ($M(acac)_n$, M:metal ion; $acac^-$:$CH_3COCHCOCH_3^-$) revealed that, on the basis of diamagnetic muon yield (P_D), they were classified into two groups: group A for compounds with P_D values of about 0.3 which consist of typical elements (e.g. Al,Ga,Zn) as M, and group B for compounds with P_D values of near unity containing transition elements (e.g. Mn, Fe, Co) as M. Since acetylacetone is an unsaturated organic compound and $M(acac)_n$ has benzenoid structure, P_D of the group A compounds is as expected whereas the group B compounds with the extreme P_D value of unity appear unusual. In this study we carried out μSR experiments on solid solutions consisting of cobalt compound and aluminum or gallium compound, $(Al_xCo_{1-x})(acac)_3$ and $(Ga_xCo_{1-x})(acac)_3$, in order to investigate the effect of the presence of a group B compound on the chemical form of muons in the group A compounds.

P_D values in $(Ga_xCo_{1-x})(acac)_3$ system at room temperature showed that while P_D values in mechanical mixtures fell on the straight line connecting two end members, $Co(acac)_3$ and $Ga(acac)_3$, those in the solid solutions gave an upward concave curve. In all the solid solutions studied P_D values decreased at low temperatures as observed in neat $Co(acac)_3$. A Gaussian zerofield muon spin relaxation rate of $3.0 \times 10^{-5}s^{-1}$ did not depend on the concentration of $Co(acac)_3$ in all the solid solutions except for neat $Ga(acac)_3$ (Feg.1). The presence of $Co(acac)_3$ affected the volume of its vicinity: thus it can be more influential than $Ga(acac)_3$ on the apparent chemical form of the muons in solid solutions and all the diamagnetic muon species could be formed and reside in the vicinity of $Co(acac)_3$ molecules.

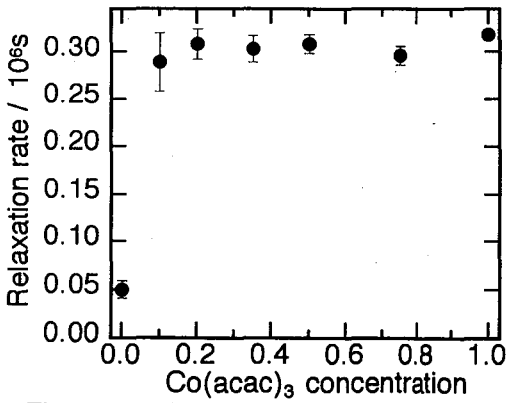

Fig. 1. Zerofield muon spin relaxation rate of diamagnetic muon in $(Ga_xCo_{1-x})(acac)_3$

FAX: +81-3-3814-2627, E-mail: kubo@chem.s.u-tokyo.ac.jp

P117
s.21

MÖSSBAUER SPECTROSCOPY OF ^{133}Cs FOLLOWING THE DECAY OF ^{133}Xe ATOMS IMPLANTED IN METALS

H. Muramatsu[1], H. Ishii[1], E. Tanaka[1], H. Ito[1], M. Misawa[1], T. Miura[2], S. Muto[2], M. Koizumi[3], A. Osa[3] T. Sekine[3] and M. Yanaga[4]

[1]*Department of Chemistry, Faculty of Education, Shinshu University, Nagano 380, Japan*

[2]*High Energy Accelerator Research Organization, Tsukuba 305, Japan*

[3]*Department of Chemistry and Fuel Research, Japan Atomic Energy Research Institute, Takasaki 370-12, Japan*

[4]*Department of Chemistry, Faculty of Science, Shizuoka University, Shizuoka 422, Japan*

Summary: Mössbauer effect measurements have been performed with ^{133}Xe-implanted sources prepared by means of an isotope separator. The behavior of the isomer shift of the 81 keV transition in ^{133}Cs was studied for ^{133}Cs atoms in various metals.

Key words: Mössbauer effect, isomer shift, ^{133}Cs, ^{133}Xe implantation

^{133}Cs is one of two isotopes of alkali metals for which the Mössbauer effect has so far been observed; another is ^{40}K, whose $\Delta\langle r^2\rangle$ is, however, so small that its widespread application would be inhibited. Therefore, ^{133}Cs is an invaluable probe for the elucidation of the nature of chemical bondings in highly ionic compounds. In this work, Mössbauer emission spectra of ^{133}Xe-implanted metal sources prepared by means of an isotope separator have been measured for the 81 keV transition of ^{133}Cs in order to understand the behavior of the isomer shift of ^{133}Cs atoms in various metals.

Ion-implantation of ^{133}Xe ($T_{1/2}$=5.25d), which decays to the Mössbauer level of ^{133}Cs, was carried out at a terminal voltage of 20 kV at room temperature. As host materials, Al , Cr , V , Mo and Rh foils were chosen. The ^{133}Cs Mössbauer spectra were measured using a single-line absorber of CsCl with 360 mg/cm^2 Cs thickness while keeping both the source and absorber at liquid-helium temperature. Referring to the systematic isomer-shift studies on ^{133}Cs by Pattyn and his coworkers[1], and considering the quadrupole splitting of the 81 keV($5/2^+$) state, the complex spectra obtained were analyzed by the least-squares method under the assumption that three single lines and two quadrupole triplets exist in the spectrum. The largest isomer shift is attributable to the normal substitutional site in the host lattice, and others may be assigned to vacancy-associated sites, where there exist xenon-vacancy clusters that contains up to five vacancies.

Several attempts have been made to find a correlation between the isomer shifts corresponding to the substitutional site and some physical and chemical properties of host materials: the atomic volume, the metallic bond radius, the Debye temperature, the Debye force-constant, the bulk modulus, the *d*-character in chemical bonds, the electronegativity difference between host and impurity atoms, and so on. For the isomer shifts and the bulk moduli, a correlation was found, which means that the rigidity of the host lattice strongly correlates to the isomer-shift value.

[1] See, for example, I.Dézsi, H.Pattyn, E.Verbiest and M.Van Rossum, Phys. Rev.**B39**(1989)6321

FAX: +81-26-232-5144, e-mail: hmurama@gipnc.shinshu-u.ac.jp

P118 s.21 ^{237}Np Mössbauer Spectroscopic Study on Heptavalent Neptunium Compound

T. Nakamoto*[1], M. Nakada[1], N. M. Masaki[1], M. Saeki[1], T. Yamashita[2], and N. N. Krot[3]

[1]*Advanced Science Research Center, Japan Atomic Energy Research Institute, Ibaraki 319-11, JAPAN*
[2]*Department of Chemistry and Fuel Research, Japan Atomic Energy Research Institute, Ibaraki 319-11, JAPAN*
[3]*Institute of Physical Chemistry, Russian Academy of Sciences, Leninskii pr. 31, Moscow, 117071, RUSSIA*

Summary: ^{237}Np Mössbauer spectrum of a heptavalent neptunium compound, $[Co(NH_3)_6][NpO_4(OH)_2]\cdot 2H_2O$, was measured at 4.9 K. The spectrum could not be fitted by using one quadrupole set, and also not by using two quadrupole sets.

Key words: ^{237}Np Mössbauer spectroscopy, Heptavalent neptunium compound

In a previous study on heptavalent neptunium compound, it was reported that ^{237}Np Mössbauer spectrum of $[Co(NH_3)_6][NpO_4(OH)_2]\cdot 2H_2O$ consists of two sets of quadrupole-split absorption lines with the same isomer shift (δ = -62.8 mm/s relative to NpO_2) and large asymmetry parameters (η = 0.69, 0.83) at 4.2 K. Based on this result, it was supposed that two nonequivalent Np(VII) sites exist and their coordination environments are in very low symmetry. In contrast to the Mössbauer result, a crystallographic study for the compound confirmed that there is only one Np(VII) site in the crystal and its coordination polyhedron is slightly distorted tetragonal bipyramid at room temperature. The problem concerning this inconsistency will be solved by finding a possible phase transition between 4.2 K and room temperature. However, it cannot be also disregarded a possibility that the polycrystalline sample used in the Mössbauer measurement contained another phase, or that the single crystal used in the structure determination was in a quite different phase from the Mössbauer sample.

In the present study polycrystalline sample of the compound was prepared and its ^{237}Np Mössbauer spectra were remeasured. ^{237}Np Mössbauer spectrum at 4.9 K was quite similar to that at 4.2 K presented by Stone et al. However, the analysis of our spectrum as done by them did not give a good approximation due to its asymmetric shape. Data analysis and other measurements will be presented.

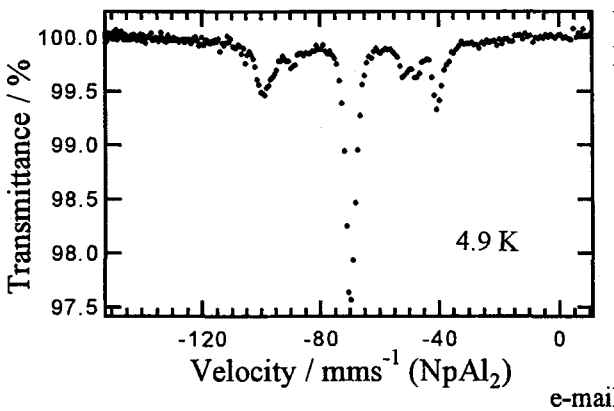

e-mail: nakamoto@analchem.tokai.jaeri.go.jp

P119
s.21

IN-BEAM MÖSSBAUER SPECTROSCOPY IN MATERIALS SCIENCE AT RIKEN ACCELERATOR RESEARCH FACILITY

Y. Kobayashi, *Y. Yoshida, *K. Hayakawa, *K. Yukihira, J. Nakamura, **H. Häßlein, **R. Sielemann, ***S. Nasu, N. Inabe, Y. Watanabe, A. Yoshida, M. Kase, A. Goto, S. Yano, E. Yagi, and F. Ambe

The Instituteof Physicaland ChemicalResearch(RIKEN), Saitama351-01, Japan.
** Shizuoka Instituteof Science andTechnology, Shizuoka 437, Japan.*
*** Hahn-Meitner-InsitutD-14109 Berlin, Germany*
**** Facultyof EngineeringScience, Osaka University, Osaka 560, Japan.*

The interest in materials science research using heavy-ion accelerators will certainly shift from conventional "off-line ion implantation" to "on-line ion implantation". In-beam Mössbauer spectroscopy is on-line Mössbauer measurement providing us directly with significant information on atomic-scale phenomena in wide varieties of materials. In RIKEN Accelerator Research Facility, we have developed three different types of the in-beam Mössbauer spectroscopy combining with (i) the nuclear reaction of ^{56}Fe(d,p)^{57}Fe, (ii) the Coulomb excitation and recoil-implantation technique, and (iii) the radioactive secondary beam, ^{57}Mn. We will introduce our in-beam experimental apparatus and discuss some results as followings.

(i) In the in-beam experiment using the (d,p) reaction, we measured the angular dependence of Mössbauer spectra at different crystal orientations of the Fe single crystal in order to elucidate the dynamical effects due to jump processes of the produced self-interstitial ^{57}Fe atoms.

(ii) ^{57}Fe atoms were implanted into solid rare-gas samples with the FCC structure immediately after the Coulomb excitation via a pulsed Ar ion beams and the in-beam Mössbauer spectra were simultaneously measured.

(iii) It is expected that in-beam Mössbauer experiments using the unstable short-lived RI beams lead to unique information concerning the change of crystal structure, the rearrangement of the irradiation damage, the generation of atoms with high degree of ionization, and the synthesis of exotic chemical species and states in matrices, because they are nearly bare atoms and have much higher implantation energy of several hundred MeV than ones by the other ordinary implantation processes. We report here a result from the in-beam Mössbauer experiment on ^{57}Fe (←^{57}Mn) in a sample of silicon wafer.

Fax 048(467)4662 kyoshio@postman.riken.go.jp
" " 9423 ,

P120
s.21

MOSSBAUER CHARACTERIZATION AND PROMPT γ -RAY ANALYSIS OF PRODUCTS OF THERMIT REACTIONS

Y. Sakai, K. Ohshita, M. K. Kubo [1], C. Yonezawa [2], H. Matsue [2], H. Sawahata [3], Y. Ito [3], S. Iwama

Department of Chemistry, Daido Institute of Technology, Hakusui-cho, Nagoya 457, Japan
[1] *School of Science, The University of Tokyo, Hongo, Tokyo 113, Japan*
[2] *Department of Chemistry and Fuel Research, Japan Atomic Energy Research Institute, Tokai, Ibaraki 319-11, Japan*
[3] *Research Center for Nuclear Science and Technology, The University of Tokyo, Tokai, Ibaraki 319-11, Japan*

Summary: Iron and boron species in the thermit-reaction products of the mixture of aluminium, iron oxide , and boron oxide were characterized by Mossbauer spectroscopy and prompt γ -ray analysis, respectively.
Key words: Thermit reaction, Mossbauer spectroscopy, Prompt γ -ray analysis

It is well known that an explosive thermit reaction takes place when a powder mixture of aluminium and a metal oxide is strongly heated in air, in which aluminium is oxidized forming Al_2O_3 while the metal oxide is reduced to metal. The thermit reaction is accompanied by instantaneous emission of large amount of heat. In the present work we characterized the chemical states of iron species in the thermit-reaction products of the mixture of Al, iron oxide, and boron oxide using Mossbauer spectroscopy. Also the physical and chemical states of boron species in the thermit-reaction products were examined by prompt γ -ray analysis (PGA). Recently, it was proved in our investigations that the PGA technique can be applied to characterization of boron by analyzing the Doppler broadening of the 478 keV prompt γ -rays from ^{7*}Li produced in the $^{10}B(n, \alpha)^{7*}Li$ reaction. Both the iron and boron states in the products prepared under various conditions were investigated non-destructively by the two independent methods. The Mossbauer spectrum at 293 K of the thermit-reaction product of Al, Fe_2O_3, and B_2O_3 is shown in Figure 1, where we can see a single absorption peak with an isomer shift of about 0 mm/s . The stable phase of metallic iron is ferromagnetic α -Fe at room temperature. However, the iron species observed here showing a single peak in the Mossbauer spectrum might be assigned to paramagnetic iron species with oxidation number of 0. The Doppler-broadened line shape of the prompt γ -rays at 478 keV of ^{7*}Li in the same product is also shown in Figure 1. The degradation constant of ^{7*}Li estimated from the line shape analysis is close to that for metallic boron, suggesting that the reductive transformation from B_2O_3 to B occurred in the thermit reaction.

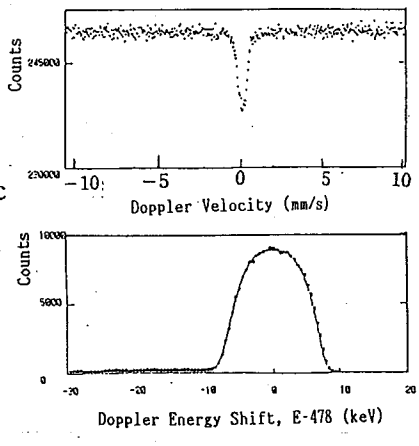

(Figure 1) ^{57}Fe-Mossbauer spectrum (top of the figure) and spectral line-shape of prompt γ -rays at 478keV from ^{7*}Li produced in the $^{10}B(n, \alpha)^{7*}Li$ reaction (bottom of the figure) for a thermit-reaction product of Al (351mg), Fe_2O_3 (60mg), and B_2O_3 (61mg).

Fax +81-52-612-5571, E-mail; yocsakai@daido-it.ac.jp

P121
s.24

DEVELOPMENT AND APPLICATION OF RADIOISOTOPE METHODS FOR SULFIDE HYDROTREATMENT CATALYST TESTING

V.M Kogan[1] and N.M. Parfenova[2]

[1]*N.D.Zelinsky Institute of Organic Chemistry, Russian Academy of Sciences, 47 Leninsky prospect, Moscow 117913, Russian Federation;*

[2]*Institute of Chemistry, Turkmenian Academy of Sciences, 92 Pogranichnicov st, Ashgabat 744012, Turkmenistan.*

Summary: A comparative radioisotope study into alumina- and silica supported Co, Ni and Co+Ni catalysts has permitted us to put forward some criteria to design a catalyst composition optimum for a definite refining process.

Key words: Catalysts, Hydorodesulfurization, Radioisotope study, Residual oils, Sulfides.

Involving heavy residual oils into processing makes it of major importance to have effective catalysts for oils hydrotreating. When developing such catalysts many parameters are taken into account - the type of residua, the range of products obtained, as well as their quality. Actually a special catalyst is made for every specific processing.

The given investigation shows possibilities of effective usage of Co and Co-Ni catalysts supported on silica and alumina for hydrotreating fuel oils of West-Sibirian petroleum. Two forms of catalysts were used: one was reduced in a flow of hydrogen and the other was sulfidized. For comparison commercial NiMo/alumina catalyst was taken.

It has been shown that the reduced and sulfidized catalysts differ in all the parameters analysed. Catalyst Co/silica in its reduced form proved to be the most effective. Catalyst (Co+Ni)/alumina proved to be the most active in its sulfidized form. Under mild experimental conditions the sulfidized commercial (Ni+Mo)/alumina catalyst did not show its characteristic activity but at 380°C one could observe significant coke deposits on its surface. The reduced catalysts showed very good ability towards demetallization. One can suppose that this is so due to different mechanisms of fuel oils hydrotreating on sulfidized and reduced catalysts.

To estimate the hydrodesulfurization (HDS) activity of Co-Ni catalysts on the basis of the data about the types of sulfide sulfur on the catalysts, the samples were tested by a radioisotope pulse technique in a thiophene HDS reaction. During sulfidation catalysts were labelled by radioactive isotope ^{35}S. It has been established that surface sulfur of the catalyst participates in hydrogen sulfide formation. In the course of HDS reaction some sulfur of the catalyst (mobile sulfur) is replaced by thiophene sulfur. The amount of mobile sulfur in sulfide catalysts depends on the composition of the catalyst and sulfiding procedure. Two types of HDS active sites containing mobile sulfur have been found - "rapid" and "slow".

The amount of mobile sulfur affects the general desulfurization degree of fuel oils and the most important role belongs to "slow" sulfur.

The study has permitted us to put forward some criteria to evaluate the results of radioisotope testing with the aim of designing a catalyst composition optimum for a definite refining process. Some cheap catalysts-adsorbents for preliminary treating of heavy crudes, before they are applied to the main oil refining processes have been designed.

Fax: + 7 095 - 135-53-28, E-mail: vmk@ioc.ac.ru

P122
s.24

STRUCTURAL INFORMATION FROM THE INTERFERENCE EFFECT OF ELECTRON-CAPTURE X-RAYS

Y. C. Sasaki*(1), K. Yasuda(1), M. Takahashi(2), I. Satoh(2), S. Ishiwata(3)

(1) Advanced Research Laboratory, Hitachi Ltd., Saitama 350-03, Japan
(2) Institute for Materials Research, Tohoku University, Sendai 980-77, Japan
(3) Department of Physics, Waseda University, Tokyo 169, Japan

Summary: The nanometer-level positional information for the radioactive atoms(for example, ^{51}Cr, ^{111}In and ^{125}I) on the substrate surface can be obtained from the interference effect of electron-capture x-rays.

Key words: radioactive atom, electron-capture x-rays, interference fringes

Abstract:
In 1994, we succeeded for the first time the observation of the interference effect for electron-capture x-rays emitted by nuclear transformations in radioactive atoms[1]. We observed the Lloyd's mirror-type interference effect [2]of monochromatic x-rays from the radioactive atoms embedded in noncrystalline material. This monochromatic x-ray is spontaneously emitted from electron-capture-type radioactive atom; for example, the K-electron capture in the radioactive decay is accompanied by emission of K x-rays. X-ray emissions from a radioactive atom above a substrate can take two optical paths: a direct emission and a totally reflected emission when the take-off angle (θ_t) is smaller than the critical angle (θ_c) for the x-ray total external reflection. The optical path difference from two sources depends on both the distance (z) of the radioactive atom from the substrate and the phase shift at the total reflection. Thus, the nanometer-level positional information for the radioactive atoms can be obtained from the period of the observed interference fringes.

A monolayer of ^{51}Cr above a Pt substrate was used as a model sample[1]. The observed pattern is monitored with a non-energy-dispersive two-dimensional detector (imaging plate; IP) and is quantitatively measured by scanning the slit with an energy-dispersive detector (pure Ge detector). Next, we tried to measure the interference fringes from the monolayer of the azobenzene and the protein labeled with radioisotopes (^{111}In and ^{125}I) in an aqueous solution. In the case of the azobenzene molecules, we observed nanometer-level structural changes by the trans-cis transition[3]. In the case of the protein molecules, we obtained the information about the orientation of the labeled protein on the substrate under the aqueous solution[4].

This paper reports the observations of the conformational changes in the monolayer of the arranged myosin molecules on the substrate under the wet conditions. Myosin molecule is an enzyme that, in conjunction with actin, transduces the chemical energy from the hydrolysis of ATP into directed mechanical movement. Thus, the large conformational changes of the myosin molecules are expected during ATP hydrolysis. The amino groups of myosin subfragment 1(S1) molecules were labeled from ^{125}I. The labeled S1 molecules were arranged on the gold substrate through the bioreactive maleimide headgroup of the self-assembled monolayer. We obtained information about the position of the labeled ^{125}I in the arranged S1 molecules in some aqueous conditions.

References:
[1] Y. C. Sasaki, Y. Suzuki, Y. Tomioka, T. Ishibashi, I. Satoh, and K. Hirokawa, Phys. Rev. **B50**(1994)15516.
[2] M. Born and E. Wolf, Principles of Optics, 6th ed.(Pergamon, New York, 1980).
[3] Y. C. Sasaki, Y. Suzuki, Y. Tomioka, T. Ishibashi, M. Takahashi, and I. Satoh, Langmuir **12(17)**(1996)4173.
[4] Y. C. Sasaki, K. Yasuda, Y. Suzuki, T. Ishibashi, I. Satoh, Y. Fujiki, and S. Ishiwata, Biophys. J. **72**(1997)1842.

Y. C. Sasaki. Fax number: +81-492-96-6006; E-mail number: ycsasaki@harl.hitachi.co.jp

P123 s.24 NATURAL ALPHA ACTIVE ISOTOPES CONTAINED IN HIGH PURITY MEMORY DEVICE MATERIAL

T.Mitsugashira[1]*, M. Hara[1], Y.Suzuki[1], M.Watanabe[1], S.Hirai[2], Y.Okada[2], M. Mori[2]

1;Oarai-branch, Institute for Materials Research, Tohoku University
Narita-machi, Oarai-machi, Higashiibaraki-gun, Ibaraki, 311-13, Japan
2;Atomic Energy Research Laboratory, Musashi Institute of Technology,
Ozenji, Asou-ku Kawasaki 215 Japan

Summary: SmF_3 coprecipitation for determining natural U and Th isotopes and $BaSO_4$ coprecipitation for Ra isotopes were successfully applied to determine traces of alpha emitters contained in memory device materials, SiO_2 and Pb.
Key words: SmF_3, $BaSO_4$, coprecipitation, alpha-spectrometry, soft-error

The probability of soft-error increases with increasing memory density and recent progress in computer technology calls for numbers of new materials to fabricate modern semiconductor memory. The authors have investigated the radiochemical activation analysis(RNAA) to determine uranium and thorium contained in various memory materials. RNAA is sensitive to ^{238}U and ^{232}Th but not sensitive to the other natural alpha emitters. It seems necessary to develop more sophisticated procedure to determine decay series alpha emitters. As the first attempt, we measured ^{210}Po in high purity lead by using alpha scintillation spectrometry coupled with pulse shape discrimination technique and found that the lead contained about 1Bq/gPb of ^{210}Po, unexpectedly higher than the content of natural uranium. This finding suggests the importance of the determination of natural decay series alpha emitters.

One of the authors have developed a samarium trifluorides coprecipitation method to determine actinides using natural alpha active isotope ^{147}Sm as an inner standard. The same procedure is useful for determining natural uranium and thorium isotopes. For radium isotopes, we selected a coprecipitation method with barium sulfates using ^{223}Ra as an inner standard. Taking high purity lead and medium grade silica as specimens, the following results were obtained:
For 7 lead samples; ①The contents of ^{210}Po were 0.7～1Bq/g. ②The contents of ^{226}Ra were less than 3～16 μ Bq/g. ③The contents of ^{238}U were less than 16 μ Bq/g. ④The contents of ^{232}Th were less than 4.4 μ Bq/g.
For silica sample;①The contents of ^{238}U,^{234}U, and ^{235}U were less than 0.02Bq/g. ②The content of ^{232}Th was 0.06Bq/g. ③The content of ^{228}Th was 0.73Bq/g. ④The content of ^{230}Th was 0.072Bq/g. ⑤The content of ^{226}Ra was 1.8Bq/g.

The procedures for these measurements will be given in the presentation. For both samples, the non-radioequilibrium was clearly demonstrated. For the evaluation of modern memory device materials with respect to the soft-error probability, presently proposed methods are quite useful.

FAX: 81-29-267-4947
E-mail: mitsug@ob.imr.tohoku.ac.jp

P124
s.24/13

RADIATION DAMAGE IN $Si_{1-x}Ge_x$ HETEROEPITAXIAL DEVICES

H. Ohyama, E. Simoen[1], C. Claeys[1], J. Vanhellemont[1, 2], K. Hayama, J. Tokuyama, Y. Takami[3], H. Sunaga[4], J. Poortmans[1] and M. Caymax[1]

Kumamoto National College of Technology, 2659-2 Nishigoshi Kumamoto, 861-11 Japan

[1]*IMEC, Kapeldreef 75, B-3001 Leuven, Belgium*

[2]*Present address: Wacker Siltronic AG, D-84479 Burghausen, Germany*

[3]*Rikkyo University, 2-5-1, Nagasaka Yokosuka Kanagawa, 240-01 Japan*

[4]*Takasaki JAERI, 1233 Watanuki Takasaki Gunma, 370-12 Japan*

Summary : Results are presented of an extended study on the radiation damage in $Si_{1-x}Ge_x$ heteroepitaxial devices by high energy electrons, neutrons and alpha rays. The radiation source dependence isalso discussed taking into account the energy transfer.

Key Words : $Si_{1-x}Ge_x$ heteroepitaxial devices, radiation damage, induced lattice defects

$Si_{1-x}Ge_x$ heteroepitaxial devices have received a lot of attention due to their excellent performance with respect to high speed and large carrier mobility. The radiation damage in $Si_{1-x}Ge_x$ devices is reported as a function of germanium content and radiation source together with the calculation of the number of knock-on atoms (N_d) and the nonionizing energy loss (NIEL). $Si_{1-x}Ge_x$ epitaxial diodes and heterojunction bipolar transistors (HBTs) are used. The germanium content of the strained $Si_{1-x}Ge_x$ epitaxial layer is x = 0.08, 0.12 and 0.16. The devices are irradiated at room temperature by 1-MeV electrons, 1-MeV neutrons and 20-MeV alpha rays. Before and after irradiation, the electrical performance of irradiated devices is measured with the observation of the induced deep levels in he $Si_{1-x}Ge_x$ epitaxial layer by deep level transient spectroscopy (DLTS). Figure 1 shows the typical current-voltage characteristic for the x = 0.12 diodes, which are irradiated by alpha rays for different fluence. The electrical performance degrades after irradiation. The damage coefficient of performance calculated for alpha irradiation is nearly the same as for neutron irradiation, while it is about three orders of magnitude larger than that for electron irradiation, because of the difference of mass and the possibility of nuclear collision. The radiation source dependence of the degradation can be explained by the difference of N_d and NIEL. Figure 2 shows the typical DLTS spectra in x = 0.12 diodes. Electron and hole capture levels are induced after irradiation. Most probably electron capture levels are associated with an interstitial boron complex, which are mainly responsible for the degradation of the device performance.

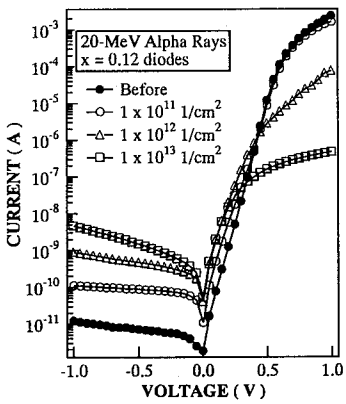

Fig. 1. Influence of 20-MeV alpha ray irradiation on electrical performance.

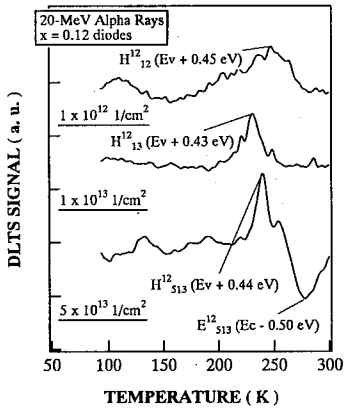

Fig. 2. DLTS spectra for x = 0.12 diodes irradiated by 20-MeV alpha rays.

Fax: +81-96-242-4190, e-mail: ohyama@cc.knct.ac.jp

P125
s.24/13

DEGRADATION OF MOSFETs ON SIMOX BY IRRADIATION

T. Hakata, H. Ohyama*, E. Simoen[1], C. Claeys[1], K. Miyahara[2], K. Kawamura[3] and Y. Ogita[4]

Kumamoto National College of Technology, 2659-2 Nishigoshi Kumamoto, 861-11 Japan

[1]*IMEC, Kapeldreef 75, B-3001 Leuven, Belgium*

[2]*Kumamoto Univeresity, 2-39-1 Kurokami, Kumamoto, 860 Japan*

[3]*Nippon Steel Co., 3434 Hikari, Yamaguchi, 734 Japan*

[4]*Kanagawa Institute of Technology, 1030 Atsugi, Knagawa, 243-02 Japan*

Summary : Results are presented of the impact of irradiation on device performance of MOSFETs on SIMOX substrate. Radiation source dependence of the degradation is also repored taking into account the energy transfer.

Key Words : MOSFETs on SIMOX, radiation damage, induced lattice defects

CMOS devices on SIMOX substrates have attracted attention due to their excellent performance with respect to high speed, low power and radiation hardness. The degradation and recovery of the electrical performance in MOSFETs on SIMOX substrate, fabricated by high and low dose oxygen implantation, after electron and alpha ray irradiation is reported. N- and p-channel MOSFETs on SIMOX substrate were processed in a standard 2 μm CMOS technology. The unbiased MOSFETs were at room temperature irradiated with 1 and 2-MeV electrons and 20-MeV alpha rays. Before and after irradiation, the electrical performance was measured together with the photoconductivity amplitude (PCA) in the front- and buried SiO_2 layer. Figure 1 shows the degradation of the input characteristics for n-channel FETs, after 1-MeV electron irradiation. In the subtheshold region of the input characteristics (Fig. 1), unstable changes of I_{DS} occurs due to the difference in irradiation-induced charge built-up at the front- and buried oxide. Figure 2, giving the PCA values as a function of fluence of the 1 and 2-MeV irradiations, shows that the PCA amplitude decreases with increasing fluence. The calculated lifetime before and after 10^{15} e/cm^2 1-MeV irradiation is 1420 and 9.9 nsec, respectively, while the value is 8.6 nsec after a 10^{15} e/cm^2 2-MeV irradiation. The radiation-induced decrease of lifetime is caused by a decrease of the carrier mobility due to the collisions with lattice defects introduced in the channel, which are also responsible for the decrease of drain current, as shown in Figure 1. Finally, the radiation source dependence on the degradation of device performance and the recovery behavior by thermal annealing will be discussed to investigate the degradation mechanism.

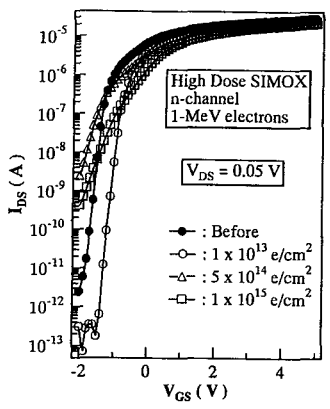

Fig. 1. Degradation of input characteristics for n-channel FETs by 1-MeV electron irradiation.

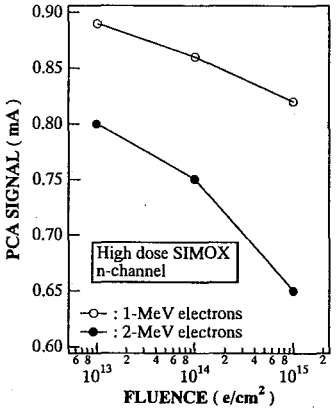

Fig. 2. PCA values as a function of fluence with 1 and 2-MeV.

Fax: +81-96-242-4190, e-mail: ohyama@cc.knct.ac.jp

P126

s.24/13

EFFECT OF IRRADIATION IN InGaAs PHOTO DEVICES

T. Kudou, H. Ohyama*, E. Simoen[1], C. Claeys[1], J. Vanhellemont[1, 2], K. Sigaki, Y. Takami[3] and A. Fujii[4]

Kumamoto National College of Technology, 2659-2 Nishigoshi Kumamoto, 861-11 Japan

[1]*IMEC, Kapeldreef 75, B-3001 Leuven, Belgium*

[2]*Present address: Wacker Siltronic AG, D-84479 Burghausen, Germany*

[3]*Rikkyo University, 2-5-1, Nagasaka Yokosuka Kanagawa, 240-01 Japan*

[4]*Kumamoto University, 39-1 Kurokami Kumamoto, 860 Japan*

Summary : Results are presented of the impact of irradiation on device performance of $In_{0.53}Ga_{0.47}As$ photodiodes. Recovery behavior by annealing is also repored together with the radiation source dependence of the degradation

Key Words : $In_{0.53}Ga_{0.47}As$ photodiodes, radiation damage, induced lattice defects

Results are presented of an extended study on the degradation of device performance and the induced lattice defects in $In_{0.53}Ga_{0.47}As$ pin photodiodes irradiated by 1-MeV electrons, 1-MeV fast neutrons and 20-MeV alpha rays. The radiation source dependence on the degradation and recovery behavior of device performance is also reported taking into account the number of knock-on atoms (N_d) and the nonionizing energy loss (NIEL). Pin photodiodes fabricated in n^--$In_{0.53}Ga_{0.47}As$ epitaxial layers were used in this study. The diodes were irradiated by 1-MeV electrons, 1-MeV neutrons and 20-MeV alpha rays at room temperature. The device performance was measured before and after irradiation. The deep levels in the $In_{0.53}Ga_{0.47}As$ epitaxial layer were studied using the deep level transient spectroscopy (DLTS) method. To investigate the recovery behavior, isochronal thermal anneals were also carried out. Fig. 1 shows the typical photo current characteristics for irradiation of 20-MeV alpha rays. Similar degradation is observed for different radiation sources. The damage coefficient of device performance calculated for alpha ray irradiation is nearly the same as that for neutron irradiation, while it is about three orders of magnitude larger than that for electron irradiation. This is due to the different N_d and NIEL, which is correlated with the difference of mass and the possibility of nuclear collision. Electron capture levels around (Ec - 0.38 eV) after irradiation are thought to be associated with the Ga vacancy. Fig. 2 shows the result of annealing of photo current characteristics. In this figure, the recovery behavior has a radiation source dependence, while the device performance degraded by the irradiation recovers by thermal annealing The recovery increases with increasing annealing temperature. The radiation source dependence of recovery behavior is thought to be due to the different type of induced radiation damage.

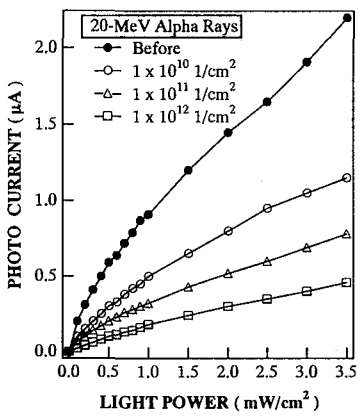

Fig. 1. Degradation of photocurrent by alpha ray irradiation.

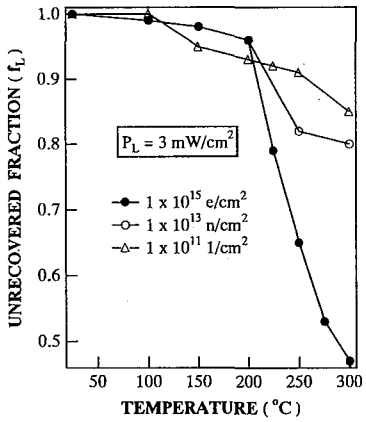

Fig. 2. Fig. 2 Recovery behavior of photo curent by thermal annealing.

Fax: +81-96-242-4190, e-mail: ohyama@cc.knct.ac.jp

P127
s.42/24

TRITIUM AUTORADIOGRAPHIC STUDY OF HYDROGEN INGRESS INTO OXIDIZED ZIRCALOY-2

H.Hanada, K.Isobe, Y.Hatano and M.Sugisaki

Department of Nuclear Engineering, Faculty of Engineering, Kyushu University, Fukuoka 812-81, Japan

Summary: The mechanism of hydrogen ingress into oxidized Zircaloy-2 is studied with tritium autoradiography and secondary ion mass spectroscopy. The results suggest that the mechanism of hydrogen ingress during cathodic charging is not necessarily same as that during oxidation.
Key words: tritium autoradiography, secondary ion mass spectroscopy, hydrogen, Zircaloy-2

The ingress mechanism of hydrogen into Zircaloy-2 through a zirconium oxide layer has been studied by examining the spatial distribution of hydrogen in the zirconium oxide layer formed on the matrix alloy, in which experimental techniques of tritium microautoradiography and secondary ion mass spectroscopy (SIMS) are adopted. In the present study, two cases of hydrogen ingress process are examined. One is the case that hydrogen is taken up through the oxide layer by cathodic charging in an aqueous media at room temperature, in which the specimen is beforehand oxidized in steam at high temperatures. The other is the case that hydrogen is picked up during the oxidation in steam at high temperatures.

In the experiment, H_2O, D_2O and HTO are used depending upon the cases; e.g. deuterium is used in the SIMS analysis to eliminate the influence of background due to protium residually present in the apparatus. In these measurements, two kinds of specimens including fine (less than 50 nm) or coarse precipitates (less than 2 μm) are used to examine the influence of the precipitates, in which the thickness of the oxide layer is adjusted as 1-2 μm.

The obtained results of SIMS analysis suggest that hydrogen transport rate through the oxide layer is not controlled by the dissolution process at the surface in both cases of cathodic charging and oxidation but by the diffusion of hydrogen in the oxide layer. The tritium microautoradiographs in both cases suggest that tritium is concentrated in the region near the precipitates (Fig.1). The radiographs in the case of cathodic charging show also that a large amount of tritium penetrates into the base alloy through the oxide film although the diffusion coefficient of tritium in the oxide film reported in literature is appreciably small at room temperature. This result suggests that the mechanism of hydrogen ingress during cathodic charging is not necessarily same as that during oxidation.

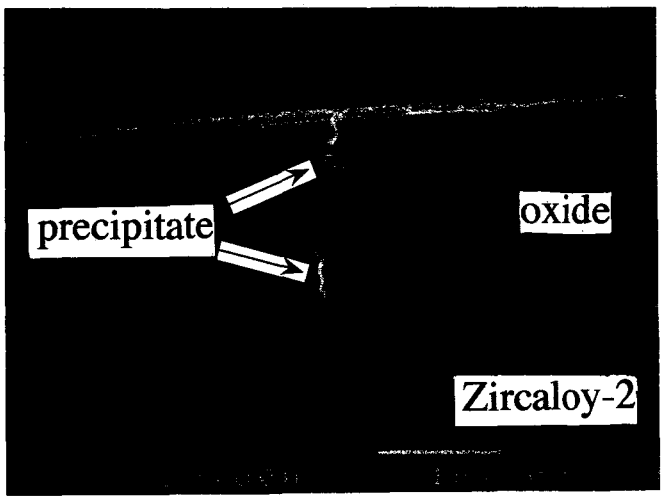

Fig.1 Tritium microautoradiograph of Zircaloy-2

FAX:+81-92-642-3800, E-mail: yhata@nucl.kyushu-u.ac.jp

P128
s.21

MÖSSBAUER PHASE DIAGRAM IN THERMALLY TREATED EUROPIUM IRON MIXED OXIDE

P. A. de SOUZA Jr.[1] V. K. GARG[2]

[1] *Departamento de Física, Centro de Ciências Exatas, Universidade Federal do Espírito Santo 29060-900 Vitória, E. S., Brazil*

[2] *Departomento de Física, Instituto de Ciências Exatas, Universidade de Brasília 70910-900 Brasília, D. F., Brazil*

Summary :

Key words:

Europium iron mixed oxides in the ratio of Eu : Fe = 1 : 9 and annealed at 500, 850, 1000 and 1250 ℃ have been investigated by X-ray diffraction, thermal differential analysis and Fe-57 and Eu-151 Mössbauer spectroscopy between RT and liqiud nitrogen temperature. The Mössbauer spectra are complex, showing upto three six line subspectra, which have been attributed to $EuFeO_3$ (europium iron perovskite), $Eu_3Fe_5O_{12}$ (europium iron garnet) and (α -Fe_2O_3 (hematite)). Mössbauer spectra of the thermally untreated gel sample at room temperature showed a well defined doublet and at 85 K showed an unresolved magnetic structure with very large linewidths, indicating the start of crystallization during the storage of the sample for nearly 6 years. The Eu-151 spectrum shows that the europium is trivalent. The XRD indicated that the sample is amorphous. Fe-57 Mössbauer spectra at room temperature of the sample thermally treated at 500 ℃ show a better resolved magnetic hyperfine structure, however the linewidths are still large, of the order of 1.0 mm/s. Somewhat better resolved spectra were obtained at 85 K, indicating that thermal treatment at 500 ℃ for 12 hours was not sufficient for the phase crystallization. The TDA curve indicate that at 443 ℃ there is a phase transition. The sample thermally treated at 1000 ℃ shows one Mössbauer sextet (Hint = 51.6 Tesla) corresponding to hematite. The XRD shows the presence of europium iron perovskite, but, only at 85 K , this substance was confirmed by Fe-57 Mössbauer spectroscopy. The europium iron perovskite has been detected at room temperature and 90 K using Eu-151 Mössbauer spectroscopy. The sample thermally annealed at 1250 ℃ shows a complex spectrum, analyzed as 83 % in the form of hematite and 17 % europium iron garnet. This is in full agreement as with the Eu-151 Mössbauer studies, which exhibit a clear europium iron garnet spectrum. These results are also confirmed by the XRD studies. It is thus verified that the increase of the thermal treatment temperature leads to crystallization of europium iron perovskite at 1000 ℃, and europium iron garnet at 1250 ℃. The behaviour of Eu : Fe = 1 : 9 system formation was analysed at 1050 ℃, 1100 ℃, 1150 ℃ and 1200 ℃, observing the transition of EuIP to EuIG phase. The whole amount of europium atoms formed first EuIP and, up to 1250 ℃, EuIG.

Fax: +55-27-335-2460, E-mail: souza@cce.ufes.br

P129
s.51

EFFECT OF PRESSURE ON THE ELECTRICAL RESISTIVITY OF α–Ce

G. Oomi and T. Kagayama

Department of Mechanical Engineering and Materials Science, Kumamoto University, Kurokami 2–39–1, Kumamoto 860, Japan

Summary: Temperature dependence of electrical resistivity have been measured for α–Ce at high pressure up to 2.0 GPa. A T^2–dependence is seen at low temperature and its coefficient becomes small with pressure. The result was analyzed associated with Kondo effect.
Key words: High pressure, Electrical resistance, Kondo temperature, Grüneisen analysis

It is well known that the electronic states of concentrated Kondo systems (CKS) are strongly dependent on a change in pressure or volume. The electronic states of CKS are characterized by the so–called Kondo temperature T_K, which is usually low for the heavy fermion (HF) compounds having extremely large effective mass but high for the intermediate valent (IV) compounds. The fact mentioned above implies a large change of T_K by an application of pressure. It has been well established that T_K increases with pressure showing a crossover from HF state to IV state[1].

Metallic Ce has several phases depending on pressure and temperature[2]. Among these phases the α–phase, which is stable below 110 K at ambient pressure or above 0.7 GPa at room temperature, has attracted paramount attention of many workers, because it exists between the magnetic γ–phase (2.53 μ_B/Ce atom) and the superconducting α'–phase T_c=1.7 K at 5 GPa and shows a exchange–enhanced Pauli paramagnetism. However it is very difficult to obtain a single phase of α–Ce at ambient pressure because of the existence of β–phase, which shows an antiferromagnetic order at 12.5 K. For this reason, there have been many discrepancies between experimental results on α–Ce. It is considered that a cooling under hydrostatic pressure above at least 0.3 GPa is needed to obtain a single phase and non–strained α–Ce[3].

In the present work we made an attempt to measure the electrical resistivity $\rho(T)$ of pressure–prepared α–Ce at low temperature. The experimental procedure to make a single phase of α–Ce was the same as described before[3]. The $\rho(T)$ curve of α–Ce was measured up to 2.0 GPa. It is found that $\rho(T)$ below 10 K is fit well as $\rho(T)=\rho_0+AT^2$, where ρ_0 is the residual resistivity. The magnitude of A decreases with pressure having a tendency to saturate above 1 GPa. Since A is proportional to T_K^{-2}, this result indicates that T_K increases with pressure. These results will be analyzed by using Grüneisen parameter for T_K.

References

[1] T. Kagayama et al., Phys. Rev. B **44** (1991) 7690.
[2] E. King et al., Phys. Rev. B **1** (1970) 1380.
[3] G. Oomi, J. Phys. Soc. Jpn. **49** (1980) 256.

Fax: +81–96–342–2749, E–mail: c3170@gpo.kumamoto-u.ac.jp

P130
s.51

THE SIZE DISTRIBUTIONS OF Po-210 IN THE ATMOSPHERE AROUND Mt. SAKURAJIMA IN KAGOSHIMA PREFECTURE, JAPAN

N. Ashikawa[1]*, N. Matsuoka[1], S. Takao[1], Y. Takashima[1], N. Syojo[2] and H. Imamura[2]

[1] *Kyushu Environmental Evaluation Association*
1-10-1 Matsukadai, Higashiku, Fukuoka 813, Japan
[2] *Kagoshima Prefectural Institute for Environmental Science*
18 Jonan-cho, Kagoshima 892, Japan

Summary: The size distributions of Po-210 in the atmosphere were measured around the active volcano, Mt. Sakurajima. The size distribution curve showed that Po-210 was condensed to fine particles smaller than 2 μm in diameter. The highest concentration of Po-210 was 2940 μBq/m³.
Key words: Polonium-210, volcano, particulate matter, size distribution

Introduction: One of the major sources of Po-210 is the volcanic plume. The measurements of Po-210 concentrations around volcano give useful information for geochemistry, health physics and others. Mt. Sakurajima is one of the most active volcanoes in Japan. So we collected the particulate matters in the atmosphere using a cascade impactor, and measured the size distributions of Po-210 in particulate matters.

Experimental: Particulate matters in the atmosphere were collected on the membrane filters by using a cascade impactor. The samples were collected at four stations around Mt. Sakurajima for the period from June 1994 to January 1996. The sample filters were dissolved in aqua regia. Known amount of Po-208 was added as a yield tracer. The Po isotopes deposited spontaneously on the silver disk. The activity of Po-210 was determined by alpha spectrometry with a surface barrier detector.

Result and discussion: The concentrations of Po-210 in atmospheric particulate matters are shown in Fig. 1.

The distances from the crater of Mt. Sakurajima to Akamizu and Kagoshima are 2 km and 5 km, respectively. On the other hand, Sendai and Kohira locate about 50 km away from the mountain. The Po-210 concentrations ranged from 63 to 2940 μBq/m³ at Akamizu, from 53 to 328 μBq/m³ at Kagoshima, from 66 to 279 μBq/m³ at Sendai and from 65 to 261 μBq/m³ at Kohira. The concentrations decreased in order of the distance from Mt. Sakurajima. The highest concentration of Po-210 (2940 μBq/m³) was observed at Akamizu in June 1995.

The size distribution of Po-210 collected at Akamizu in June 1995 is shown in Fig. 2. The size distribution curve indicates that the Po-210 in the atmosphere was condensed to fine particles smaller than 2 μm in diameter.

In addition, it was suggested that the Po-210 concentrations in particulate matters collected at Akamizu were affected by the wind direction above Mt. Sakurajima.

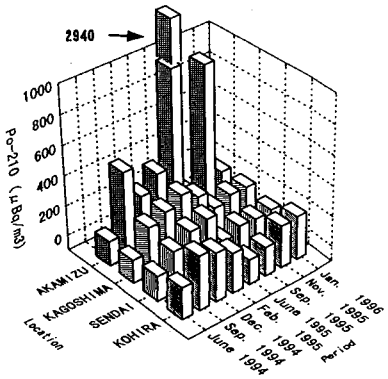

Fig.1 Concentrations of Po-210 in particulate matters

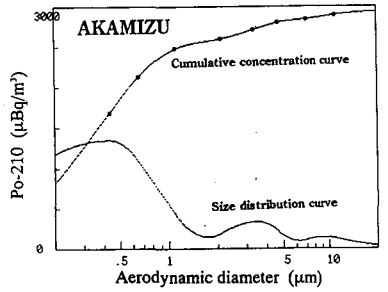

Fig.2 The size distribution of Po-210 in particulate matters in June 1995

Fax: +81-92-662-0990, E-mail: app-anal@keea.or.jp

P131
s.51

DETERMINATION OF ^{137}Cs, FALLOUT Pu and ^{90}Sr IN THE VOLCANIC SOIL OF KOREA

M.H. LEE, C.W. LEE, J.H. LEE
Korea Atomic Energy Research Institute, P.O. Box 105, Yusung, Taejeon, Korea

Summary : Volcanic soils were sampled from Cheju island and analyzed for ^{137}Cs, fallout Pu and ^{90}Sr concentrations. The concentrations of ^{137}Cs, fallout Pu and ^{90}Sr in the volcanic soil are higher than that in other forest site. The activity ratios of $^{239,240}Pu$, ^{137}Cs and ^{90}Sr were close to the fallout values due to atmospheric nuclear test.
Key words : concentrations, ^{137}Cs, fallout Pu, ^{90}Sr, volcanic soil, activity ratio, global fallout

Soil samples were collected from 5 sites in Cheju island in 1996. In each site, 5 to 10 soil samples were taken with a core sampler (4.5 cm in diameter) within an area of about 50 m × 50 m to a depth of about 5 cm. The samples were dried at 110 ^{o}C for 48 h after pebbles and fragments of plant root were removed and then sieved through a 1.0 mm screen. For ^{137}Cs analysis, a HPGe detector with counting efficiency of 25%, FWHM of 1.7 keV was used. Radiochemical analyses of $^{239,240}Pu$, ^{238}Pu and ^{241}Pu were carried out on aliquots of 100 g soil. The purified Pu fraction was divided into two nearly equal parts: one part was subjected to beta (^{241}Pu) by a low background liquid scintillation counter, and the other part was used for the measurement of other Pu isotopes ($^{239,240}Pu$, ^{238}Pu) by means of alpha-ray spectrometry. For the determination of ^{90}Sr, a solvent extraction method using crown ether was used.

The results of the mean values with standard deviation in the volcanic soil were 167.94 ± 83.99 Bq/kg for ^{137}Cs, 3.69 ± 1.29 Bq/kg for $^{239,240}Pu$, 0.155 ± 0.042 Bq/kg for ^{238}Pu, 13.73 ± 5.12 Bq/kg for ^{241}Pu, and 43.74 ± 9.61 Bq/kg for ^{90}Sr. The concentrations of ^{137}Cs, fallout Pu and ^{90}Sr are higher than that in other forest site. This result can be explained by geological and geographical location of sampling and the characteristic of the volcanic soil. Cheju island has more precipitation than any other area. When rain falls on the volcanic soil which has the porosity and permeability of the lavas, it easily percolate on the volcanic soil. The loss of the radionuclides by the rainwater rolling off on the volcanic soil is smaller than that on other soil. Also the organic matter (more than 40 %) forms complexes with fallout radionuclides such as plutonium compound and fix fallout radionuclides in the soil.

The activity ratios of $^{239,240}Pu/^{137}Cs$ and $^{90}Sr/^{137}Cs$ vary according to the source and can be utilized to identify the different sources of release. The mean activity ratio of $^{239,240}Pu/^{137}Cs$ in volcanic soils was calculated to be 0.022. This value is very close to 0.021, the estimated value commonly attributed to the fallout of these radionuclides due to atmospheric nuclear test. However, the activity ratio of $^{90}Sr/^{137}Cs$ was calculated to be 0.260, which is lower than the value of 0.602 which is characteristic of fallout from nuclear weapon testings. The difference in the values of activity ratio can be explained by the relative migration of ^{90}Sr to ^{137}Cs. Also, the activity ratios of $^{238}Pu/^{239,240}Pu$ and $^{241}Pu/^{239,240}Pu$ are close to those observed in the cumulative deposit from the global fallout of nuclear weapon testing.

mhlee1@nanum.Kaeri.re.kr
Fax: 82-42-863-1289

P133
s.51

KINETICS OF ELEMENT PROFILE PATTERN DURING LIFE CYCLE STAGE OF MORNING-GLORY

T.M.Nakanishi and M.Tamada

Graduate School of Agricultural and Life Sciences, The Univ. of Tokyo, 1-1-1, Yayoi, Bunkyo-ku, Tokyo, Japan 113

Summary: We present the kinetics of seven element profiles, Na, Mg, Al, Cl, K, Ca and Br in every tissue of morning-glory (*Ipomoea nil* L. c.v. Murasaki) during life cycle. Barriers formed for element were found even in the same tissue and between juvenile and adult phase.
Key words: neutron activation analysis, kinetic of element profile, morning-glory

Abstract: To study the kinetics of element profiles for Na, Mg, Al, Cl, K, Ca and Br during life cycle of morning-glory (*Ipomoea nil* L. c.v. Murasaki), the plant at several growth stages was harvested and the element concentrations in every tissue were determined by neutron activation analysis. Five to ten tissues of the plants at the same growing stage, from 0 day to 78 days, were collected and were irradiated by thermal neutrons (total neutron flux: $4.5 \times 10^{13} n/cm^2$). The samples we analyzed were, root (divided into two parts), each stem between the nods (two to three parts in each stem), leaf (three parts), leaf petiole, bud, flower and seed (two to four parts). There were systematic barriers appeared according to the plant development. First barrier was found between root and upper part of the plant. Most of Al and Na, absorbed from root was remained in root tissue. As the plant grows, there appeared a distinct barrier between juvenile phase and adult phase. Especially for Ca and Mg, the tissues lower than cotyledon, i.e. stem between root and cotyledon as well as petiole of cotyledon, seemed to store the elements during juvenile phase. The stored elements gradually moved up from cotyledon area to the upper part of the plant while the adult phase developed. Though the elements concentration upper than cotyledon gradually increased with respect to the decrease of the barrier formed around cotyledon, the barrier did not disappear completely until seed ripening stage, except for K. Generally, late developing stem showed lower accumulation of the elements, which seemed to regulate the inflow of Mg, Ca, Cl and Br into flowering tissue. The concentrations of K, Ca, Cl and Br in leaf were kept constant in spite of higher concentration of those in leaf petiole. The concentrations of these elements in leaf petiole became two to three times higher than those in leaf, which tendency was prominent especially at an early adult phase. When element profile of Cl and Br was compared, Cl was found to be easier to move within the tissue than Br, which induced higher osmotic pressure of leaf petiole to that of leaf and lower concentration of Br at the upper part of the cotyledon area. After flowering, selective element accumulation was observed while seed development, where most of the elements were accumulated into seed wall, not in seed. In the case of Al, accumulation in seed was relatively high, similar amount to that of seed wall. Higher concentration of the elements in elder leaf, which falls into ground and will be reused as plant nutrient, might reflect the recycling system of the element in plant.

Fax: +81-3-5689-7297, E-mail:atomoko@hongo.ecc.u-tokyo.ac.jp

P134
s.51

PHOTON ACTIVATION ANALYSIS OF I, TL, AND U IN ENVIRONMENTAL MATERIALS

K. Masumoto, T. Ohtsuki[1]*, Y. Miyamoto[2]*, J. H. Zaidi[2]*, A. Kajikawa[2]*, H. Haba[2]*, K. Sakamoto[2]*

Radiation Science Center,High Energy Accelerator Research Organization, Tanashi, Tokyo 188
[1]*Laboratory of Nuclear Science, Faculty of science, Tohoku University, Sendai, Miyagi 982*
[2]*Faculty of science, Kanazawa University, Kanazawa, Ishikawa 920-11*

Summary: Several elements including iodine, thallium and uranium were determined by PAA. Two electron accelerators, KURRI-Linac and Tohoku Linac were used for the comparison of analytical results of several kinds of environmental materials issued by NIES, NIST and IAEA.
Key words: PAA, Environmental materials, Iodine, Thalium, Uranium

Photon activation analysis (PAA) is effective for multielement analysis of envirnmental materials as the complementary technique to NAA, because of its suitable chracteristices, such as high sensitivity for trace elements and low sensitivity for major and minor elements in environmental materials. Iodine, thallium and uranium are difficult or not easy to analyse by NAA in spite of their environmental concerns. Terefore, several elements including I, Tl, U in various environmental samples were determined by PAA.

Samples were several kinds of environmental materials issued as the certified reference sample by NIES, NIST and IAEA. Irradiations were performed at 300-MeV electron linear accelerator of Tohoku University (Tohoku-Linac) and the electron linear accelerator of Research Reactor Institute of Kyoto University (KURRI-Linac). At the Tohoku-Linac, samples were irradiated by using 20-MeV electron beam at the average current of 70 μA for 5 hrs or by using 30-MeV electron beam for 3 hrs at the average current of 100 μA. At KURRI-Linac, typical irradiation was performed for 2 hours. Electron energy was 20 to 27 MeV, pulse width was 4 μs and repetition rate was 80 pps. After irradiation, samples were transfered to a new alminium foils and shaped into the same size again and setted on the sample holder for automatic counting, respectively. The pure Ge detector and MCA were connected to the automatic measurement system using micro-robot for sample changing. In order to get a good SN ratio of gamma-ray peaks from the nuclides to be determined, all samples were measured several times which intervals were several days, 1 week and 2-3 weeks after irradiation.

Trace elements including I, Tl, U etc in a variety of environmental samples were successfully determined and their detection limits were below ppm concentration level.

Table 1 shows the results of I in biological reference materials. As electron beam was defocused at KUR-Linac, samples sealed separately into a quartz ampoule were rotated to irradiate homogeneously and to reduce a radiation damage. The results of KUR-Linac were agreed with the literature values.

Table 1. Analytical results of iodine in biological reference materials. (μg/g)

Sample	Code	KUR-Linac	Tohoku-Linac	Literature
Body Fluids				
Milk Powder	IAEA A-11	0.18±0.03	0.30±0.01	1.5
Milk Powder	BCR CRM 63	0.41±0.11	4.9±0.3	-
Non-fat Milk Powder	NIST SRM-1549	3.18±0.07	3.13±0.11	3.38±0.02
Animal				
Bovine Liver	NIST SRM-1577a	0.23±0.07	0.79±0.02	0.243
Human Hair	NIES CRM No.5	3.02±0.11		-
Mussel	NIES CRM No.6	6.24±0.32		-
Mussel Tissue	IAEA MA-M-2	21.13±0.16		-
Oyster Tissue	NIST SRM-1566	3.05±0.12	2.54±0.09	2.8
Plant				
Citrus Leaves	NIST SRM-1572	1.94±0.11	1.89±0.04	1.84±0.03
Chlorella	NIES CRM No.3	0.35±0.09		-
Orchard Leaves	NIST SRM-1571	0.24±0.02		0.17
Peach Leaves	NIST SRM-1547	0.41±0.06		0.3
Pepperbush	NIES CRM No.1	0.59±0.12		-
Tomato Leaves	NIST SRM-1573	0.30±0.08		0.27

Concentration of I in environmental samples obtained by Tohoku-Linac and KURRI-Linac were good agreement with each other but not agreed with reference values. The results of Tl and U of environmental samples were good agreement with their reference value. It was shown that PAA will be able to offer valuable data for certification of environmental reference materials.

Fax:+81-424-69-2145, E-mail: masumoto@tanashi.kek.jp

P135
s.51

AEROSOL SIZE DISTRIBUTION OF RADON DAUGHTERS IN THE ACCELERATOR TUNNEL AIR

Y. Oki, K. Kondo,* Y. Kanda, T. Miura

Radiation Science Center, High Energy Accelerator Research Organization,
Oho 1-1, Tsukuba-shi, Ibaraki-ken, 305, Japan

Summary: Aerosol size distributions of Rn-daughters were determined for the accelerator tunnel air and the basement air of a concrete building. Their size distributions largely depend on the size distributions of ambient non-radioactive aerosols.

Key words: Rn daughters, size distributions, diffusion battery, unattached fraction

Rn-222($T_{1/2}$=3.82d) emanates to the atmosphere from soils and concrete walls of a building. Rn-222 is chemically inert and gaseous, while its decay product, Po-218($T_{1/2}$=3.05m), is positively charged at its birth and interacts instantly with surrounding molecules in the atmosphere. The processes of neutralization and aerosol formation of Po-218 in the atmosphere depend on the concentrations of ambient non-radioactive aerosols and their size distributions, chemical species, humidity and so on. We study the aerosol size distributions of radon daughters for the air in an accelerator tunnel and the basement air of a concrete building. These airs are largely different each other in non-radioactive aerosol size distributions and aerosol concentrations, being considered to be appropriate for the study on physico-chemical behavior of Rn-daughters in the atmosphere.

The aerosol size distributions of radon daughters were determined by using a wire screen diffusion battery(500 mesh). That is, radon daughters with high diffusivity are removed in the battery by becoming attached to the wire screens, and their size distributions were obtained from the relation between the number of wire screens and the ratio of the number of daughter atoms emerging from the battery and entering it. The fractions of unattached Po-218 that are not attached to ambient aerosols were also measured.

The measured distributions of radon daughters were of a log-normal, and the results are well explained based on attachment reactions of radon daughters onto ambient non-radioactive aerosols. The Po-218 aerosols have size distributions with geometric mean radii of about 0.03 μm and 0.06 μm for the accelerator tunnel air during machine operation and beam-off, respectively. Non-radioactive aerosols with a geometric mean radius of about 0.01 μm were observed during beam-on, while the size distributions were of a bi-modal for the air at beam-off. Whereas the size distribution for the basement air was about similar to those obtained for the accelerator tunnel air during beam-off. It was also indicated that the unattached fractionslargely depend on ambient aerosol numbers.

Fax:+81-298-64-4051, E-mail:kenjiro.kondo@kek.jp

P136
s.51

COMBINATION OF MICROWAVE DIGESTION AND INDUCTIVELY COUPLED PLASMA MASS SPECTROMETRY FOR DETERMINATION OF LEAD ISOTOPE RATIOS

H. Kawamura*, H. Tagomori, T. Nagano, N. Matsuoka, S. Takao, Y.Takashima, K. Saeki[1], M. Koike[1], N. Momoshima[2]

Kyushu Environmental Evaluation Association
1-10-1, Matsukadai, Higashiku, Fukuoka 813, Japan
[1]Energy Research Section, Research Laboratory, Kyushu Electric Power Co., Inc.
2-1-47, Shiobaru, Minamiku, Fukuoka 815, Japan
[2]Department of Chemistry, Faculty of Science Kyushu University
6-10-1, Hakozaki, Higashiku, Fukuoka 812-81, Japan

Summary: Microwave digestion was applied to pretreatment of atmospheric particulate matter samples for determination of lead isotope ratios by inductively coupled plasma mass spectrometry (ICP-MS). The method was proved to be suitable for pretreatment of samples for ICP-MS.
Key words: Microwave digestion, ICP-MS, Lead isotope ratios, Atmospheric particulate matter.

Introduction: Lead isotope ratios, $^{207}Pb/^{206}Pb$, $^{208}Pb/^{206}Pb$ are highly variable and source dependence. If lead released into the atmosphere retains the isotope ratios of their sources, it would be possible to identify pollutant sources by lead analysis. In this study pretreatment of atmospheric particulate matter samples was investigated for determination of lead isotope ratios by ICP-MS.

Experimental: Atmospheric particulate matter samples were collected on membrane filters using a cascade impactor. Sample and acid (HNO_3 and HF) were placed in a PTFE digestion vessel[1)](Fig.1: San'ai, P-70) and sealed tightly. The vessel with the sample and acid was heated with a microwave oven. The digested sample was evaporated to dryness on a hot-plate and the residue was dissolved in HNO_3. The lead isotope ratios were determined with a ICP-MS (HEWLETT PACKARD, 4500). The influences of matrix on an accuracy of measurement and lead blank level were investigated.

Result and discussion: Lead level of blank sample was confirmed to be sufficiently low compared to the atmospheric particulate matter sample. The lead isotope ratios in the digested sample were able to be measured directly without purification because most of the matrix elements did not affect the accuracy. Microwave digestion is an easy and quick pretreatment method for atmospheric particulate matter samples to determine lead isotope ratios. It is concluded that this method is suitable for routine work.

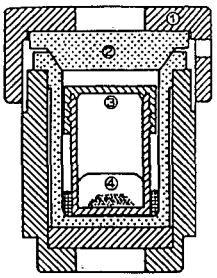

Fig.1. Digestion vessel
1) Polypropylene jacket
2) PTEF outer vessel
3) PFA inner vessel
4) Sample and acid mixture

Reference: 1) H.Isoyama et al., Anal. Sci., 6, 385-388 (1990)

Fax: +81-92-662-0990, E-mail: kawamura@keea.or.jp

P137
s.51

cancelled

P201
s.51

OPTIMIZATION OF LIQUID SCINTILLATION COUNTING TECHNIQUES FOR THE DETERMINATION OF CARBON-14 IN ENVIRONMENTAL SAMPLES

H. J. WOO, S. K. CHUN, S. Y. CHO, Y. S. KIM[1], D. W. KANG[2]

[1] *Korea Institute of Geology, Mining and Materials, P. O. Box 111, Daedeok Science Town, Taejon, Korea, 305-350*

[2] *Korea Electric Power Research Institute, Munji-dong 103-16, Yusung-gu, Taejon, Korea, 305-380*

Summary :

Key words:

The goal of this work is to optimize the liquid scintillation counting techniques for the determination of C-14 in stack effluent gases and in environmental samples such as biological and air samples. Carbon-14 activities in most environmental samples are measured with direct CO_2 absorption method. Highest figure of merit was found through the variation of Carbosorb E and Permafluor V ratio, and measurement windows. The best condition was 1:1 volume ratio. Average 2.35 g of CO_2 is reproducibly absorbed in the 20 ml mixture within 30 min. The counting efficiency determined by repeated analysis of NIST oxalic acid standard and the background count rate are measured to be 58.4± 2.0 % and 1.88 cpm, respectively in case of saturated solution. The correction curve of counting efficiency for partially saturated solutions is prepared, however the difference of corrected counting efficiency is not larger than 0.5 % when the amount of absorbed CO_2 is more than 1.6 g. The overall uncertainty of sample specific activity for near background levels is estimated to be about 7 % for 4 hours counting at 95 % confidence level. Due to the limitation of the available sample amount in case of reduced carbon species, stack effluent gas samples are measured by gel suspension counting method. After precipitation of CO_2 in the form of $BaCO_3$, 400 mg of which is mixed with 6 ml H_2O and 12 ml of Instagel XF. The counting efficiency is measured to be 57.7 ± 1.1 % and the typical sensitivity of this technique is about 130 mBq/m^3 for a 100 min count at a background count rate of 1.69 cpm. The overall uncertainty of specific activities (dpm/gC) of stack gas samples is estimated to be about 2 % at 95 % confidence level. For the benzene counting method measurements are performed with a mixture of 3 ml benzene 1 ml of scintillation cocktail (5 g of butyl-PBD in 100 ml of scintillation grade toluene) in a low potassium 7 ml borosilicate glass vial. The counting efficiency and the background count rate are measured to be 67.5 ± 1.2 % and 0.54 cpm, respectively at the highest figure of merit condition. The long-term stability of samples has been checked for all the counting techniques over a two week period, in which no apparent change in counting efficiency and background level was seen.

Fax: +82-42-861-9727, E-mail: bjwoo@rock25t.kigam.re.kr

P202
s.51

RADIOCARBON DATING FOR ACCIDENTAL RELEASES OF CHERNOBYL NPP

Michael Buzinny

Research Center for Radiation Medicine Academy of Medical Sciences of Ukraine, 254050, Melnikova 53, Kiev, Ukraine

Summary:
Key words:

RBMK-1000 (former Soviet Union) reactor at Chernobyl NPP was accidentally destroyed on April, 1986. Different direct and retrospective (indirect) methods were used to estimate radiological consequences of the subsequent radioactive releases to the environment and human health. To understand radioactivity transportation and distribution in the environment one have to take account of releases fractions, wind directions, weather conditions. Two main significant releases fractions are gases and aerosols. Each fraction play its own role in the formation of the radioactive contamination trace for different places. To estimate the Chernobyl NPP's accident trace I consider using of radiocarbon. It is one of the long-lived radionuclide observed in the Chernobyl accidental releases. Though its radiological impact is very significant it forms the trace in the environment that stays for long. Radiocarbon dating is mostly developed technique. Similarity in behavior (environmental transportation) of gaseous releases including C02 and aerosols including graphite dust was a prerequisite for this radiocarbon dating.

More than 60 trees were sampled around the Chernobyl NPP for radiocarbon dating and estimation of the gaseous transportation of radioactivity. The traditional radiocarbon dating technology (based on benzene synthesis and following liquid scintillation measurement on base of modern liquid scintillation spectrometer Quantulus 1220TM) was used for radiocarbon determination. To determine the excessive 14C ((14C) spatial destribution 14C levels were compared for the 1985-1987 annual rings for each tree analyzed. Dating of separate early and late wood samples for the 1986 annual tree ring were carried out to increase sensitivity and precision of the measurements. The maximum observed level for (14C was found to be 270 Bq kg-1 of Carbon (Bq kg-1C).

Background data point at an accumulation of the 14C specific activity of up to 25 kBq kg-1C in graphite of the 4th reactor of the Chernobyl NPP. The following computation of 14C destribution in the ground surface layer gave levels comparable with naturally occured 14C level in the organic matter at a distance of more than 10 km from the 4th reactor. Thus forest litter was used as an accumulator of the graphite dust for an estimation of aerosols transportation. The radiocarbon dating method was the same as that for the annual tree rings.

Radiocarbon levels for annual tree rings and forest litter will be presented and discussed, spatial distribution parameters and discharge level will be also estimated.

Fax: 380-44-213-7202, E-mail: buz@rpi.kiev.ua

P203
s.51

RADIOCARBON DATING FOR TREE RINGS OF DENDRO-CHRONOLOGICALLY DATED JAPAN CEDARS BURIED IN THE PADDY FIELD AT FUKUI.

S.Shibata[1], E.Kawano, K. Kimura[2], T.Mine[3] and M.Harada.

[1]*Isotope Center, Research Institute for Advanced Science and Technology Osaka Prefectural University*
[2]*The National Institute for Environmental Studies.*
[3]*SUNTORY Limited , Research Center.*

Summary: ^{14}C dating was made for rings of Japan Cedars whose relative growing ages were known. In comparison with INTCAL, their growing ages were determined (BC 1110-2430). ^{14}C variation in air was also studied.
Key word: ^{14}C Dating, Dendrochronology, Japan, MEOH-LSC method

Abstract: Kimura determined relative growing ages of Japan Cedars buried in the paddy fields at Fukui (70 cedars) by using tree-ring age determination. We extracted 6 cedars among them, dividing into 87 ring samples (20 yr. unit) for ^{14}C dating (MEOH-LSC method). They were numbered from the youngest ring sample (cal. yr. was termed X-YR) as shown below. B109 : 55-315, B63 : 153-453, B74 : 436-896, A103 : 820-1020, A15 : 982-1197 and A77 : 1140-1320. In comparison with INTCAL of CALIB program (M. Stuiver and P. J. Reimer), we attempted to obtain actual growing ages of these cedars and to estimate the atmospheric ^{14}C variation at that time in Japan. From the 87 data of ^{14}C age, we obtained ^{14}C age data set (COR-OR) composed of 64 data continuing at 20 yr. intervals for 1320 years. Setting a proper cal. yr. (Xn) for X-YR, we calculated ^{14}C age data, COR-OR(Xn) from COR-OR. With shifting Xn at interval of 1 yr. (2930-3045 yr. BP), we calculated COR-OR(Xn). The square root of average quadratic deviation between the ^{14}C ages of COR-OR(Xn) and INTCAL at the same cal. yr. (SQRT(AV(DEV)^2) was calculated for every COR-OR(Xn). When Xn is set to 2995 yr. BP, we attained the least value of SQRT(AV(DEV)^2), 45 years (0.989 of correlation coefficient), assuming that 2995 yr. BP is most probable as X-YR. Figure 1 shows ^{14}C age variation curves of COR-OR(2995) and INTCAL. On the basis of COR-OR(2995), we calculated ^{14}C variation ($\delta\ ^{14}C$, per mil) in air at that time in Japan. The ^{14}C variation curve obtained gives 0.78 of correlation coefficient and 9.60 of t-value (n=64) against INTCAL.

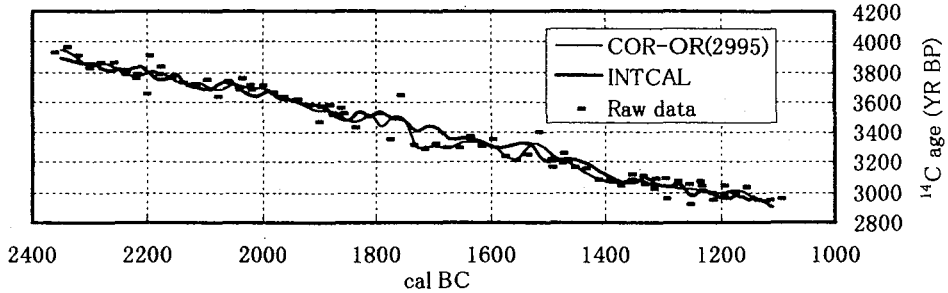

Fig.1 ^{14}C age variation curves (INTCAL and COR-OR(2995)).

Fax:+81-722-36-3876, E-mail:Shibata@riast.osakafu-u.ac.jp

P204
s.51

TRANSFER OF ^{137}Cs FROM SOIL TO PLANTS IN A WET MONTANE FOREST IN SUBTROPICAL AREA

C.-Y. Chiu[1], S.-Y. Lai[2], C.-J. Wang[2], and Y.-M. Lin[2]

[1]Institute of Botany, Academia Sinica, Taipei, 11529 Taiwan
[2]Taiwan Radiation Monitoring Center, Kaoshiung, 833 Taiwan

Summary: Although the soil is extremely acidic and the rainfall is high, conspicuous amount of ^{137}Cs is retained in the organic layer of a wet montane forest soil. The results suggest a rapid recycling of ^{137}Cs between soil and understory plants in this undisturbed multistoried forest ecosystem.

Key words: ^{137}Cs, ecosystem, forest, subtropical, soil, Taiwan

The distribution of ^{137}Cs was intensively investigated in an undisturbed wet montane ecosystem surrounding Yuanyang Lake which lies at the elevation of 1670 m in northeastern part of Taiwan. This area is occupied by a mossy forest, and thus represents a rare perhumid temperate locality in subtropical region. The radioactivity concentration of ^{137}Cs was determined by γ-spectroscopy with Ge (Li) detector. Although the soil is extremely acidic (pH=3.4) and the rainfall is high, ^{137}Cs seems to be retained in the organic layer. Radioactivity of ^{137}Cs in surface soil ranges from 28 to 71 Bq/kg. The migration of ^{137}Cs downward from the organic layer to the lower horizons of the soil profiles was found negligible. The concentrations of ^{137}Cs in the ground moss layer and litter were much lower than that in the soil organic layer; this suggests that ^{137}Cs detected is not from the newly deposited radioactive fallout. ^{137}Cs is easier translocated to juvenile plant tissues such as leaves and twigs than to woody branches. The radioactivity and transfer factor of ^{137}Cs are varied with plant species. Fern and weeds have higher values than the shrub and coniferous trees do. It indicates a rapid recycling of ^{137}Cs between soil and understory plants in the undisturbed multistoried forest ecosystem.

Fax: 886-2-782-7954, E-mail: bochiu@gate.sinica.edu.tw

P205
s.51

RELATION BETWEEN TRITIUM CONCENTRATION AND CHEMICAL COMPOSITION IN RAIN IN FUKUOKA

Y. Hayashi, N. Momoshima*, H. Kakiuchi, and Y. Maeda
Department of Chemistry, Faculty of Science, Kyushu University, Hakozaki, Higashiku, Fukuoka 812-81, Japan

Summary: Tritium concentrations in rain collected in Fukuoka were measured and their variations seem to be governed by meteorological conditions. Cations and anions concentrations as well as pH changed each rain, probably suggesting a long distance transport of pollutant from Asia continent.
Key words: tritium, sulfur, chemical composition, rain

In Japan the regulation of SO_2 emission put into practice in 1969 to improve air pollution and now atmospheric SO_2 concentration satisfies the environmental quality standard. However an average value of pH in rain is 4.6 in Japan, showing acidification. To examine the origin of air pollutant, we collected rain samples from 1996 and measured the tritium concentrations and the chemical compositions. Tritium concentrations were analyzed with a low back-ground liquid scintillation counter (LBLSC) after electrical enrichment of tritium in rain. The concentrations of cations were determined by atomic absorption method and those of anions by ion chromatography.

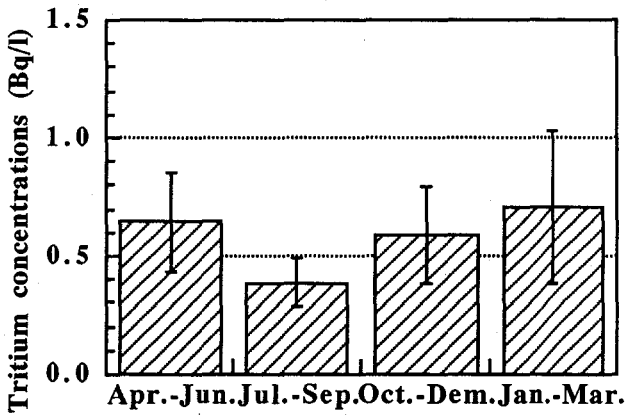

Fig. 1 Average values of tritium concentraions in rain in Fukuoka in 1996-1997

Tritium concentration in rain reached its maximum in early 1960s by atmospheric nuclear tests and has decreased after the Test Ban Treaty in 1963. The annual average value in Fukuoka's rain returned to the natural level after 1988. The recent tritium levels in rain are shown as an average of each quarter in Fig. 1. Tritium levels in rain are low in July-September and high in January-March. Recent rain shows a variation of tritium concentration in relation to meteorological conditions rather than the spring peak which had observed in 1960s and 1970s. High tritium level was observed in rain when Fukuoka was covered by continental air mass while low when covered by ocean air mass. This can be attributed to higher tritium level in Asia continent than ocean.

Fax:+81-92-642-2607, E-mail:momoscc@mbox.nc.kyushu-u.ac.jp

P206
s.51

TRITIUM CONCENTRATION IN OCEAN

H. Kakiuchi[1], N. Momoshima[1*], T. Okai[2], Y. Maeda[1]

[1]Department of Chemistry, Faculty of Science, Kyushu University, Hakozaki, Higashi-ku, Fukuoka 812-81, Japan.
[2]Department of Nuclear Engineering, Faculty of Engineering, Kyushu University, Hakozaki, Higashi-ku, Fukuoka 812-81, Japan.

Summary: Tritium concentrations in air and surface seawater were analyzed over the Pacific and Indian Oceans. Relatively high tritium concentrations were observed on seawater near continents while low those from open sea.
Key words: tritium, the Pacific Ocean, the Indian Ocean

Tritium is a radioactive isotope of hydrogen and its half life is 12.34 years. Most of the tritium in the environment exist as tritiated water and a variation of tritium activity in water can be explained by movement and mixing of water bodies with different tritium levels. In general, tritium concentrations in continental area are relatively higher than that in ocean area owing to slow turn-over rate of water in continent, slow mixing of continental water with seawater.

As a part of a global survey program of the environmental tritium, we have designed to analyze tritium concentration in air and seawater over the Pacific and Indian Oceans. During the R/V Hakuho-maru cruise in 1996, we collected many tritium samples and were shipped to the laboratory for analysis. Tritium in the surface seawater samples were measured with a low-back ground liquid scintillation counter for 1000 min after electrically enriched tritium concentration.

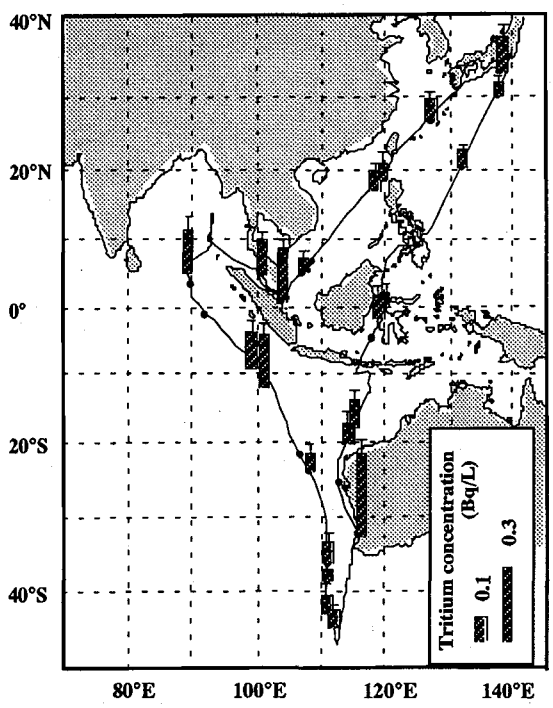

Fig. 1 Tritium concentrations in the surface seawater during the cruise KH-96-5.

The tritium concentrations in the surface seawater is shown in Fig. 1. The distribution of tritium concentrations in seawater samples collected near continent are ranged from 0.2 to 0.4 Bq/L, and most of those from open sea show under 0.1 Bq/L. The tritium level observed in the Pacific and Indian Oceans was lower than that in Japan sea where the tritium concentrations from 0.3 to 1.5 Bq/L have been reported. The relatively high tritium concentrations could be attributed to mixing of continental water with high tritium concentrations.

Fax: +81-92-642-2607, E-mail: momoscc@mbox.nc.kyushu-u.ac.jp

P207
s.51

VARIATION OF ATMOSPHERIC TRITIUM CONCENTRATIONS IN THREE DIFFERENT CHEMICAL FORMS IN FUKUOKA, JAPAN

T. OKAI, N. MOMOSHIMA[1] and Y. TAKASHIMA[2]
Departmemt of Nuclear Engineering, Faculty of Engineering, Kyushu University 33, Hakozaki, Higashi-ku, Fukuoka 812-81 Japan
[1]Department of Chemistry, Faculty of Science, Kyushu University 36, Hakozaki, Higashi-ku, Fukuoka 812-81 Japan
[2]Kyushu Environmental Evaluation Association 1-10-1, Matsukadai, Higashi-ku, Fukuoka 813, Japan

Summary : Tritium concentrations of atmospheric HTO, HT and CH_3T in Fukuoka, Japan are 19.3-23.3, 28.2-48.5 and 11.8-15.6 mBq/m^3-air, respectively. The specific activities (TU) are about 15, $6x10^5$ and $3.3x10^4$ for HTO, HT and CH_3T, repectively.

Key words : Tritium, Atmospheric Tritium, Tritium concentrations, HTO, HT, CH_3T

National Institute of Fusion Science (NIFS) is now constructing a new fusion device and related facilities at Toki city in Gifu prefecture, Japan. Tritium is present in the atmosphere in the three different chemical forms, tritiated water vapor (HTO), tritiated hydrogen (HT) and tritiated hydrocarbons (primarily tritiated methane, CH_3T). Thus, tritium concentrations of atmospheric HTO, HT and CH_3T have been measured on the campus of Kyushu University in Fukuoka Prefecture, Japan from 1984 to the present to establish the general database on behavior of atmospheric tritium before large-scale tritium handling is begun for developing a fusion reactor.

Average monthly HTO concentrations expressed in Bq/L-H_2O vary within ranges of 1.06 to 2.45, giving an overal average value of 1.85 ± 0.078. The minima of the HTO concentrations in each year are all observed in July or August. This is understandable because the Fukuoka area in July and August is covered by an oceanic air mass that has a low tritium level of water vapor, of 0.26-0.50 Bq/L, evaporated from sea water. Atmospheric HTO concentrations expressed in mBq/m^3-air vary within ranges of 7.8 to 46.1. HTO concentration has a strong correlation with the atmospheric humidity, being high in summer and low in winter.

On the contrary, in the case of HT and CH_3T, no seasonal variations were observed with average monthly values of 23.1 to 61.0 mBq/m^3-air and 8.3 to 23.9 mBq/m^3-air, respectively. The present HTO concentration has been already close to the tritium level before nuclear era. However, the present concentartions of HT and CH_3T are still higher by a factor of about 140 and 30, respectively, than those before the tests. The specific activities of these species are 15, $6x10^5$ and $3.3x10^4$ TU for HTO, HT and CH_3T, repectively. The apparent difference in the specific activities suggests very slow transformation of these species in the atmosphere.

FAX : 092 - 642 - 3833
E-mail : okaitne@mbox.nc.kyushu-u.ac.jp

P208
s.52

RAPID DETERMINATION OF Sr-89 AND Sr-90 FOR AQUEOUS SAMPLE BY LIQUID SCINTILLATION SPECTROMETRY

C.W. Lee, M.H. Lee, H.K. Park, D.W. Park, G.S. Choi, K.H. Hong
Korea Atomic Energy Research Institute, P.O. Box 105, Yusung, Taejon, Korea

Summary : The strontium isotopes from aqueous medium were isolated using Sr-Spec™ resin. The isolated Sr-89 and Sr-90 were determined simultaneously by a single liquid scintillation spectrometry.
Key words: strontium, Sr-Spec resin, liquid scintillation spectrometry

In the event of the release to the envronment, the radiologically important nuclides Sr-89 and Sr-90 would have to be monitored as rapidily as possible, in environmental samples such as milk, drinking water. However the standard methods for isolating and measuring Sr-89 and Sr-90 in environmental samples are very laborious and time consuming. Almost all techniques depends on the equilibrium between Sr-90 and its radioactive daughter Y-90. It takes about 2 - 3 weeks to reach the secular equilibrium state after the separation of strontium. Then the yttrium is separated from the equilibrium state to count beta-ray of Y-90 with gas-flow proportional counter. The long chemical separation steps may give rise to analytical uncertainty to the results.

The simple and rapid method for isolating strontium from aqueous medium using Sr-Spec™ resin was described in this paper. The method was based on a preliminary precipitation of the alkaline earths e.g. Ca, Sr, Ba by treating the sample with oxalic acid. Strontium was then isolated from this nitric acid medium by chromatographic separation using strontium selective binding resin(Sr-Spec™) with a suitable nitric acid concentration of mobile phase solution. The pure beta-emitting nuclides Sr-89 and Sr-90 were determined simultaneously in the isolated eluent by a single liquid scintillation measurement. The total spectra of scintillation in a multichannel analyzer was isolated into sub-regions of counts for Y-90, Sr-89, Sr-90 and background. The activities of stromtium were calculated from this spectral analysis of scintillation..

Detection limits of 0.018 Bq for Sr-89 and 0.014 Bq for Sr-90 were obtained in 16 hrs measurement. The method was particulary suited for rapid monitoring of these two isotopes since it was independent of the stage of the Sr-90/Y-90 equilibrium.

cwlee@nanum.Kaeri.re.kr
Fax: 82-42-863-1289

P209
s.51

Determination of Thoron and Radon Activity by Liquid Scintillation Spectrometry

M.Sakama, Y.Oura, K.Kawamura, H.Yoshikawa[1], K.Sueki, and H.Nakahara*
Tokyo Metropolitan University, 1-1 Minami-Ohsawa Hachioji, Tokyo 192-03
[1]Power Research and Nuclear Fuel Development Coorporation, Tokai , Ibaraki 319-11

Summary: A new spectral method is proposed for the determination of ^{220}Rn and ^{222}Rn contents in fumarolic gas using the radon extraction by toluene followed by alpha spectrometry by a LSC/MCA potable counter.
Key words : ^{220}Rn, ^{222}Rn concentrations, fumarolic gas, LSC/MCA portable counter

A new spectral method using a liquid scintillation counter is explored for the determination of the thoron, ^{220}Rn, content in fumarolic gas in the presence of a comparable amount of ^{222}Rn. Radon, an inert gas, is easily soluble in toluene, and this fact allows quantitative analysis of the alpha and beta-emitting nuclides of ^{222}Rn, ^{220}Rn and their daughter nuclides by a liquid scintillation counter. This sampling method of radon by toluene extraction has a great advantage that the initial toluene sample contains only radon and no other daughter nuclides. For an absolute determination of radioactivity, the so-called "integral counting method " is used to correct for the quenching effect. This method is essentially based on an extrapolation of the integral counts observed with various discriminator levels to that expected for the zero discriminator level, and, in practice, the number of events integrated over the whole alpha and beta spectra is read from a scaler,and no spectral information is used. Therefore, for the direct determinations of ^{220}Rn in gas samples by the integral counting method, in which ^{222}Rn and its daughters are inevitably present, decay analysis of the observed counts has to be applied to obtain the 55s component of the radioactivity due to ^{220}Rn and its daughters. The problem involved in such a decay analysis is that ^{218}Po which builds up from the parent nuclide of ^{222}Rn obscures the decay of the 55 s component. Therefore, if the activity ratio of thoron to radon is close to unity or less than unity, an observation of the 55 s component becomes extremely difficult since an actual counting begins only,at best, 3 min after the sampling.

The aim of the present work is to investigate a new alpha spectrometric method for the determination of the ^{220}Rn content in fumarolic gas by use of a portable liquid scintillation counter equipped with a function of MCA, and also to develop an automatic radon sampling and extraction method which allows shortening the time required before starting the counting. The alpha spectrometric method is essentially based on the following procedure. On the alpha-ray spectrum observed by a portable LSC/MCA analyzer brought to the sampling site, the ROI is so set on the alpha peaks of ^{220}Rn(6.29MeV) and ^{216}Po(6.78 MeV) that the least number of alpha counts due to ^{222}Rn(5.49 MeV) and ^{218}Po(6.00 MeV) are included as depicted in the figure as an example. Then, the decay of the counts in the ROI are followed and submitted later to the decay analysis for evaluation of the 55 s component. The problems inherent to this method are that (1) the alpha counts of ^{220}Rn are usually too few to form an alpha peak and that (2) the alpha spectrum is sensitively affected by the quenching effect. In the symposium, several attempts to overcome those problems will be discussed and the ^{220}Rn detection limit of this spectral method under the presence of ^{222}Rn and its precision and accuracy will be shown. Some preliminary results of the automatic sampling and solvent extraction method will also be presented.

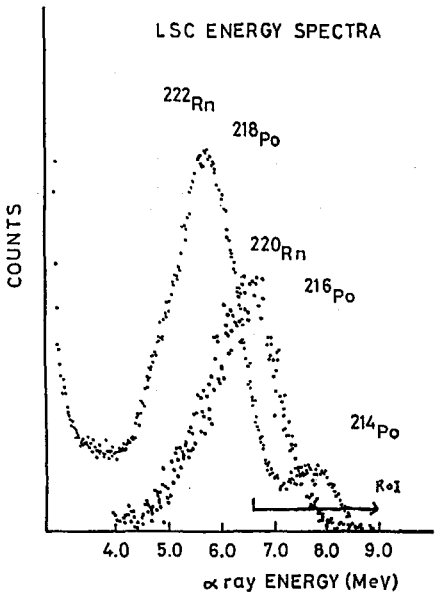

Fig. LSC Energy spectra of ^{222}Rn and ^{220}Rn with their daughter nuclides.

Fax:+81-426-77-2525, E-mail: nakahara-hiromichi@c.metro-u.ac.jp

P210 s.51 CALIBRATION OF LIQUID SCINTILLATION COUNTER FOR MEASURING LOW-LEVEL CONCENTRATION OF RADON IN WATER SAMPLE

M. N. Al-Haddad, I. Al-Jabri, M. A. Islam

Energy Research Laboratory. Research Institute. King Fahd University of Petroleum and Minerals. Dhahran 31261, Saudi Arabia.

Summary : Liquid Scintillation Counter (LSC) has been calibrated to measure low-level concentrations of radon gas in water samples in order to check the compliance of local groundwater with the recommended USEPA limit of 11,100 Bq m^{-3}

Key words : LSC, calibration, radon, water, LLD, water-to-flour ratio, Saudi Arabia, Al-Hassa

The purpose of this work is to calibrate the liquid scintillation counter model LKB-Wallac 1217 RackBeta available at the Energy Research Laboratory to measure low-level concentrations of radon gas in water samples in order to check the compliance of local groundwater with the recommended level. Important counting parameters such as water-to-fluor ratio, counting window, lower limit of detection, and calibration factor have been investigated and optimized. The water-to-flour ratio has been investigated using various water-to-fluor ratio with a fixed amount of tritium standard activity. The optimum water-to-fluor ratio is obtained at 4:15. A set of radon standard sources covering various radon activities were prepared using a weighted amount of a tracable radium-226 standard solution made by Amersham Laboratories. The prepared set of standards have been measured daily for 40 days to allow the radon and radon daughters to equilibrate with dissolved radium. The calibration factor of the LSC was then found to be 875 ± 6 Bq m^{-3}/cpm. The growth curve of the highest radon activity standard is obtained. The spectrum of the highest radon activity standard is plotted as count rate versus 0-256 channel number (energy) with an increment of eight channels. The spectrum shows clear peaks fall between the endpoint of the unquenched ^{14}C and ^{32}P beta spectra (0.156 -1.71 MeV) as shown in the Figure. The lower limit of detection was obtained for full and optimized window and found to be 3,848 and 2,600 Bq m^{-3} for 1-hour counting at a 99.9% confidence level, respectively.

The radon concentration in groundwater samples from Al-Hassa oasis of Saudi Arabia have been examined. The results show that the radon concentration varies from below the detection limit to a maximum of 13,264 Bq m^{-3}.

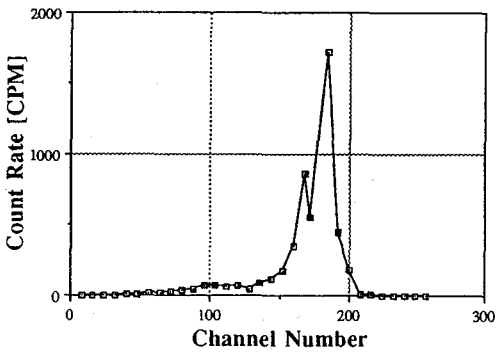

Radium/Radon spectrum using LSC

Fax : +00 966 3 860 4281 E-mail : meyassar @ dpc.kfupm.edu.sa

P211
s.51

A RADON MEASUREMENT SYSTEM FOR STANDARDIZATION

J. M. LEE, T. S. PARK AND P. J. OH

Korea Research Institute of Standards and Science, 1 Doryong-dong, Yusong-gu, Taejon 305-600, Korea

Summary :
Key words:

A radon measurement system based on two pulse ionization chambers for standardization in Korea has been developed at KRISS. The system consists of a radon generator, a gas handling and purification system, and a multichannel acquisition system. Radon gas following radium decay is separated by bubbling radium solution with ionization gas, N2. Water vapour and other impurities in radon gas are removed during passing through purification system which consists of traps and furnaces. Radon gas transfered into pulse ionization chamber decays radiating alpha particles which are measured by multichannel acquisition system. Filled gas can be evacuated immediately if necessary. The whole gas handling system except for radon generation part was constructed with stainless steel pipe and vacuum valves. The generation of radon gas from radium tested successfully, and transfering to background and alpha particle from radon decay were obtained with two pulse ionization chambers.

Some parameters and characteristics of the radon measurement system will be given, and alpha particle spectra aquisited with pulse ionization chambers will be shown.

Fax: +82-42-868-5042, E-mail: jmlee@krissol.kriss.re.kr

P212
s.51

FISSION TRACK METHOD IN THE INVESTIGATION OF NATURAL RADIOACTIVITY OF SOME GEOLOGICAL SAMPLES

B. S. BAJWA AND H. S. VIRK

Department of Physics, Guru Nanak Dev University, Amritsar - 143005, India

Summary :
Key words :

Uranium, thorium and their daughters are significant sources of natural radioactivity in the environment. They may constitute health hazard effects, if their concentration is considerably high enough.

The results of radioactivity of some rocks and fossil bones samples collected from Siwalok Himalayas of India, are reported. Uranium concentration in these samples are estimated through the Fission Track Techniques using Solid State Nuclear Track detectors (SSNTDS).

The qualitative analysis of fission track radiographs of some radioactive fossil bones has been came out, which indicated the inhamogeneous distribution of uranium, dependent upon the matrix of fossil bones.

Fax: 091-0183-258820, E-mail: pcse@gndu.ernet.in

P213
s.51

MICROANALYSIS OF URANIUM IN INDIAN WATER SAMPLES USING U(n,f) REACTION

PADAM SINGH, M. MUJAHID, A.H. NAQVI AND D.S.SRIVASTAVA*

Department of Applied Physics, Z.H. College of Engineering & Technology, Aligarh Muslim University, Aligarh 202 002 (INDIA)

Summary: Trace quantities of uranium in water samples are determined using U(n,f) reaction and detecting the resulting fission fragments by plastic track detectors. The average U-content in water samples collected from different sources in the cities of Allahabad, Jhansi, Kanpur, Ghaziabad, Agra and Aligarh are 2.14 μg/l, 3.25 μg/l, 4.71 μg/l, 7.31μg/l, 14.62 μg/l, 13.27 μg/l respectively.

Key words: Trace quantities, U(n,f) reaction, Plastic detector.

Abstract: The concentration of uranium in water plays a significant role to enhance the radiation level in human beings. The radionuclides enter the human body mainly through food and drinking water. A concentration of uranium beyond 10 pci/l (or 14.92 μg/l) is true carcinogenic (Lappenbusch, 1979), however the maximum permissible quarterly intake of natural uranium (in soluble form) has been set at 1.2 μg/l (Morgan, 1986). This amounts to an oral intake of 19.85 mg of uranium per day beyond which damaging effects in human kidney may appear. The reported data will help the environmental protection agencies to set radioactive standards for human population to survive safely from unduly high exposures of radiation due to uranium at certain places.

The U-content level in 111 water samples collected from hand pumps, jet pumps and rivers in six different cities of Uttar Pradesh (India) was found to vary from location to location and city to city. The average value of U-content in water samples of these cities are shown in the given table

TABLE: U-CONTENT LEVEL IN INDIAN WATER SAMPLES

S.No.	Name of City	Range of U-content μg/l	Mean value μg/l
1.	Agra	4.300.01-31.780.07	14.62
2.	Ghaziabad	3.040.05-11.360.33	7.31
3.	Kanpur	2.560.08 - 9.080.10	4.71
4.	Jhansi	0.870.01- 6.450.19	3.25
5.	Allahabad	0.920.01- 3.790.15	2.14
6.	Aligarh	.070.25-20.490.27	13.27

*Author for correspondence
E-mail chairap@amu.nic.in
Univ. Telex 564-230 AMU in

P214
s.51

SETTLING VELOCITY OF PARTICLES BEARING PLUTONIUM IN THE PACIFIC WATER COLUMN

M. A. Haque[1] and T. Nakanishi[2]*
[1]*Graduate School of Natural Science and Technology*
[2]*Department of Chemistry, Faculty of Science*
Kanazawa University, Kakuma-machi, Kanazawa, Ishikawa 920-11, Japan

Summary : To estimate the mean settling velocity of particles which transport and remove Pu from seawater to depositional sinks, two different models were applied to the measured results of Pu inventories in water and sediment columns in the North Pacific.
Key words: ^{239,240}Pu, seawater, deep-sea sediment, settling particles, settling velocity

To estimate the mean settling velocity of particles which transport Pu from seawater to depositional sinks, inventories of ^{239,240}Pu in water and sediment columns have been measured at 6 stations in the North Pacific as of 1988, and two different models (model-1 and -2) were applied to the measured results. Model-1 is based on the following assumptions: (1-1) the total amount of ^{239,240}Pu which fell during 1945-1980's can be assumed to be delivered instantaneously onto the earth's surface in 1963 when the maximum of annual deposition of the nuclides was observed worldwide, (1-2) most of the nuclides delivered to the surface of the ocean has been trapped at the sub-surface layer, (1-3) since 1963, the nuclides in the sub-surface seawater have been scavenged at a constant distribution ratio by particles which settle to seabed at a constant flux (hence, the decrease of ^{239,240}Pu inventory in water column has followed first-order kinetics). On the other hand, model-2 is based on the following assumptions: (2-1) the delivery of fallout ^{239,240}Pu to the sea area and land surface at comparable latitude were same, and the data set of annual ^{239,240}Pu deposition measured in Japan is applicable to the North Pacific, (2-2) each annual deposition can be treated as an instantaneous annual injection and (2-3) ^{239,240}Pu delivered to the oceans equilibrated rapidly to the environment and associated with particles to follow successive settling through water column at finite velocity.

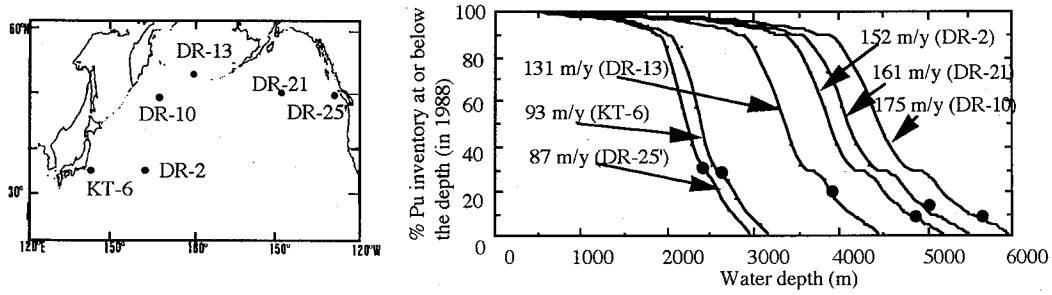

Fig.1 The fraction of "^{239,240}Pu inventory in water and sediment columns below given depth of water column" to "total ^{239,240}Pu inventory in water and sediment columns" in the North Pacific as of 1988. Closed circles represent the fractions found in the sediments. Solid curves represent the fractions calculated according to the model-2 in which settling velocities indicated in the figure are assumed.

The estimated mean settling velocities of particles which carry down ^{239,240}Pu in the water columns of the North Pacific were in a range from 97 to 217 m y^{-1} by model-1, and 87 to 175 m y^{-1} by model-2 (Fig.1). The good agreement between results by two models suggests that the simplifying assumptions for the models were made without leading to serious errors, but the calculation according to the model-2 cannot reproduce the actual depth profile of ^{239,240}Pu in the Pacific. Mean diameter of these particles was then estimated from the value of mean settling velocity to be in a range from 3.6 to 7.2 μm by assuming an appropriate values for densities of seawater and settling particles and for viscosity of seawater. The mean diameter was found to increase with the increase of depth of water column, and this suggests a size growth of settling particles in deeper layers.

Fax: +81-76-264-5742, E-mail: nakanisi@cacheibm.s.kanazawa-u.ac.jp

P215
s.51

SR ISOTOPE RATIOS AND REE ABUNDANCES IN SILICEOUS SEDIMENTARY ROCKS FROM SOUTHWEST JAPAN: TRACERS INDICATING CHANGE OF THEIR SOURCES AND DEPOSITIONAL ENVIRONMENTS FROM THE PERMIAN TO THE TRIASSIC.

T.Kunimaru [1,3], H. Shimizu [1,2], K. Takahashi [3] and S. Yabuki [3]
1 Department of Environmental Science, Graduate School of Science and Technology, Kumamoto University, Kumamoto 860, Japan.
2 Department of Environmental Science, Faculty of Science, Kumamoto University; Kumamoto 860, Japan.
3 The Institute of Physical and Chemical Research, Saitama 351-01, Japan.

Summary: Sr isotopic ratios, REE abundances and major element compositions were reported for the Permian and Triassic cherts from the Southwest Japan. The nature of their sources and depositional environment of these cherts and their change from the Permian to the Triassic were discussed.
Key words: Sr isotopic ratio, REE abundances, chert, Permian, Triassic

Sr isotopic ratios, REE abundances and major element compositions were reported for the Permian and Triassic cherts from Kuma and Saiki areas in the Southern Chichibu (Sambosan) terrane, the Outer Zone of Southwest Japan, in order to elucidate the nature of sources, depositional environment and their change from the Permian to the Triassic.

Higher contribution of detrital components for the Triassic Sambosan cherts than for the Permian Sambosan cherts is suggested by Ce-anomaly degree in REE pattern, MnO/TiO_2 ratio and initial $^{87}Sr/^{86}Sr$ ratio of these cherts. Small negative Ce anomalies ($Ce/Ce^* = 0.75$-0.95) are observed for the Permian cherts from both Kuma and Saiki areas, in contrast to small positive Ce anomalies ($Ce/Ce^* = 1.1$-1.3) for the Triassic cherts from the both areas. It should be noted that the Sambosan cherts show neither large negative Ce anomalies ($Ce/Ce^* = 0.2$-0.5) observed for deep-sea cherts nor large variation in Ce anomalies ($Ce/Ce^* = 0.3$-1.5) observed for cherts from the Franciscan terrane, California. MnO/TiO_2 ratios are larger than 0.5 for the most of the Permian Kuma cherts and the early Permian Saiki cherts, while the ratios are smaller than 0.5 for the Triassic Kuma cherts and late Permian and Triassic cherts from the Saiki area. Initial $^{87}Sr/^{86}Sr$ ratios for the Permian Saiki cherts are 0.706-0.707 and are slightly lower than those for the Triassic Kuma cherts (0.707-0.709). These $^{87}Sr/^{86}Sr$ ratios for the Permian and Triassic Sambosan cherts are close to the coeval marine $^{87}Sr/^{86}Sr$ ratios (Burke et al., 1982) and are clearly lower than that for cherts from the Mino terrane (0.713), Inner Zone of Southwest Japan (Shibata and Mizutani, 1982).

Our geochemical and isotopic data of the Sambosan cherts suggest the change of depositional environments from more or less ocean-basin floor feature at Permian to less pelagic one at Triassic, although geochemical features showing deposition at typical deep-ocean floor are not observed even for the Permian cherts. The following depositional environments are suggested. (1) The late Permian Kuma cherts and the early Permian Saiki cherts were deposited between continental margin and ocean-basin floor or deposited at the location ranging from continental margin to ocean-basin floor. (2) The Triassic cherts from Kuma and Saiki areas and the middle and late Permian Saiki cherts were deposited at marginal sea or continental shelf and slope. (3) The Permian and Triassic Sambosan cherts were deposited at more open-ocean environment than the Triassic cherts in the Mino terrane.

FAX: +81-96-342-3419
E-mail ADRESS: kunimaru@sci.kumamoto-u.ac.jp

P216 s.52 PROMPT GAMMA-RAY ANALYSIS OF METEORITE SAMPLES, WITH SPECIAL REFERENCE TO Si

Sk. A. Latif,[1] Y. Oura,[1] M. Ebihara*,[1] H. Nakahara,[1] C. Yonezawa,[2] T. Matsue,[2] and H. Sawahata[2]

[1]*Department of Chemistry, Faculty of Science, Tokyo Metropolitan University, Hachioji, Tokyo 192-03, Japan*
[2]*Department of Chemistry and Fuel Research, Tokai Research Establishment, JAERI, Tokai, Ibaraki 319-11, Japan*

"Summary: Prompt gamma-ray analysis (PGA) was used to determine Si and other elements (e.g. , H, B, S) in meteorite samples. PGA has high sensitivities for these elements compared to other conventional methods."

"Keywords: Neutron-induced PGA, meteorite samples, Si, mono-standard"

Neutron-induced prompt gamma-ray analysis (PGA) was applied to several meteorite samples (Allende, Zagami, Acfer 209, ALH 77005, ALH 84001, EETA 790001 and Neagari). Both thermal neutron and cold neutron guided beams of JRR-3M were used. In this study, we are concerned with the determination of Si because Si can't be reliably determined by non-destructive NAA. Silicon was determined in two different ways: the comparison method using a Si reference, and the mono-standard method. In the latter case, Fe is used as a reference element. The Si values determined by these two ways are consistent within 6.8%. In addition to Si, H, B, Na, Mg, Al, S, Ca, Ti, V, Mn, Fe, Sm and Gd were determined. Among these elements, few data have been reported in the literature for H, B and S in meteorites. The analytical sensitivity of Si using the cold neutron guided beam is 12.24 times higher than that for the thermal neutron guided beam. Our data for Si in Allende meteorite reference sample (average:16%) are consistent with the recommended value in the literature (16.02%).

Fax: +81-426-77-2525
e-mail: ebihara-mitsuru@c.metro-u.ac.jp

P217
s.52

DETERMINATION OF IMPURITIES IN GRAPHITE BY NEUTRON GENERATOR ACTIVATION ANALYSIS

S.A.Makarov and A.V.Andreev

State Institute for Rare Metals, National Scientific Center "GIREDMET"
Bol.Tolmachevsky per.5, Moscow, 109017, Russia

Summary: The neutron activation analysis using a neutron generator (NGAA) was applied for impurity determination in pure materials with activation by 3 and 14 MeV and moderated neutrons and gamma activity registration by high efficiency HPGe detector.
Key words: activation analysis, neutron generator, polyethylene moderator, nuclides, impurity.

Instrumental neutron activation analysis using thermal and fast neutrons of the neutron generator was applied to determine light and others elements in pure graphite at the ppm level. Compact samples of mass 5 – 10 g and reference standards prepared from high–purity powdered materials were irradiated at a "SAMES" T-400 modernized neutron generator with 3 and 14 MeV and thermal (slowed down) nominal neutron flux densities of $6 \cdot 10^8$, $5 \cdot 10^{10}$, $3 \cdot 10^7$ neutr/cm^{2}s, respectively. The slowed down neutrons were produced by polyethylene moderator with a lead–beryllium converter of 14 MeV neutrons. Irradiation times were chosen from seconds (short-lived nuclides) up to hours (long-lived nuclides). A fast pneumatic transport system was used for short-lived nuclides. A monitor standardization technique for long-lived nuclides was proposed. Standard yields of analytical γ-lines were measured using monitors (Al, Ni, Mn) of neutron flux. The accuracy of these measurements (about 10 for each γ-line) was 5 % rel. The samples activity was measured by a 45 % HPGe ("PGT") or NaJ(Tl) ("Harshaw") and "Ortec" spectrometric systems. The design and equipment of the activation analysis installation are described. The three irradiation modes enabled us to correct account for interferences using different nuclides for element determination. Data processing was performed using IN-96 and IN-120 ("Intertechnique") multichannel analyzers and a computer utilizing the softwere developed by our group. One of the main goals of this work was to evaluate the potentialities of neutrons with different energies in determining impurities at ppm level and less. Due to the absence of matrix effect interferences such an object of analysis as graphite can show the potentialities of NGAA for determining trace elements. In specific cases the cyclic activation and measurement are feasible. The sensitivities of O, F, Na, Mg, Al, Si, Cl, Ar, Ca, Sc, Ti, Fe, Ni, Zr, Nb, Au determination of below 1 ppm are achieved. The error of the results of analysis at ppm level was 20 % rel. The examples of results of analysis and the sensitivities of various element determination in graphite are presented.

Fax : (7 095) 247 2317
E-mail: smak@inrran.msk.su

P218
s.52

NEUTRON GENERATOR ACTIVATION ANALYSIS (NGAA) FOR HIGH–PRECISE AND HIGH–SENSITIVE ELEMENT DETERMINATION

A.V.Andreev and S.A.Makarov.

State Institute for Rare Metals, National Scientific Center "GIREDMET"
Bol.Tolmachevsky per.5, Moscow, 109017, Russia

Summary: Instrumental neutron activation analysis using three types of neutrons (3 and 14 MeV and thermal) was applied for the whole sample determination of the impurities with the sensibility below 1 ppm and component macroconcentrations with total error 0,5-2,0 % rel.
Key words: activation analysis, neutron generator, component, impurity, precise analysis.

The neutron activation analysis using a neutron generator (NGAA) is conventionally associated with 14 MeV neutrons (dt–neutrons). However, this compact accelerator — generator of neutrons can be used efficiently as a universal radiation source in the material analysis. The possibilities and advantages of neutrons of various energies were studied using a modernized T-400 "SAMES" neutron generator. The three types of neutrons were produced: dt–neutrons ($\varphi = 1–4\cdot10^{10}$ n/cm^{2}s), dd-neutrons ($\varphi = 5–7\cdot10^{8}$ n/cm^{2}s) and slowed down dt-neutrons ($\varphi = 3–5\cdot10^{7}$ n/cm^{2}s) to be used in activation analysis techniques both for impurity determination at ppm level and high-precision determination of components.

One of the key problems of the techniques elaboration is the investigation and correct accounting of all possible sources of the systematic errors. They arise due to the self–absorption of γ–ray emission in sample material, self–screening of neutron flux, gradient of neutron flux density at the neutron generator, interferences of γ–lines, and other effects. The ways to determine correction factors and to eliminate errors are described. A procedure for calculating the general error of results of analysis is proposed.

The main NGAA results are presented for different materials. The concentration range of elements determination was equal to $n\cdot10^{-6}$ up to 100 % mass. The techniques of high-precision determination of macroconcentrations (> 5 % mass.) with a precision 0,5-2.0 % rel. are described. Furthermore, the data on various element determination (B, N, O, F, Na, Mg, Al, Si, P, Cl, Ar, K, Ca, Sc, Ti, V, Mn, Fe,Co, Ni, Cu, Zn, Ga, As, Se, Br, Sr, Y, Zr, Nb, Mo, Ru, Rh, Pd, Ag, In, Sn, Te, J, Ba, La, Ce, Pr, Nd, Sm, Eu, Gd, Er, W, Re, Ir, Pt, Au, Hg, Tl, Pb) are presented in the whole concentration range.

Fax : (7 095 247 2317
E-mail : andreev@inrran.msk.su

P219
s.52

EPITHERMAL NEUTRON ACTIVATION ANALYSIS AT IBR-2 PULSED FAST REACTOR AT DUBNA FOR STUDYING THE ENVIRONMENT

M. V. FRONTASYEVA

Joint Institute for Nuclear Research, Frank Laboratory of Nuclear Physics, 141980 Dubna, Moscow Region, Russia

Summary :
Key words:

Epithermal neutron activation analysis (ENAA) has certain advantages over the conventional instrumental neutron activation analysis (INAA) for many trace elements in terms of improvement in precision and lowering of detection limits. INAA has shown to be useful for a number of sample types of interest in environmental studies, and should find more extensive use in this area. Experience in the use of ENAA at IBR-2 pulsed fast reactor at Dubna (Russia) for monitoring the environment is summarized. It is shown that the analysis of airborne particulate matter is a case where ENAA should be particularly useful. A similar case where ENAA has shown strong performance is in the analysis of mosses used as biomonitors of atmospheric deposition, where 45 elements were determined. In this and other cases, however, induction-coupled plasma mass spectrometry is a very strong competitor, offering data for even more elements. A comparison of INAA and ICP-MS for moss analysis is presented, and cases where INAA is unique are discussed.

Fax: 7(09621)65085, E-mail: marina@nf.jinr.ru

P220
s.52

PROMPT GAMMA RAY ANALYSIS OF ARCHAEOLOGICAL BRONZE

Y. Oura[1], K. Sueki[1], H. Nakahara[1], T. Tomizawa[2], and T.Nishikawa[3]

[1]*Graduate School of Science, Tokyo Metropolitan University.*
1-1 Minami-Ohsawa, Hachioji-shi, Tokyo 192-03, Japan.
[2]*Faculty of Literature, Keio University.*
2-15-45 Mita, Minato-ku, Tokyo 108, Japan.
[3]*Osaka board of education*
Ohtemae, Cyuo-ku, Osaka 540, Japan.

Summary: Prompt gamma ray analysis using the internal monostandard method was applied to bronze samples. Sn/Cu content ratio was found nondestructvely determined by this method down to the level of a few hundredths.
Key words: prompt gamma ray analysis, internal monostanadard method, archaeology, bronze

We have developed an internal monostandard method of the prompt γ-ray neutron activation analysis (PGAA) which is applicable to voluminous samples[1)], and analyzed major element concentration ratios of Mn, K, Na, Ti, Fe, Al, and Ca to Si and minor ones of B, Sm, and Gd to Si in archaeological pottery bowls as a practical application. Then, the prompt gamma ray analysis using the internal monostandard method has proved very useful to classify the pottery bowls. In this article the application of PGAA to archaeological bronze samples is reported. The archaeological bronze consists mainly of Cu, Sn, and Pb, whose concentrations differ among the samples of different production era and area.

The experiments were performed using the prompt γ-ray analyzing system attached to the thermal neutron guide tube of JRR-3M, at the Japan Atomic Energy Research Institute. As samples, eleven bronze blocks whose Cu and Sn concentrations are known were selected and irradiated with thermal neutron beam for about 5000 sec. Data analysis was carried out as described in our previous report[1)].

Most of the observed prompt γ-rays in the whole energy region could be assigned to Cu with a few γ-rays from Sn. No γ-ray from Pb was observed. The content ratios of Sn to Cu were calculated by using $\sigma_{Sn}b_{Sn}/\sigma_{Cu}b_{Cu}$ values (shown in Table) obtained from the standard sample prepared with a known amount of CuO and SnO. The Sn/Cu values obtained by the present method were in agreement with the known values, and this analytical method was found applicable to the bronze with the Sn/Cu content ratio even down to a few hundredths. We plan to analyze Sn/Cu ratios in archaeological bronze mirrors (dokyo), by this analytical method.

Table. Selected γ ray energies and measured ratios ($\sigma_{Sn}b_{Sn}/\sigma_{Cu}b_{Cu}$) using thermal neutrons.

element	energy[keV]	$\sigma_{Sn}b_{Sn}/\sigma_{Cu}b_{Cu}$
Sn	1171.3	0.118 ± 0.002
	1293.3	0.179 ± 0.003

The γ ray energy selected for Cu was 278.2 keV.
σ : neutron capture cross section.
b: number of photons emitted per neutron capture.

Reference: 1) K.Sueki et al., Anal. Sci. **68**, 2203 (1996).

Fax: +81-426-77-2548, E-mail: oura-yasuji@c.metro-u.ac.jp

P221
s.52

VERTICAL DISTRIBUTION OF ELEMENTS IN NON-POLLUTED ESTUARINE SEDIMENTS DETERMINED BY NEUTRON INDUCED PROMPT GAMMA-RAY AND INSTRUMENTAL NEUTRON ACTIVATON ANALYSES

A. Kuno[1], K. Sampei[1], M. Matsuo[1]*, C. Yonezawa[2], H. Matsue[2] and H. Sawahata[3]
[1]*Graduate School of Arts and Sciences, The University of Tokyo, 3-8-1 Komaba, Meguro, Tokyo 153, Japan*
[2]*Japan Atomic Energy Research Institute, Tokai-mura, Ibaraki 319-11, Japan*
[3]*Research Centre for Nuclear Science and Technology, The University of Tokyo, Tokai-mura, Ibaraki 319-11, Japan*

Summary: Neutron induced prompt gamma-ray analysis (PGA) and instrumental neutron activation analysis (INAA) have been applied to the sediments collected from the Yasaka River estuary in Oita Prefecture, Japan, in order to investigate the vertical distribution of elements.
Keywords: PGA, INAA, estuarine sediments, vertical distribution, the Yasaka River

Environmental monitoring of estuarine areas receives much attention in these days. The authors have already studied the distribution of elements in urban estuarine sediments collected from the Tama River in Tokyo, Japan, by neutron induced prompt gamma-ray analysis (PGA) and instrumental neutron activation analysis (INAA). Although several elements such as Cd were considered to be enriched by human activities, the natural contents of the elements in non-polluted estuarine sediments must be estimated to discuss the anthropogenic contribution. In this study, PGA and INAA have been applied to the sediments collected from the Yasaka River estuary in Oita Prefecture, Japan (Fig. 1). The river is one of the cleanest rivers in Japan and its estuary is known for one of limited places where spawns a horseshoe crab, which is designated as a natural treasure.

Fig. 1. Sampling location.

The sediment cores of approximately 50 cm in length were collected at two stations in the estuarine area. Each of them was subsampled at every 3 cm length, air-dried for more than 2 weeks, and then ground into powder. For detection of B, Cd, Gd, H, S and Si, samples were irradiated with cold guided neutrons of JRR-3M in the Japan Atomic Energy Research Institute, and prompt gamma-rays were counted for 3600 seconds. For detection of Al, As, Au, Ba, Br, Ca, Ce, Cl, Co, Cr, Cs, Eu, Fe, Hf, K, La, Lu, Mg, Mn, Na, Nd, Rb, Sb, Sc, Sm, Ta, Th, Ti, V, W, Yb and Zn, samples were irradiated in the reactor at the Institute for Atomic Energy, Rikkyo University, and gamma-rays were counted after cooling. Three different conditions of irradiation and cooling were applied depending on the half-lives of the resulting nuclides.

The vertical profiles of many elements in the Yasaka River estuarine sediments were more fluctuated than those in the Tama River estuarine sediments probably because of higher biological activity and/or higher sedimentation rate in the Yasaka River estuary. On the other hand, the S content in the Yasaka River estuarine sediments increased with increasing depth, which was the same trend as that in the Tama River estuarine sediments. However, the Cd content in the Yasaka River estuarine sediments was lower than the detection limit of PGA (0.5 ppm) throughout the cores, while Cd in the Tama River estuarine sediments was highly concentrated in the deeper layer where sulphate ion is reduced to hydrogen sulphide. This fact indicates that Cd content in estuarine sediments is affected by human activities and sulphate reduction. The Cd content in estuarine sediments would be a good environmental indicator because it is easily detectable due to accumulation as sulphides.

Fax: +81-3-3485-2904
E-mail: cmatsuo@komaba.ecc.u-tokyo.ac.jp

P222
s.52

NEUTRON AND PHOTON ACTIVATION ANALYSES OF GEOCHEMICAL AND PLANT SAMPLES — EFFECTS OF INTERFERING NUCLEAR REACTIONS —

Y. Miyamoto[1], A. Kajikawa[2], H. Haba[1], K. Masumoto[3], T. Nakanishi[2] and K. Sakamoto[2]

[1]*Division of Physical Sciences, Graduate School of Natural Science and Technology, Kanazawa University, Kanazawa 920-11, JAPAN*

[2]*Department of Chemistry, Faculty of Science, Kanazawa University, Kanazawa 920-11, JAPAN*

[3]*KEK (Tanashi), Tanashi, Tokyo 188, JAPAN*

Summary: Geochemical reference rocks and plant (spices and pulses) samples were determined for up to 40 elements by NAA and PAA. Contribution from interfering nuclear reactions were not negligible for the analytical results, for which the correction methods are proposed.
Key words: NAA, PAA, interference, spices, pulses, reference rock

Geochemical reference rock (15 GSJ and 6 KIGAM) samples and plant samples (15 spices and 12 pulses of various origins) were determined for up to 40 elements by INAA and IPAA by cross-checking with use of two reactor sites of different neutron spectra (the thermal-column connected by a pneumatic tube (TC-pn) and at a core site connected by a pneumatic tube #2 (pn-2) of Kyoto University Research Reactor (KURR)), electron LINAC (uncollimated bremsstrahlung beam of maximum end-point energy of 30 MeV from the electron LINAC of Kyoto University Research Reactor Institute (KURRI)) and ICP-MS (SEIKO SPQ-9000, Kanazawa University). Three geochemical reference rocks issued from GSJ and three biological reference samples were used for the reference standards. The spice and pulse samples were crushed, ground and sieved under foreign contamination-free condition. Some high-pure reagents were also neutron- and photon-irradiated together with the samples to correct the contribution of the interferences in activation analysis (AA).

The analytical results of the plant samples irradiated at TC-pn, pn-2 and LINAC were in good agreement with each other except for Mg and Fe. In case of rock samples, the results of Na, Al and Mn from TC-pn and LINAC irradiation agreed well with each other, but the analytical results for some elements from pn-2 were appreciably higher than those from TC-pn and LINAC due to the interfering nuclear reactions, (n, α) and (n, p) reactions. In Na determination, contributions from the interferences were not negligible for samples of Na/Al (weight) ratios more than 2.5. In case of PAA, the products of (n, γ) reaction induced by the secondary neutrons contributed to the analytical results seriously. The analytical results for Mg in the rock samples of Na/Mg ratio less than 1.1 and those for Fe in the samples of Mn/Fe ratio less 0.04 were found to be obtainable by subtracting the contributions of the interferences with use of NaCl and MnO reagents, respectively, in the same irradiation. The Mg and Fe in the plant samples, however, could not be corrected for the respective interferences due to their high ratios of Na/Mg and Mn/Fe. Wrapping the samples with a Cd-foil (1 mm thick) was effective to reduce the interferences, and Mg in the plant samples became to be analyzed. The results from ICP-MS are added to check the AA results and also to increase the analytical results.

PHONE : +81-76-264-5691, FAX : +81-76-264-5742,
E-mail : yutakam@kenroku.ipc.kanazawa-u.ac.jp

P223
s.52

LOSSES TO THE ELEMENTS IN PLANT SAMPLES UNDER THE DRY ASHING PROCESS

T. Aoki[1], S. Koh[2], and Y. Katayama[2]
[1]*Radioisotope Research Center, Kyoto University, Sakyo, Kyoto 606-01, Japan*
[2]*Graduate School of Agriculture, Kyoto University, Sakyo, Kyoto 606-01, Japan*

Summary: Losses to the elements occurring in plant samples when they are subjected to the dry ashing process were investigated. The amounts of elements which remained after heating were determined by instrumental neutron activation analysis (INAA).
Key words: plant, pretreatment, dry ashing, element loss, INAA.

Ashing is used in order to detect low levels of trace elements in plant samples. Dry ashing in particular has been used because of its simplicity and low rate of contamination. However, there is some loss to the elements due to volatilization during the dry ashing process.

In this work, losses to the elements occurring in plant samples when they are subjected to the dry ashing process were investigated. Plant samples obtained from (1) the stems of sugi (*Cryptomeria japonica* D. Don) and hinoki (*Chamaecyparis obtusa* Endl); (2) the leaves of matebashii (*Lithocarpus edulis* Nakai), sakura (*Prunus virginia* Linn. var. demissa Torr.), sugi, and hinoki; and (3) a seitaka-awadachi-sou (*Solidago Altissima* L.) plant were used. Standard reference materials (apple leaves (NIST), peach leaves (NIST), and pepperbush leaves (NIES)) were also used. The samples were heated to different temperatures (range 105°C-600°C) in an electric furnace and some samples were also heated at constant temperatures (350°C and 450°C). The amounts of elements which remained after heating were determined by instrumental neutron activation analysis (INAA).

Amounts of Cl and Br in the samples taken from the sugi and hinoki stems decreased steeply over the range 105°C to 400°C (Fig.1). But over half the amounts of these elements remained in the sakura leaves and the standard reference samples (apple leaves and peach leaves), even at 600°C. Amounts of Al in the samples taken from the hinoki and sugi stems decreased over the range 350°C to 600°C. Almost no losses to K and Rb were observed in the range 400°C to 600°C. The amount of Na increased over the range 450°C to 600°C, possibly because of contamination from the porcelain crucibles that the samples were heated in. No changes in the amounts of alkaline earth elements (Ca, Sr, Ba) were observed. Amounts of other elements (La, Sm, Mn, Fe, Co, Cu, Zn, Sb) in the samples remained almost constant over the range 105°C to 600°C. The element concentrations in the the samples taken from stem of a hinoki are shown in Fig. 2.

The dry ashing method using porcelain crucibles is suitable for analyzing most elements in plant samples, but great losses to the amounts of Cl and Br, and the possible contamination of Na from the porcelain crucibles has to be taken into consideration in the case of these elements.

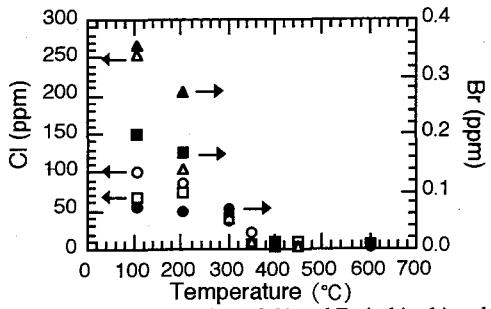

Fig. 1. Concentration of Cl and Br in hinoki and sugi stem samples after dry ashing.
○, ●: hinoki △, ▲: sugi (heartwood)
□, ■: sugi (sapwood)

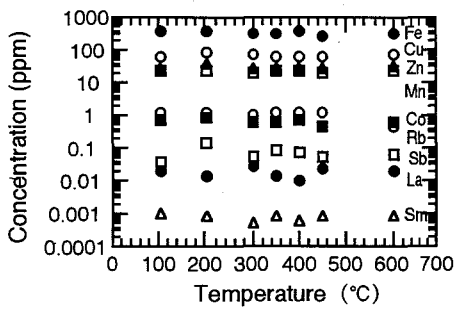

Fig. 2. Concentration of certain elements in hinoki stem samples after dry ashing.

Fax: +81-75-753-7540, E-mail: a50846@sakura.kudpc.kyoto-u.ac.jp

P224
s.52

ACTIVATION ANALYSIS OF TRACE METALS IN THE SEVERAL KINDS OF TISSUES OF EVEN-TOED UNGULATES

M. Fukushima, H. Tamate, S. Sato, S. Terui[1], and S. Mitsugashira[2]

[1]*Faculty of Science and Engineering, Ishinomaki Senshu University, Shinmito Minamisakai, Miyagi 986-80, Japan*
[2]*Laboratory of Nuclear Science, Tohoku University, Sendai, Miyagi 980-77, Japan*

Summary: The concentration levels of trace metals in several kinds of tissues of even-toed ungulates were determined by instrumental neutron activation analysis, photon activation analysis, and flame atomic absorption spectrometry.
Key words: Trace elements, Tissues of even-toed ungulates, Activation analysis

The concentration levels of trace metals in several kinds of tissues of even-toed ungulates were determined. For the samples the livers of Japanese sika deer, the livers, spleens and kidneys of one-month-old calves and fetus of pigs were used. We have used instrumental neutron activation analysis (INAA) and photon activation analysis (IPAA) for the tissues of Japanese sika deer, IPAA and flame atomic absorption spectrometry (FAAS) for the calves, and FAAS for the fetus.
For INAA and IPAA the samples were cut into pieces, pulverized in a porcelain mortar filled with liquid nitrogen, freeze-dried, and finally fractionated through a stainless steel sieve of 200 mesh. Then approximately 100-300 mg of the sample was wrapped in an aluminum foil of high purity, and shaped into a pellet with a diameter of 10 mm and a thickness of 1-3 mm. As comparative standards three different materials were used: NIST SRM-1577b Bovine Liver, BCR No.186 Pig Kidney and NRCC TORT-1 Lobster. The pellets of the samples and the comparative standards were sealed in a silica tube, and were irradiated for 6 or 24 hours in the JMTR reactor at Japan Atomic Energy Research Institute, Oarai, Ibaraki, Japan for INAA, and 3 hours by 30 MeV bremsstrahlung irradiation with a linear electron accelerator of Tohoku University, Sendai, Japan for IPAA. After a suitable period, the aluminum foils were removed, and the samples were rewrapped with non-activated foils. Pure Germanium detectors with multichannel pulse-hight analyzers were used for gamma-ray measurements. The gamma-ray spectra were measured after a decay period of approximately 1 week, 2 weeks, and 1 month for INAA, and 1 day, 1 week, and 1 month for IPAA.
For FAAS approximately 1-5 g of the sample was digested with nitric acid and hydrogen peroxide. The solution obtained by this process was sprayed into a flame by means of a nebulizer.
In the present work, the concentrations of six elements (Ag, Co, Fe, Rb, Se, and Zn), eight elements (Br, Ca, Fe, Mg, Mn, Mo, Na, and Rb), and four elements (Cu, Fe, Mn, and Zn) were analyzed by INAA, IPAA, and FAAS respectively.

Fax:+81-225-22-7746, E-mail: fukusima@isenshu-u.ac.jp

P225 s.60 ADSORPTION AND INTERFACE ACCUMULATION OF AQUASOL AND ORGANOSOL CARBON PARTICLES LABELLED WITH ^{99m}Tc

T. Nozaki,[1] A. Satoh,[1] S. Muraoka,[1] J. Ishiguro,[2] K. Yoda,[2] and K. Ogawa[2]

1: Purex Co., 735, Nippachou, Kouhoku-ku, Yokohama, 223 Japan

2: School of Allied Health Sciences, Kitasato University, Sagamihara, Kanagawa, 228 Japan

Summary: The adsorption of ^{99m}Tc-labelled fine carbon particles in various liquids was measured in view of the dependence on the adsorbing substance, its surface treatment, applied electric potential, and the medium. Also, the particles were found to often accumulate on aqueous-organic interfaces.
Key words: ^{99m}Tc, carbon aquasol, carbon organosol, adsorption, interface accumulation

Behaviour of ultra-fine aquasol and organosol particles cannot be observed easily, principally because of the lack of suitable detection methods. A commercial apparatus called Technegas gives ultra-fine aerosol carbon particles labelled with ^{99m}Tc. We prepared aquasol and organosols of the ^{99m}Tc-carbon, by shaking the aerosol with the liquid media.[1)] Almost no ^{99m}Tc was eluted into water from the carbon. We studied (1) the adsorption of the labelled particulates on several substances and (2) its accumulation on aqueous-organic interfaces, both under various conditions

Plates of the substances (2x2 cm) after suitable surface treatments were kept standing in the sols under gentle stirring for 20 min, and the radioactivity both adsorbed and remaining were measured. Some results are given in Table 1; fairly clear dependences of the adsorptivity on the substance and medium is seen. The surface property was almost masked by coverage with 2 layers of Langmuir-Brodgette films of arachic acid. Application of electric potential enhanced the adsorption on either positive or nagative side or both, depending on the medium. Filtration of the sols through a 0.2 μm micropore filter resulted in noticeable lowerings of adsorbability. For semiconductor silicon, etching with NH_4OH-H_2O_2 gave surface the least adsorptive of the etchings used in semiconductor industry; Si in Table 1 had been etched with this agent. This etching was also the most effective for the removal of the adsorbed particulates.

Table 1. Adsorptivity (mm)*

	n-Octane	Xylene	Water	MIBK**	s-Butanol
Al	4.62±0.33	6.87±0.82	2.65±0.14	0.91±0.05	0.477±0.040
Cu	16.76±0.34	4.68±0.04	0.29±0.02	0.53± 0.02	0.139±0.026
Polyethylene	8.89±0.88	6.07±0.32	0.87±0.05	0.24±0.03	0.177±0.022
Teflon	14.54±1.44	5.56±0.56	0.47±0.02	0.21±0.02	0.153±0.023
Fe	9.41±1.43	4.65±0.06	2.08±0.49	0.68±0.08	0.135±0.049
Si	5.40±0.28	2.63±0.76	0.15±0.02	0.25±0.04	0.109±0.056

* Thickness of the sol layer containing equal activity of ^{99m}Tc as adsorbed on the surface.

** Methyl-isobutyl ketone.

The ^{99m}Tc-carbon particulates often accumulated on liquid-liquid interfaces. Using a gamma-camera, we observed the accumulation on MIBK-water interface. Markedly different camera images were obtained, according to the concetration of electrolytes in the aqueous phase. In the absence of electrolytes, a much stronger activity was observed in water than in MIBK, with a slight interface accumulation. In about 0.1 N NaOH, the concetration difference became much smaller. In 0.15 N NaCl, the accumulation was quite significant with some adsorption on the wall in contact with the aqueous phase, but without any notable decrease of radioactivity concetration in MIBK.

1) T. Nozaki et al., Appl. Radiat. Isotopes, **46**, 157, 1995.

Fax: 801-0463-92-3136

P226
s.62

SPECanalSuite97 for Win95

Y. Hamajima

Department of Chemistry, Faculty of Science, Kanazawa University, Kakuma-machi Kanazawa, 920-11, Japan

Summary: SPECanalSuite97 delivers a set of spectrum analysis applications designed to help radiochemists. The Suite includes peak area calculation, spectrum and nuclear data viewer, decay analysis, and some utilities with GUI of Windows95 and NT.
Key words: SPECanal, gamma-ray, X-ray, spectrum analysis, nuclear data viewer, PC

Personal computer(PC) is usually used for data taking of gamma- and X-ray measurement. As modern PC has very high computing power, it is possible to use PC for peak area, decay, and efficiency calculation, and for search for nuclear data. Two years ago, I reported SPECanal95 on SORC95(Niigata university), which was DOS based suite. Recently, user friendly operating system, Windows95, is loaded on most of PC. In this paper, I introduce new SPECanalSuite97 with GUI of Windows95. I will also perform demonstration of new Suite by small computer.

SPECanalSuite97 delivers a set of 32 bit applications and gamma- and X-ray catalog database designed to take advantage of Windows 95 and Windows NT. The application in the suite includes wPKarea(peak area calculation based on gaussian + exponential tail + arc-tangent bkg curve fitting), wPKview(spectrum and nuclear data viewer), wPKidnt(automatic nuclide identification derived from peak energy position and branching ratio corrected by detector efficiency), wPKdecay(decay analysis based on least square fitting), wPKeff(detector efficiency estimation by standard source method), and some other utilities of data printing and maintenance designed to help radiochemists.

Gamma- and X-ray catalog database of SPECanal was compiled from ENSDF(evaluated nuclear structure data file) of NNDC(National Nuclear Data Center, BNL, USA), and was adapted for personal computers. This database consists 103 element ASCII files containing over 2400 entries of radionuclides with half life of longer then 1 micro second and over 54000 gamma- and X-ray lines with branching ratio of grater than 0.1%. Every data of nuclide includes half-life, decay mode, error of energy line and branching ratio, and classification of gamma- and X-ray. Installer automatically constructs two binary files of energy list. One is full list included all energy lines, and the other is small one with branching ratio of grater then 5 %. User easily browses these nuclear data by wPKview.

Fax: +81-76-246-5742, E-mail: hama@cacheibm.s.kanazawa-u.ac.jp

P227
s.62

SIMPLE MEASUREMENT OF ^{14}C IN THE ENVIRONMENT USING GEL SUSPENSION METHOD

G. Wakabayashi, H. Ohura, T. Okai, M. Matoba, A. Nohtomi[1], H. Kakiuchi[2], N. Momoshima[2] and H. Kawamura[3]

Department of Nuclear Engineering, Faculty of Engineering, Kyushu University, 6-10-1 Hakozaki Higashi-ku Fukuoka 812, Japan
[1]Proton Medical Research Center, Tsukuba University, Ibaraki 305, Japan
[2]Department of Chemistry, Faculty of Science, Kyushu University, Fukuoka 812, Japan
[3]Kyushu Environmental Evaluation Association, Fukuoka 813, Japan

Summary : We applied new gelling agent, N-lauroyl-L-glutamic-α,γ-dibutylamide, for simple liquid scintillation counting of environmental ^{14}C as $CaCO_3$. The properties of this method was evaluated and it was shown that this method had enough precision for the environmental monitoring.
Keywords : carbon-14, liquid scintillation counting, gel suspension method

Environmental ^{14}C is of interest because of the biological importance of carbon and long half-life (5730 years) of this isotope. The conventional sample preparation procedure for liquid scintillation counting of environmental ^{14}C such as benzene synthesis method is complex and requires expensive equipment, therefore it is not adequate for the purpose of the environmental monitoring. The purpose of this study is to develop the simple liquid scintillation counting technique for the routine assay of ^{14}C in the environment.

For this purpose, we applied new gelling agent, N-lauroyl-L-glutamic-α,γ-dibutylamide, for liquid scintillation counting of ^{14}C as $CaCO_3$ (gel suspension method). The sample preparation procedure of this method was much simpler than conventional methods and required no special equipment.

Sample $CaCO_3$ (468.2 dpm/g-$CaCO_3$) used for counting was produced from active-$NaHCO_3$. Vials of 7 ml, 20 ml and 100 ml were used for counting. Sample $CaCO_3$ dispersed in a gel-forming liquid scintillator was measured with a low background liquid scintillation counter (Aloka LB-1) and quenching effect was compensated by efficiency tracing method.

Counting samples of 100, 20 and 7 ml vial could contain $CaCO_3$ up to 30, 6 and 2.1 g, respectively. Figure of merit was calculated to assess the optimum condition of measurement. The maximum value of figure of merit (the optimum condition) was obtained when the maximum amount of sample $CaCO_3$ was incorporated in the vial. Under the optimum condition, lower detection limit of counting sample of 100 ml was appx. 0.3 dpm/g-C for counting interval of 2000 min, and that of 20 ml was appx. 0.5 dpm/g-C for 4000 min. These values are low enough for present level of environmental ^{14}C. Moreover, the samples were very stable at least 1 year after preparation. Therefore the samples prepared by gel suspension method are adequate for long term preservation.

As a conclusion, it was shown that gel suspension method could be applied for the monitoring of environmental ^{14}C.

Fax : +81-92-642-3800, E-mail : gensan@nucl.kyushu-u.ac.jp

P228
s.62

COMPARISON OF THE TEVA • SPEC RESIN AND LIQUID-LIQUID EXTRACTION METHODS FOR THE SEPARATION OF TECHNETIUM IN SOIL SAMPLES

K. Tagami and S. Uchida

Environmental and Toxicological Sciences Research Group, National Institute of Radiological Sciences, 3609 Isozaki, Hitachinaka-shi, Ibaraki, 311-12 JAPAN

Summary: A separation method using a novel chromatographic resin was compared with a liquid-liquid extraction method for Tc-99 in soil samples. ICP-MS was used for the determination of Tc-99. Molybdenum concentrations in the separated solutions by both methods were also measured.
Key words: Technetium, molybdenum, TEVA • Spec resin, liquid-liquid extraction, ICP-MS, soil.

Analysis of global fallout Tc-99 in environmental samples should provide useful information for predicting this nuclide's behaviour under natural conditions which is important from the viewpoint of radioecology. Previously we developed the following separation method for soil samples. A soil sample is first incinerated at 450℃, then Tc is separated from it by volatilization, i.e., by combustion of the sample at 950℃ and trapping of the element in a potassium carbonate solution. The solution is extracted into cyclohexanone to remove Ru which has an isotopic abundance of 12.7% at mass of 99. Then Tc in the organic layer is back-extracted into deionized water by addition of carbon tetrachloride. After adjusting acidity to 2% of the aqueous phase with nitric acid (super-analytical grade), the Tc-99 concentration in the solution is measured by ICP-MS (Yokogawa, PMS-2000).

When ICP-MS is used, a solution which contains no isotopes except Tc at mass 99 is preferable. The liquid-liquid extraction method has a high recovery of Tc and a high decontamination factor for Ru. However, using an organic reagent might cause a higher background level in the final solution than that in deionized water for ICP-MS measurement. Further, the organic reagent can not remove Mo. Large amounts of Mo-98 and Mo-100 might interfere with Tc-99 count although there is no natural abundance at 99 for Mo.

In this study, a novel extraction chromatographic resin (TEVA • Spec resin) was compared with the liquid-liquid extraction method for separation and concentration of Tc-99 in the trap solution obtained by combustion of environmental soil samples. Previously, we found that the resin retained Tc efficiently and selectively from several kinds of solutions. To introduce the trap solution to the resin, the solution was neutralized and then adjusted to 0.1M nitric acid with conc. nitric acid. Tc was extracted on the resin from ca. 0.1M nitric acid solution with almost 100 % recovery and stripped from the resin with 5 mL 8M nitric acid. Tc could be completely separated from Ru with high recovery as pertechnetate ion. Additionally, Mo could be removed from the final solution.

FAX: +81-29-265-9883, E-mail: k_tagami@nirs.go.jp

P229
s.62

OPTIMIZATION OF LIQUID SCINTILLATION COUNTING TECHNIQUES FOR THE DETERMINATION OF CARBON-14 IN ENVIRONMENTAL SAMPLES

H.J. Woo[1], S.K. Chun[1], S.Y. Cho[1], Y.S. Kim[1], D.W. Kang[2] , C. Huh[2]

[1]*Korea Institute of Geology, Mining and Materials, P.O. Box 111, Daedeok Science Town, Taejon, Korea, 305-350*
[2]*Korea Electric Power Research Institute, Munji-dong 103-16, Yusung-gu, Taejon, Korea, 305-380*

Summary: Liquid scintillation counting technique of direct CO_2 absorption, gel suspension and benzene synthesis are described for C-14 measurements in stack effluent gases and environmental samples of biota and field air.
Key words: LSC, C-14, stack gas, environmental samples

The goal of this work is to optimize the liquid scintillation counting techniques for the determination of C-14 in stack effluent gases and in environmental samples such as biological and air samples. Carbon-14 activities in most environmental samples are measured with direct CO_2 absorption method. Highest figure of merit was found through the variation of Carbosorb E and Permafluor V ratio, and measurement windows. The best condition was 1:1 volume ratio. Average 2.35 g of CO_2 is reproducibly absorbed in the 20 ml mixture within 30 min. The counting efficiency is measured to be 58.4±2.0% by repeated analysis of NIST oxalic acid standard, and the background count rate is measured to be 1.88 cpm in the case of saturated solution. The correction curve of counting efficiency for partially saturated solutions is also prepared, however the difference of corrected counting efficiency is not larger than 0.5 % if the amount of absorbed CO_2 is more than 1.6 g. The overall uncertainty of sample specific activity for near background level is estimated to be about 7 % for 4 hours counting at 95% confidence level. Due to the limitation of the available sample amount in case of reduced carbon species, stack effluent gas samples are measured by gel suspension counting method. After precipitation of CO_2 in the form of $BaCO_3$, 400 mg of which is mixed with 6 ml H_2O and 12 ml of Instagel XF. The counting efficiency is measured to be 57.7± 1.1 % and the typical sensitivity of this technique is about 130 mBq/m^3 for a 100 min count at a background count rate of 1.69 cpm. The overall uncertainty of specific activities of stack gas samples is estimated to be about 2 % at 95 % confidence level. For the benzene counting method measurements are performed with a mixture of 3 ml benzene and 1 ml of scintillation cocktail (5g of butyl-PBD in 100 ml of scintillation grade toluene) in a low potassium 7 ml borosilicate glass vial. The counting efficiency and the background count rate are measured to be 67.5±1.2 % and 0.54 cpm, respectively at the highest figure of merit condition. The long-term stability of samples has been checked for all the counting techniques over a two week period, in which no apparent change in counting efficiency and background level was found.

Fax: +82-42-861-9727, E-mail: skchun@rock25t.kigam.re. kr

P230
s.62

P231
s.63

A REVIEW OF HIGH SENSITIVE NEW TL DOSIMETRY PHOSPHORS OF IONISATION RADIATION

S. J. Dhoble* AND N. S. Dhoble[1]

Kamla Nehru College, Sakkardara Square, Nagpur-440009, M.S. INDIA.
[1]Sevadal Mahila Sci. College, Sakkardara Square, Nagpur-09, . INDIA

Summary : Thermoluminescence (TL) is now extensively used for dosimetry of ionising radiations. $K_2Ca_2(SO_4)_3$: Eu; $CaSO_4$: P,Dy; $K_3Na(SO_4)_2$: Eu; MgB_4O_7:Dy; $Sr_5(PO_4)_3$ Cl : Eu phosphors are prepared easily with appreciable TL efficiency.
Key Words : Thermoluminescence, high sensitivity, phosphors, dosimetry.

The thermoluminescence dosimetry. (TLD) phosphors in common use are LiF-TLD100; LiF:Mg,Cu,P;MgB_4O_7 :Dy ; $CaSO_4$:Dy etc. $CaSO_4$:Dy has good sensitivity, but poor " tissue equivalence" and the shape of glow curve changes with exposure. We have made a systematic survey of the TL studies of stable phosphors prepared in our laboratory. They show TL with appreciable efficiency. New high sensitive phosphors $K_2Ca_2(SO_4)_3$: Eu (0.1 mole %), MgB_4O_7:Dy (0.1 mol %), $Sr_2B_5O_9Cl$: Eu (2 mol%), $Sr_5(PO_4)_3Cl$: Eu (2 mol %) and $KMgF_3$: Eu (0.1 mol %) are prepared by solid state diffusion method by taking the constituents in stoichiometric ratio. The resulting compounds annealed at 950 K, 775 K, 1000 K, 1200 K, 975 K respectively for one hour and quenched to room temperature (RT). $CaSO_4$: p,Dy (1%, 0.5 mol %) is prepared by acid method, which is annealed at 973K for one hour and quenched to RT. $K_3Na(SO_4)_2$: Eu (0.1 mol %) is prepared by melting together the constitutent sulphates in stoichiometric ratio. The molten masses were slowly cooled to RT and crushed power used as a phosphor. Formation of crystalline compounds is confirmed by XRD pattern.

Fig.1 shows TL glow curves of the $K_2Ca_2(SO_4)_3$:Eu(a);$CaSO_4$: P,Dy(b); $K_3Na(SO_4)_2$: Eu(c); MgB_4O_7:Dy(d); $Sr_2B_5O_9Cl$: Eu(e); $Sr_5(PO_4)_3Cl$: Eu(f) and $KMgF_3$: Eu (g) Phosphors (exposed to 2.58 x 10^{-2} CKg^{-1} of gamma rays). They are found to be atleast 5, 1.5, 6, 0.5, 0.7, 2 and 0.2 times sensitive than the conventional $CaSO_4$: Dy phosphor respectively. The strong TL glow peaks are observed around 420 K, 500 K, 475 K, 460 K, 495 K, 430 K and 530 K respectively. High temperature glow peak could be quite suitable for applicaiton in TL dosimetry of ionisation radiation. No change in glow curve of the sample is observed for various gamma-ray exposures and excellent linearity is obtained in the range 2.5 x 10^{-3} to 0.25 CKg^{-1}. The TL emission peak of above phosphors are also in the ultraviolet and blue region of the spectrum. Effect of storage in dark at RT, shows negligible fading of the prominent glow peak. These four facts are very useful in context of the TL dosimetry for consideration of TLDs phosphor of ionisation radiation.

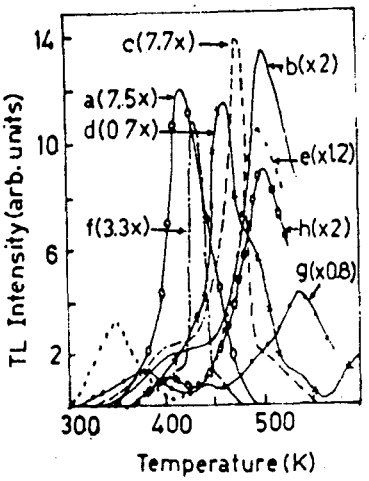

Fig.1 TL glove curves of various phosphores expressed to γ rays.

FAX +91-712-532841

P232
s.62

APPLICATION OF A YAP SCINTILLATOR TO A PHOSWICH DETECTOR FOR SIMULTANEOUS COUNTING OF ALPHA AND GAMMA RAYS

K. Yasuda and S. Usuda

Department of Fuel Cycle Safety Research, Japan Atomic Energy Research Institute, Tokai-mura, Naka-gun, Ibaraki-ken, Japan 319-11

Summary: A phoswich detector composed of a new scintillator, YAP, for γ counting and ZnS(Ag) for α counting has been devised, and properties of the phoswich are discussed from the viewpoint of simultaneous counting of alpha and gamma rays.
Key words: YAP, ZnS(Ag), phoswich detector, simultaneous counting, alpha rays, gamma rays

A YAP scintillator, crystal of yttrium-aluminum perovskite doped with Ce, seems to be a promising detector for γ rays even under the corrosive and high exposure dose circumstance. The reason is that the scintillator has the following good characteristics: fast scintillation decay time (28 ± 2 ns), relatively high scintillation efficiency (40 % of NaI(Tl) light output), high density (5.55 g/cm^3), chemical proof against acid solutions and organic solvents, high melting point (1850 °C), etc. [1].

The author et al. have developed phoswich detectors, the combinations of plural scintillators coupled to a single photomultiplier tube (PMT), for simultaneous counting of various radiations[2], and therefore noticed the YAP as an excellent element of phoswich for counting of γ (including β) rays.

The rise times of the YAP and ZnS(Ag) for α and γ rays, and FWHM (the full widths at half maximum) were obtained by measuring their distributions (see Table 1).

Table 1 Dimension of the scintillators used and their rise times.

Scintillators	[Dimension]	^{244}Cm (α source) Rise time	(FWHM)	^{137}Cs (γ source) Rise time	(FWHM)
ZnS(Ag)	[1"ϕ, 10 mg/cm^2]	476	(21.8)	-	-
YAP	[1"ϕ × 3 mmt]	211	(2.7)	211	(17.4)

The ZnS(Ag) was sensitive to only α rays and its rise time was slow. On the other hand, the YAP had high sensitivity to γ rays, its rise time was faster than that of ZnS(Ag) and the FWHM was quite narrow.

Consequently, a ZnS(Ag)/YAP phoswich detector for simultaneous α and γ counting was devised (see Fig. 1). The pulse shape discrimination (PSD) properties between the radiations were excellent (figure of merit: 6.8) and the tailings of the α and γ peaks in the rise time distributions to each other were negligibly small.

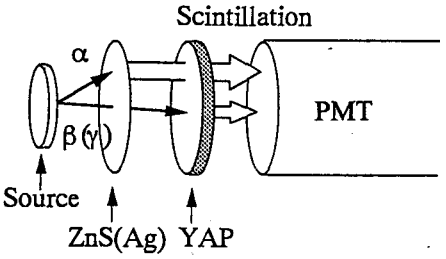

Fig. 1 Arrangement of ZnS(Ag)/YAP phoswich detector.

In addition, it was ascertained that an optical sharpcut filter made the PSD properties to be more improved by slowing the rise time attributed to the ZnS(Ag)[3]. The devised phoswich will serve to monitor α and γ rays emitted from actinides treated with nuclear fuel cycle facilities. In the presentation, the properties of ZnS(Ag)/YAP will be discussed in detail and compared with other phoswiches.

[1]V. G.Baryshevshy et al., Nucl. Instr. Methods B58, 291 (1991)
[2]S. Usuda, S. Sakurai, K. Yasuda, Nucl. Instr. Methods A388, 193 (1997)
[3]S. Usuda, J. At. Energy Soc. Japan, 38, 715 (1996), in Japanese.

Fax: +81-29-282-6798, E-mail: yasuda@sglsun.tokai.jaeri.go.jp

P233
s.52

OPTIMIZED DATA EVALUATION FOR k_0- BASED NAA

R. van Sluijs, D.A.W. Bossus

DSM Research B.V., Section IS-MVR/RAS, P.O.Box 18, NL-6160 MD Geleen, The Netherlands

Summary: k_0-NAA allows the analysis of up-to 67 elements simultaneous. The k_0-method is based on calculations using a special library instead of measuring standards. The calculations and resulting raw data require optimized evaluation procedures for an efficient use of the method.

Keywords: matrix interpolation, efficiency, interference, nuclide identification, gamma spectrometry

k_0-neutron activation analysis allows the simultaneous analysis of up-to 67 elements without the use of standards. The flexibility regarding to reactor, detector and sample composition and geometry is one of the key success factors of the method. This flexibility is made possible thanks to the good physical-mathematical description of activation and detection on which the method is based. The measurement of standards is in the k_0-method replaced by extensive calculations using a special nuclear library containing k_0-factors and related nuclear data.

For each measurement limits of detection and/or element concentrations can be calculated for 345 analytical gamma lines from 122 isotopes. The amount of data resulting from these calculations is very large and requires some reduction. In fact only a final list of element concentrations based on several measurements is the goal of the analyst. It is obvious that isotope and element identification, gamma interference correction and mean element concentration calculation is necessary.

The procedures for isotope/element identification and gamma interference correction that are implemented in KAYZERO®, a program for evaluation of k_0-NAA data, are outlined in the paper. The procedures use concentrations and limits of detection, that can be reported as intermediate results, and can therefore be checked by hand easily. Main benefit of this approach is that the evaluation procedure is transparent and that a program will not become a black box.

The most time consuming calculations are the calculations of the full-energy detection efficiency and true-coincidence correction factors for the source-detector combination. By introducing standardized counting vials and the matrix interpolation technique the evaluation of NAA data is further optimized. The detection efficiency of a specific sample (described by density and composition) is found by reading this efficiency in a efficiency versus linear attenuation coefficient plot for the counting vial and detector configuration used. Using this method the data evaluation is simplified and calculations can be performed almost instantaneously.

Fax: +31-46-4767500, E-mail: r.sluijs-van@research.dsm.nl

P234
s.52

IMPURITY CORRECTION FACTOR OF $MnSO_4$ COMPOUND FOR THE DETERMINATION OF NEUTRON EMISSION RATE ON THE MANGANESE BATH METHOD

K. O. CHOI, Y. S. LEE[1], K. S. PARK[2]

[1] *Korea Research Institute of Standards and Science, Taejon 305-600, Korea*

[2] *Kyungbuk National University, Taegu 702-701, Korea*

Summary :

Key words: $MnSO_4$, H_2O, Manganese Bath, Neutron Source Strength, ICP.

The Manganese Sulphate Bath Method is widely used for measurements of Neutron Source Strength. In this study, the analytical chemistry method based on the Inductively Coupled Plasma Spectrometry (ICP) was used for examining the impurity contents of $MnSO_4 \cdot H_2O$, to induce $^{55}Mn(n, \gamma)^{56}Mn$ reactions. From the analytical results, mainly K, Co, and Zn as well as trace amounts of Cd, Li, etc., have turned out to be the relevant impurities absorbing the neutrons, and the fraction of neutrons absorbed by the total impurities was calculated, and determined to be 1.37 %.

Fax: +82-42-868-5042, E-mail: kochoi@krissol.kriss.re.kr

P235
s.52

AN UNUSUAL CORRELATION BETWEEN RARE EARTH ELEMENTS AND CALCIUM CONTENTS IN FERN LEAVES.

J. Takada[1], T. Sumino[1], K. Nishimura[2], Y. Tanaka[1], K. awamoto[1] and M. Akaboshi[1]

[1] *Research Reactor Institute, Kyoto University, Kumatori-cho, Sennan-gun, Osaka, 590-04, JAPAN*

[2] *University Forests, Kyoto University, Kitashirakawa Oiwake, Kyoto, 606-01, JAPAN*

Summary: Logarithmic scattering diagram between REEs and Ca characterized with respect to the sampling site revealed that the 142 fern could be separated into two or three groups on the basis of their different REE/Ca ratios.

Key words: Rare earth elements (REE), Fern leaves, Neutron activation analysis, REE/Ca ratio

Since the rare earth elements (REE) are at Their most informative as isomorphic replacements of Ca^{2+} in organisms, we analyzed these elements in 142 fern leaves collected from several samplingsites in Japan by instrumental neutron activation analysis (INAA), and the correlation between the REE and Ca contents was examined. In most cases, between any REEs and Ca contents, the correlation in the logarithmic scattering diagram was expressed as a single line parallel to the vertical (Y) axis. However the detailed analysis of the diagram characterized with respect to the sampling site revealed that the 142 fern could be separated into two or three groups on the basis of their different REE/Ca ratios. (Fig.) The sampling sites where the different REE/Ca ratio were observed completely agreed with that found in the preceding report, namely, in the strange correlation between Eu and the other REEs.

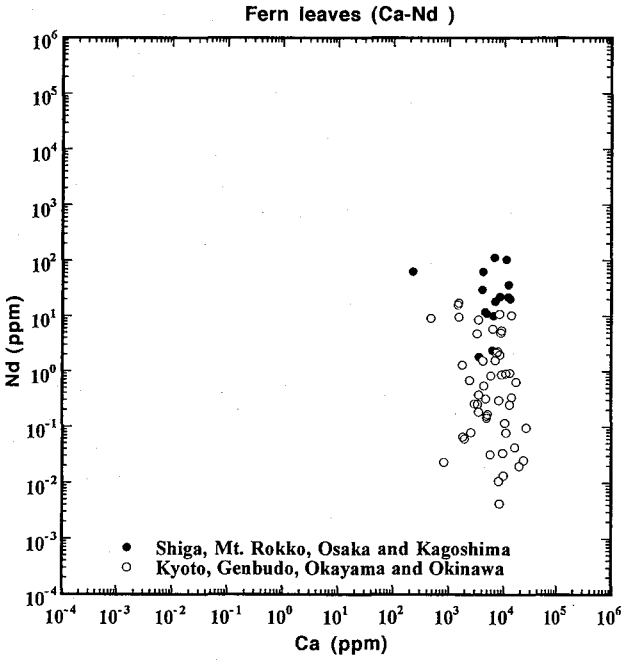

Fig. Correlation between the Ca and Nd contents characterized with respect to the sampling site.

P236 s.52 DETERMINATION OF BORON CONTENT IN VOLCANIC ROCKS BY NEUTRON-INDUCED PROMPT Γ-RAY ANALYSIS: CORRECTION OF ANALYTICAL SENSITIVITY VARIATION

T. Sano[1], T. Fukuoka[2], T. Hasenaka[3], C. Yonezawa[4], H. Matsue[4], H. Sawahata[5]

[1]*Faculty of Integrated Human Studies, Kyoto University, Kyoto, Japan*
[2]*Department of Science, Gakushuin University, Tokyo, Japan*
[3]*Faculty of Science, Tohoku University, Sendai, Japan*
[4]*Tokai Establishment, Japan Atomic Energy Research Institute, Tokaimura, Ibaraki, Japan*
[5]*Tokai Establishment, Research Center for Nuclear Science and Technology, University of Tokyo, Tokaimura, Ibaraki, Japan*

Summary: We report the results of examinations for accurate neutron-induced prompt γ-ray analysis of boron in volcanic rock samples. The analytical sensitivity variation was corrected by normalization using the peaks of Si.

Key words: prompt γ-ray analysis, boron, volcanic rocks, GSJ standard rocks

Boron is an excellent tracer of crustal recycling at convergent plate margins such as Japan and central/south America, where oceanic plates undergo volcanic arcs. Because the budget of this element in arc magmas is dominated by the subduction component (ocean sediments, altered crust, or melts/fluid derived therefrom), it is strongly enriched in many volcanic arc lavas compared to those erupted on other tectonic settings. Neutron-induced prompt γ-ray analysis (PGA) is a suitable way of B determination, because boron is one of the most sensitive elements. Moreover, it is a non-destructive method, which is free from evaporation loss or contamination, contrasting to the decomposition by HF-mannitol method for ICP-AES. Errors in PGA analysis will be introduced from the flux fluctuation and the sample geometry during neutron irradiation. Previous workers adopted an average of more than five measurements to improve the accuracy and precision. However, we have to develop other improvements, since the irradiation time is limited. The following describes our procedures for sample preparations and data reductions.

Volcanic rock powder was cold-pressed into a disk (12 mm in diameter and 4-6 mm in thickness), and was then heat-sealed in a bag of FEP film. This bag was situated in PGA system at neutron beam guide of JRR-3M reactor in He atmosphere for cold or thermal neutron irradiation, and simultaneous γ-ray spectrometry for 1,000-10,000 sec (Yonezawa *et al.*, 1993). The pressed powder gains 3-6 times increase in density. Therefore, we could greatly reduce irradiation time. However, Yonezawa and Wood (1995) reported that analytical sensitivity (cps/g) of each element decreased with increasing weight of the sample. This change in sensitivity of boron was corrected by normalization. When the Si content was determined by another analytical method (*e.g.*, XRF), we could normalize B peak count rates by using those of 2093 and 3539 keV Si peaks. Analyses of standard rock powder samples revealed the efficiency of this method. This normalization can simultaneously correct the analytical sensitivity variation caused by the flux fluctuation.

Calibration lines were made from a series of prompt γ-ray counting of pressed powdered disks that contain known amount of B standard solution. Powders of SiO_2 and GSJ standard rocks (JB-1a, JA-2, JR-2 and JG-1a) were used and dried in atmosphere. Peak count rates of B, when normalized by Si contents, indicate a good linear relationship with B contents for each standard rock or SiO_2 powder. However, the slopes of calibration lines for different standard powders show differences greater than the analytical error. The slope for SiO_2 powder is especially steeper than the rest. Because this slope angle correlates with the peak count rates of H for each standard powder, we deduced that this phenomenon was caused by the neutron scattering with matrix H.

When we use the above analytical procedure, we can determine the accurate B content in volcanic rock with short irradiation time. Analyses of GSJ standard rocks, using the above procedure, agree well with the reported values of Imai (1986) and Yonezawa and Wood (1995).

Fax: +81-75-753-6872, E-mail: sano@geo01.gaia.h.kyoto-u.ac.jp

APSORC '97 LIST OF ABSTRACTS

ORAL SESSIONS

A00s, B00s, C00s & D00s

Wednesday morning, 8 October 1997

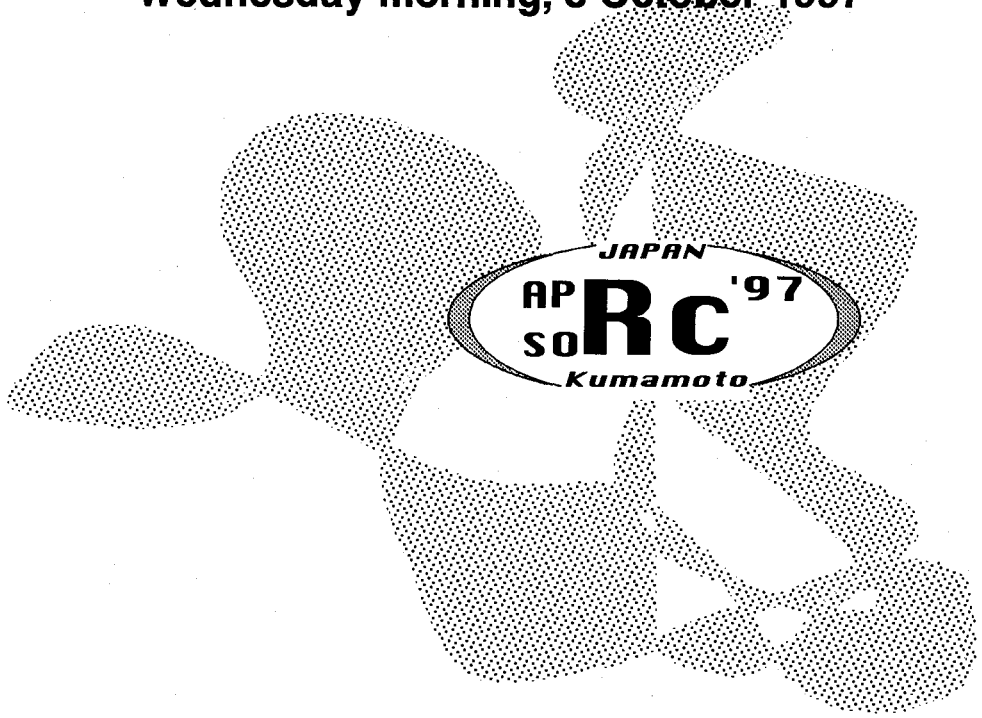

- KEYNOTE THEME -

EVER ONWARD TOWARDS THE FRONTIERS OF RADIOCHEMISTRY IN THE SECOND CENTURY OF RADIOACTIVITY DISCOVERY

A01
s.02

Bremsstrahlung Emission in α-Decay of ^{244}Cm and ^{210}Po

T. Ohtsuki, J. Kasagi, H. Yamazaki, N. Kasajima, H. Yuki, M. Yukishima

Laboratory of Nuclear Science, Tohoku University

Summary: We have measured bremsstrahlung emission associated with the α-decay of ^{210}Po and ^{244} in α-γ coincidence measurements with Si and Ge detectors. From the measurement, we found that the emission probabilities were at least one order of magnitude smaller than the calculated results by the Coulomb acceleration model. This seems due to the destructive interference of the photons emitted at the inside and outside of the barrier.
Key word: Bremsstrahlung emission, α-decay of ^{210}Po and ^{244}Cm

Bremsstrahlung associated with α-decay is of particular interest, since α-particles must pass through a large Coulomb barrier so that bremsstrahlung photons may contain plentiful information on the tunneling motion, if the α-particles emit photons inside the barrier. In order to investigate such a possibility, we have measured bremsstrahlung emission associated with the α-decay of ^{210}Po and ^{244} in α-γ coincidence measurements with Si and Ge detectors. The measurements were performed with a ^{244}Cm source for about 80 days and subsequently with a ^{210}Po source for about 120 days, so far. The source and Si detector were placed in a small vacuum chamber and the distance between them was only 4.5 mm. The Ge detector was placed outside the chamber at 20 mm from the source. Data(E_α, E_γ, T) were accumulated with CAMAC in event-by-event mode and written on an MO disk for off-line analysis. The total number of observed α-decay was about 3.3×10^9.

Events with $E_\alpha+E_\gamma=E_\alpha^{g.s.}$ were analysed to deduce those of the bremsstrahlung photons associated with α-decay to the ground state of the daughter nucleus. They were selected by setting a gate on the two-dimensional of E_α vs E_γ. Chance coincidence events were subtracted from the prompt coincidence events, and the correction for the detector efficiency as well as for the angular correlation were made. The bremsstrahlung emission probabilities were deduced for 160 keV $<E_\gamma<$400 keV for the α-decay of ^{244}Cm and 100 keV$<E_\gamma<$340 keV for ^{210}Po. The deduced emission probabilities are very small and seems to decrease rapidly as the photon energy increase.

The deduced probabilities are compared with calculations based on the classical radiation theory. The sudden acceleration model in which an α-particle suddenly obtains its final velocity overestimates the data by more than one order of magnitude. The Coulomb acceleration model in which an α-particle is accelerated by the Coulomb force from the classical tunneling point with zero velocity also overestimates the data. Thus, we have inferred a possibility that photons are also produced in the Coulomb barrier and performed classical calculations [1] in which bremsstrahlung emission in tunneling motion of α-particles is taken into account. The results of the calculations show that photon energies below 250 keV are emitted inside the barrier more than outside. However, they cannot be measured directly because of the interference. Due to the destructive interference of the photons emitted at the inside and outside of the barrier, the calculated results are at least one order of magnitude smaller than those of the Coulomb acceleration, and explain the trend of the experimental data very well.

[1]M.I. Dyakonov and I.V. Gornyi, Phys. Rev. Lett. **76** 3542(1996).

Mikamine, Taihaku, Sendai 982, Japan, E-mail: Ohtsuki@LNS.tohoku.ac.jp, and Kasagi@

A04
s.02

RECENT STUDIES OF UNSTABLE NUCLEI FAR FROM STABILITY WITH THE ON-LINE ISOTOPE SEPARATORS OF JAERI

T. SEKINE,[*1] S. ICHIKAWA,[2] A. OSA,[1] M. KOIZUMI,[1] H.IIMURA,[2] K. TSUKADA,[2] I. NISHINAKA,[2] Y. HATSUKAWA,[2] Y. NAGAME,[2] M. ASAI,[3] Y. KOJIMA,[3] T. HIROSE,[3] M. SHIBATA,[3] H. YAMAMOTO[3] AND K. KAWADE[3].

[1] *Department of Chemistry and Fuel Research, Japan Atomic Energy Research Institute (JAERI), Takasaki, Gunma 370-12, Japan,*

[2] *Department of Chemistry and Fuel Research, JAERI, Tokai, Ibaraki 319-11, Japan*

[3] *Department of Energy Engineering and Science, Nagoya University, Furo-cho, Chikusa-ku, Nagoya 464-01, Japan*

Summary: Studies on the decay of unstable nuclei using the two isotope separators of JAERI are reviewed. New nuclides of $^{125, 127}$Pr, ^{166}Tb, ^{165}Gd, ^{161}Sm and ^{236}Am have been identified, and the evolution of nuclear structure with neutron number has been studied on even – A Ba and Ce nuclei.
Key words: Isotope separator on-line, nuclear decay, new nuclides, half-lives, nuclear structure.

For the study of unstable nuclei, two isotope separators on-line (ISOL) have been constructed in JAERI. One, connected to the tandem accelerator at Tokai and called the JAERI-ISOL, began operating in 1982 and its scientific activities until 1991 were described elsewhere, while the other, connected to the AVF cyclotron at Takasaki and called the TIARA-ISOL, began operating in 1992. The present paper reviews the studies with both the ISOLs since 1992.

At the JAERI-ISOL, a new target-ion source system has been developed in order to explore the neutron-rich side on rare-earth nuclei and the actinide region. The system separates the target from the hot thermal ion source, which enables us to use actinide targets; the recoiling products are transported with a He-jet into the ion source. So far, the neutron-rich nuclides ^{166}Tb, ^{165}Gd and ^{161}Sm, and the EC-decay nuclide ^{236}Am have been newly identified as summarized in Table 1.

Table 1 New nuclides identified recently with the ISOLs of JAERI

Nuclide	Half-life	Decay mode	Nuclear reaction
^{125}Pr	3.3±0.7 s	β^+/EC	^{92}Mo(^{36}Ar, 1p2n)
^{127}Pr	7.7±0.6 s	β^+/EC	^{94}Mo(^{36}Ar, 1p2n)
^{166}Tb	21± 6 s	β^-	^{238}U(p, f)
^{165}Gd	10.3±1.6 s	β^-	^{238}U(p, f)
^{161}Sm	4.8±0.8 s	β^-	^{238}U(p, f)
^{236}Am	4.4±0.8 m	**EC**	**^{235}U(^{6}Li, 5n)**

At the TIARA-ISOL, the study of neutron-deficient rear-earth nuclides was extended with ^{36}Ar beams from those carried out with ^{32}S/^{35}Cl beams at the JAERI-ISOL. The new nuclides $^{125, 127}$Pr have been identified (See Table 1). The decay of even-A La and Pr isotopes was also studied using an efficient gamma-gamma angular correlation measurement system for the elucidation of the evolution of nuclear structure with neutron number. Resultingly, low-spin states in $^{124,-130}$Ba and ^{130}Ce have been established with their spins.

In the symposium, some applications of an ISOL will be presented together with the development of a laser ion source.

Fax: +81-273-46-9690, E-mail: sekine@taka.jaeri.go.jp

A05
s.01

SYSTEMATICS OF BIMODAL NATURE IN ACTINIDE FISSION

Y. Nagame[1], I. Nishinaka[1], Y.L. Zhao[1,4], K. Tsukada[1], S. Ichikawa[1], H. Ikezoe[1], M. Tanikawa[2], T. Ohtsuki[3], Y. Oura[4], K. Sueki[4], H. Nakahara[4], H. Kudo[5], Y. Hamajima[6] K. Takamiya[7], K. Nakanishi[7], and H. Baba[7]

[1] *Japan Atomic Energy Research Institute, Tokai-mura, Ibaraki 319-11, Japan*
[2] *Department of Chemistry, University of Tokyo, Bunkyo-ku, Tokyo 113, Japan*
[3] *Laboratory of Nuclear Science, Tohoku University, Sendai 982, Japan*
[4] *Department of Chemistry, Tokyo Metropolitan University, Hachioji, Tokyo 192-03, Japan*
[5] *Department of Chemistry, Niigata University, Niigata 950-21, Japan*
[6] *Department of Chemistry, Kanazawa University, Kanazawa 920-11, Japan*
[7] *Department of Chemistry, Osaka University, Toyonaka, Osaka 560, Japan*

Summary: From the systematic studies of mass division phenomena, it has been found that there are at least two independent deformation paths in low energy proton-induced fission of actinides.
Key words: actinide fission, fission barrier, scission point, two deformation paths

For mass division phenomena in low energy proton-induced fission of actinides, systematic studies, including excitation functions, angular distributions and total kinetic energy distributions of the fragments, have been performed by using the JAERI tandem accelerator.

From our earlier work, the following statements were experimentally derived; (i) there exist two different fission threshold energies, leading to symmetric and asymmetric mass divisions, and a few MeV higher threshold is required for the symmetric mass division, and (ii) at least two kinds of scission configurations for certain mass division are verified: compact and elongated scission configurations.

Our recent experiments by a double velocity time-of-flight method have revealed a correlation between the two fission threshold energies and the two scission configurations. The elongated scission configuration is related with the fission process that goes over the higher threshold energy and results in the symmetric mass division, while the compact scission configuration with the process that experiences the lower threshold and ends up with the asymmetric mass division. We claim that there are at least two fission paths from the threshold region to the scission, that is, bimodal nature in fission [1].

Further experiments are being performed to examine the effect of proton and neutron levels in a fissioning nucleus on the two paths. In the symposium, we will review the experimental results, and will discuss systematics in bimodal phenomena from particle-induced fission of light actinides through spontaneous fission of heavy actinides.

[1]. Y. Nagame *et al.*, Phys. Lett. **B387**, 26 (1996).

Fax: +81-292-82-5963, E-mail: nagame@popsvr.tokai.jaeri.go.jp

A06
s.01

RADIOCHEMICAL STUDY OF FAST FISSION MECHANISM

H. Baba, N. Takahashi, A. Yokoyama, and T. Saito
Department of Chemistry, Graduate School of Science, Osaka University, 1-1 Machikaneyama, Toyonaka, Osaka 560, Japan

Summary: Fast fission mechanism was studied radiochemically by means of the $^{238}U+^{12}C$ reaction. The fast fission component was found to reveal itself in the far-asymmetric mass region and follow the Fokker-Planck equation.
Key words: heavy ion fission, uranium-238, carbon-12, diffusion

The reaction of ^{238}U with ^{12}C was studied radiochemically with the purpose of elucidating the fast fission mechanism. From the difference in the mass distribution below and above the expected critical energy where fast fission is predicted to set in, the fast fission component was extracted in the far-asymmetric mass region and interpreted as the mass diffusion following the Fokker-Planck equation. Anomalous charge dispersion widths in the corresponding mass region and a sudden increase of the whole mass distribution width at the critical energy were also observed to support the above result. The reaction times of fast fission deduced from the width and position of the mass distribution were 4×10^{-21} s as well by taking into account the effect of neutron emission from the heavy constituent of the dinuclear system during the diffusion process, which turned out to be more than one order of magnitude longer than the corresponding life time of typical deep inelastic scattering but substantially short compared to ordinary fusion-fission life time as shown in Fig. 1. Evaluation of the driving potential for mass drift required the dinuclear configuration be of an elongated or deformed form for fast fission in contrast to a more compact form for the deep inelastic process. It is concluded that fast fission is an incomplete mass relaxation process due to mass diffusion, not a mere extension of ordinary diffusion but a rather distinctive type of diffusion involving deformation of the once-formed dinuclear system.

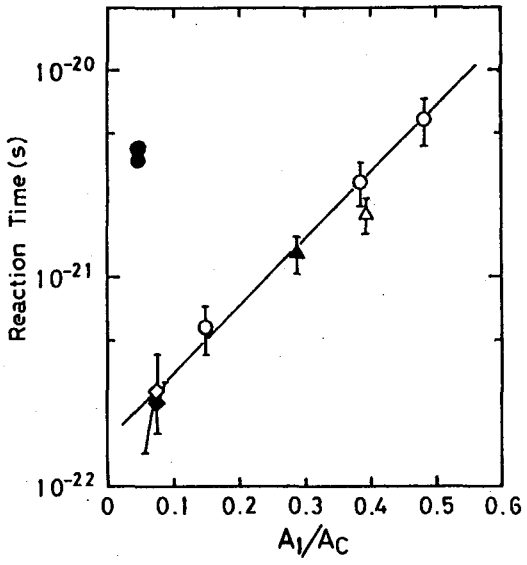

Fig.1. Reaction times deduced in the present work (solid circles) in comparison with those determined from the angular distributions of projectile-like products of the deep inelastic reactions.

A07
s.04

BEHAVIOR OF PIONIC HYDROGEN ATOMS IN GAS AND LIQUID PHASES

A. Shinohara, T. Muroyama[1], T. Miura[2], A. Yokoyama[3], K. Takamiya[3], T. Kaneko[4], T. Saito[3], J. Sanada[3], H. Araki[3], S. Kojima[5], Y. Hamajima[6], H. Muramatsu[7], H. Baba[3], M. Furukawa[8]

Department of Chemistry, Graduate School of Science, Nagoya University, Chikusa-ku, Nagoya 464-01, Japan
[1] LLRL, Kanazawa University, [2] Radiation Science Center, KEK, [3] Graduate School of Science, Osaka University, [4] Faculty of Science, Niigata University, [5] Radioisotope Research Center, Aichi Medical University, [6] Faculty of Science, Kanazawa University, [7] Faculty of Education, Shinshu University, [8] Faculty of Environmental and Information Science, Yokkaichi University

Summary: Pionic X rays and π^0 decays were measured for gas mixtures of $H_2/D_2/CH_4+SF_6$ /Ar and the individual pure gases. Chemical structural effects on the pion transfer process from pionic hydrogen to other atoms were revealed by the pionic X-ray spectrum.
Key words: pion, pionic hydrogen, gas phase, pionic atom, pion transfer, structure effect

Molecular and atomic capture processes of negative pions have not yet completely understood, especially in hydrogen-containing molecules. The transfer of the pion captured by hydrogen to other atoms plays an important role in the overall process. The pion transfer will be affected by the chemical state of hydrogen, by which the pion is captured, and the structure of the atom, to which the pion is transferred from a pionic hydrogen atom. Recently, we found such chemical effects on the transfer process in the several systems of the liquid phase.

We report here some results of the gas phase experiment that was planned to study the behavior of pionic hydrogen atoms without the effects of the intermolecular interactions. A high pressure gas chamber including the counters was newly designed to measure simultaneously the low energy pionic X rays (ex. ~18 keV for πC(3-2)) and two gamma rays from the π^0 decay (indicating the pion capture by hydrogen), and the experimental setup was revised for the gas phase measurement. The samples were the gas mixtures of $H_2/CH_4/D_2$ and SF_6/Ar, and the individual pure gases. The variation by adding hydrogen was found in the pionic X-ray spectrum for both SF_6 and Ar systems.

Figure 1 exhibits the X-ray intensity ratios F(n-2)/S(4-3) as a function of the principal quantum number n in the mixture systems of SF_6(20%). The values are represented as the relative values to those in the pure SF_6. The increase of the pionic X-rays of F with n indicates that the pion transfer to F atoms occurs more frequently than that to S atoms. The transfer parameters can be determined from the concentration dependence of the pion capture probability on hydrogen based on a proposed model involving a large mesomolecular model and an external transfer process. We discuss the structural effects on the pion transfer from the obtained parameters and our previous results in liquid phase experiments.

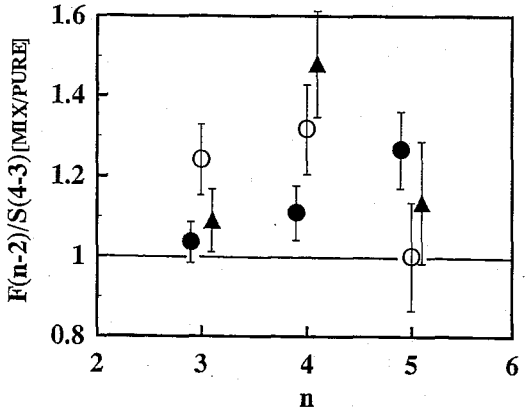

Fig.1. X-ray intensity ratios F(n-2)/S(4-3) against n for the SF_6 mixture systems.
●: H_2+SF_6, O: D_2+SF_6, ▲: CH_4+SF_6

Fax: +81-52-789-2953, E-mail: b42141a@nucc.cc.nagoya-u.ac.jp

A08
s.11

GAS PHASE CHEMISTRY OF TRANSACTINOID ELEMENTS (104 – 106)

I. Zvara, A.B. Yakushev, S.N. Timokhin

Joint Institute for Nuclear Research, Flerov Laboratory of Nuclear Reactions, RU-141980 Dubna, Moscow Region, Russian Federation

Summary: Studies of (oxo)chlorides of the first three transactinoid elements by gas–solid thermochromatography performed at JINR Dubna in recent years are reviewed and these and other data are analyzed to estimate the macroscopic volatility characteristics of the new elements' compounds.

Key words: elements 104, 105 106, thermochromatography, (oxo)chlorides, (oxo)bromides

In the recent ever first chemical identification of element 106 – ekatungsten, a ^{249}Cf target (≈1.0 mg/cm^2) was bombarded with 94-MeV ^{18}O ions (≤3·10^{12} pps) at the JINR U-400 cyclotron. 0.9-s ^{263}106 and as yet unknown ^{264}106 with comparable $T_{1/2}$ and σ could have been expected to form. The bombardment products were continuously on-line separated by gas–solid thermochromatography, i.e., in columns with a negative longitudinal temperature gradient: ≈ 450°C at the hot end and ambient temperature at the cold one; the carrier gas was argon containing some air and vapors of $SOCl_2$. Specifically, whereas, in the particular experimental conditions, Mo and W yielded volatile (oxo)chlorides, transuranium elements with $Z \leq$ 105 did not. The material of the employed open tubular column (fused silica) served as a solid state track detector of the fission fragments, which originated from the s.f. events of element 106 and/or its descendants. In about 120 hours, forty atoms were detected; their inner chromatogram peaked at ≈ 300°C, whereas the simultaneously produced 2.5-h ^{176}W was deposited at ≈ 80°C. The careful analysis showed that the elements had first yielded WO_2Cl_2 and $[106]O_2Cl_2$. The W compound was then slowly reacted to form more volatile $WOCl_4$, whereas the short-lived element 106 had decayed before an analogous conversion could have taken place.

Earlier, in similar columns, 35-s ^{262}105, produced in ^{249}Bk + ^{18}O, was studied with argon + $SOCl_2$ + $TiCl_4$ carrier gas and with argon + Br_2 + BBr_3. Several hundred atoms of the element were recorded. The adsorption behavior of the element 105 compounds was compared with the (oxo)halides of Nb, Ta and Hf. Also 3-s ^{259}104 (a few dozen atoms registered) and some Hf isotopes were compared in the same chlorinating and brominating gases.

Meanwhile, the Swiss (PSI, Villigen) group developed an isothermal gas chromatography technique for studying alpha- and/or s.f.-active isotopes of elements 104 – 106. At the column exit they measured the fraction of atoms which had survived and from this they evaluated the retention times based on the known half-lives. In the case of element 104 they are utilizing 1-min ^{261}104 rather than ^{259}104. The JINR and PSI approaches have provided independent and complementary data on the microvolatility (= adsorbability) of compounds. The consistency of the results of the two groups is analyzed and an attempt is made to evaluate macrovolatility in terms of boiling points, evaporation enthalpies, etc. These parameters are needed when searching for the so called relativistic effects in the chemical properties of the heaviest elements by confronting experimental data with the results of sophisticated relativistic molecular calculations.

Fax: +7-09621-65083, E-mail: zvara@nrsun.jinr.dubna.su

A09
s.13

STABILITY OF RADIO-METALLO-FULLERENE AGAINST BETA-DECAY

K. Sueki, K. Kikuchi, K. Tomura[1] and H. Nakahara

Department of Chemistry, Tokyo Metropolitan University, Minami-Osawa 1-1, Hachiouji, Tokyo 192-03, JAPAN

[1]*Institute of Atomic Energy, Rikkyo University, Nagasaka 2-5-1 Yokosuka, Kanagawa 240-01, JAPAN*

Summary: The aim of this work is to investigate the influence of the change of element within the fullerene cage through nuclear decay process. In the β^--decay of ^{177}Yb-^{177}Lu, the Lu@C_{82} species produced was not at all eluted at the retention time of Yb@C_{82} in the HPLC elution.
Key words: Metallo-Fullerene, M(II)@C_{82}, M(III)@C_{82}, HPLC, Retention time, Beta decay

Recently, in the study of REE endohedral metallo-fullerenes, it has become clear that the encapsulated metal atom takes the +2 oxidation state in the Sm, Eu, Tm, and Yb@C_{82} fullerenes, and the +3 state in other REE@C_{82} fullerenes. If the encapsulated atom is radioactive, its chemical property (atomic number) suddenly changes through radioactive decay. We have previously studied the effect of the β^--decay of ^{161}Gd to ^{161}Tb in the metallofullerene of M@C_{82}, and found that more than 90 % ^{161}Tb remained stable within the C_{82} cage. Such stability of the ^{161}Tb@C_{82} produced through the β^--decay reveals not only a small effect of the recoil energy but also no effective change of the electronic stability (probably both Gd and Tb are in the same oxidation state of +3) even after the change of the atomic number.

The aim of this work is to further investigate the influence which such an elemental change exerts on fullerene through radioactive decay process. Two cases of β^--decay within a C_{82} carbon cage were studied: one in ^{177}Yb-^{177}Lu in which the most stable oxidation state is expected to change from +2 for Yb to +3 for Lu, and the other is ^{171}Er-^{171}Tm in which the oxidation state is expected to change from +3 for Er to +2 for Tm. Since three kinds of isomers are reported for Tm@C_{82} with same oxidation state of +2, it would be also interesting to investigate which isomer survives must the after-effect of β^--decay.

The elution curves for a HPLC column of Buckyprep, 10mmϕx250mm, with a flow rate of 3.2 mL/min. observed by γ-ray measurements are shown in Fig. 1 for the three isotopes (^{169}Yb, ^{175}Yb and ^{177}Lu). In the system ^{177}Yb-^{177}Lu, the Lu@C_{82} species produced by the β^--decay of ^{177}Yb in C_{82} was not at all eluted at the retention time of Yb@C_{82} (at the retention time for Yb@C_{82} in the +2 state) in the HPLC elution, and, instead, about 1/20 was found eluted at the retention time for M(III)@C_{82}. Furthermore, the radioactive ^{177}Lu was observed scattered over the whole fractions of the elution curve, the fact of which might indicate that the species of Lu@C_{82} produced by β^--decay were unstable against some chemical reactions such as dimerization and oxidation and that their reaction products are soluble in toluene but not being eluted at any specific retention time.

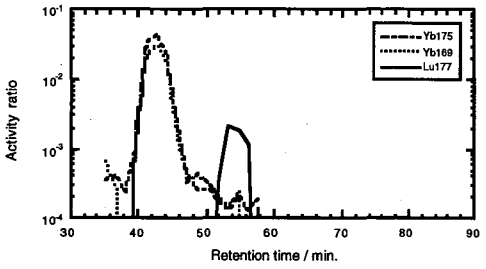

Fig.1 The HPLC elution curves observed three isotopes (^{169}Yb, ^{175}Yb, ^{177}Lu) in irradiated Yb@C_{82} sample.

The experiment on the ^{171}Er-^{171}Tm case is in progress, but results will be presented at the symposium.

Fax: +81-426-77-2548, E-mail: sueki-keisuke@c.metro-u.ac.jp

A10
s.12

REGIOSELECTIVE HYDROGEN ISOTOPE EXCHANGE REACTION IN BENZOIC ACID AND BENZAMIDE

OOHASHI K.[1], SEKI H.[2], and .HASEGAWA H.[1]
Laboratory of Radiopharmaceutical Chemistry, Faculty of Pharmaceutical Sciences, Chiba University[1].
Chemical Analysis Center, Chiba University[2].
1-33 yayoi-cyo, inage-ku, Chiba 263, Japan

Summary: The hydrogen isotope exchange reaction of benzoic acid, its alkali metal salts, and in addition benzamide with D_2O or HTO was studied in the presence of $RhCl_3 \cdot 3H_2O$. On the basis of the experimental results, the reaction mechanism is discussed.

Key word: Tritium, Deuterium, isotope exchange, regioselectivity, rhodium (III) chloride

In a regular exchange run, 158 mg of the rhodium(III) trichloride catalyst, 1.2 mmol of the substrate, and 0.6 ml of HTO or D_2O were dissolved in 3 ml of DMF and were allowed to react at 105-107°C for 11 h. In the tritium exchange, the catalyst showed greater activity towards the alkali metal salts than towards the free acid[1]). Methyl benzoate was inert for the exchange reaction. A similar tendency as described above was observed for the extent of deuterium labeling between benzoic acid and its alkali metal salts. The labeling extent was 85 % in lithium and sodium benzoates and 50 % in benzoic acid under the experimental conditions. Though the evident intermediate is not still given, it was suggested on the basis of the findings that the present highly regioselective hydrogen isotope exchange probably raised *via* an initial coordination of the negatively charged oxygen atom in benzoate ion to the rhodium(III) trichloride catalyst. In the case of benzamide, the lone pair of the nitrogen atom will substitute for the negatively charged oxygen atom.

Tritium incorporation to the lithium salt showed a steep increase with increasing amount of the catalyst and leveled off when it went up to over 30 mg (Fig.1). Further increase in the amount of catalyst resulted in a very gradual decrease in the labeling extent, though the reason is not clear. On the other hand, the incorporation to both the free acid and benzamide gradually increased with increasing amount of the catalyst to 237 mg along similar curves in both case. More than 237 mg of the catalyst deposited in the reaction mixture. The abundance of d_0 predominated in low degree region of deuterium labeling, but it greatly decreased and instead, the production of d_2 was gradually increased beyond that of d_1 with increasing extent of deuterium labeling. On the basis of the above findings, it seems likely that a reversible process is involved in the complex formation of

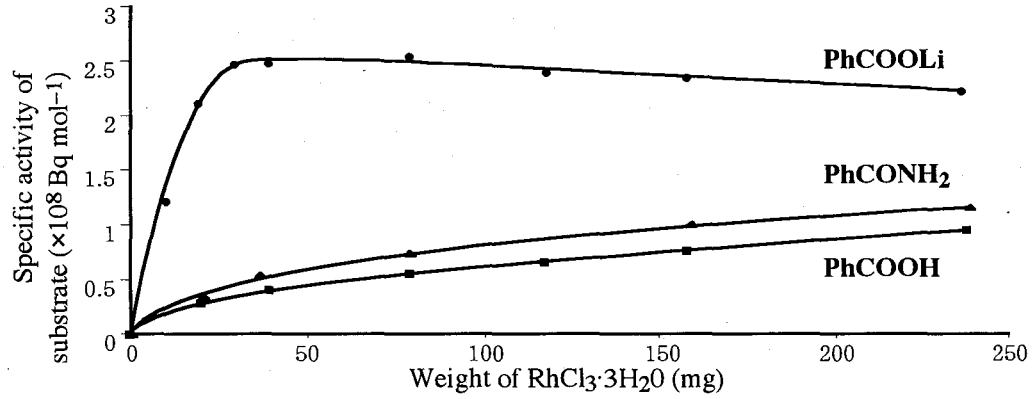

Fig.1 Changes in the specific activities of substrates with the amount of $RhCl_3 \cdot 3H_2O$

carboxylate ion or benzamide with the catalyst ([$PhCOO^-$] + [catalyst] $\rightleftarrows$ [$PhCOO^-$ – catalyst]) as seen in the homogeneous associative π-complex mechanism for the catalytic hydrogen isotope exchange reactions of hydrocarbon and derivatives with metals. The more d_1 molecules are produced, the more chance for double deuterium labeling of d_1 will be given or the more d_2 will be produced.

1) K. Oohashi, Y. Soutome, *J. Radioanal. Nucl. Chem. Letter*, **155**, 65(1991).

A11
s.02

RECOIL PROPERTIES OF RADIONUCLIDES FORMED IN THE PHOTONUCLEAR REACTIONS ON ^{27}Al, ^{nat}Cu, ^{nat}Ag, ^{nat}Ta, AND ^{197}Au AT INTERMEDIATE ENERGIES

H.Haba[1], H.Matsumura[1], Y.Miyamoto[1], K.Sakamoto[2], Y.Oura[3], S.Shibata[4], M.Furukawa[5], and I.Fujiwara[6]

[1]Division of Physical Sciences, Graduate School of Natural Science and Technology, and [2]Department of Chemistry, Faculty of Science, Kanazawa University, Kanazawa-shi, Ishikawa 920-11, Japan
[3]Department of Chemistry, Faculty of Science, Tokyo Metropolitan University, Hachioji-shi, Tokyo 192-03, Japan
[4]Research Reactor Institute, Kyoto University, Sennan-gun, Osaka 590-04, Japan
[5]Faculty of Environmental and Information Science, Yokkaichi University, Yokkaichi-shi, Mie 470-01, Japan
[6]School of Economics, Otemongakuin University, Ibaragi-shi, Osaka 567, Japan

Summary: Thick-target recoil properties of photonuclear reaction products from ^{27}Al, ^{nat}Cu, ^{nat}Ag, ^{nat}Ta, and ^{197}Au at intermediate energies have been investigated using the thick-target thick-catcher method, and the results are discussed by referring to hadron reactions and PICA calculation.
Key words: photonuclear reaction, recoil property, thick-target thick-catcher method

We have been measuring the reaction yields of bremsstrahlung-induced photopion reactions, photospallation, photofragmentation, and/or photofission from ^{7}Li to ^{209}Bi targets using radiochemical techniques systematically in terms of energy and target mass to investigate reaction mechanisms and nuclear structure. Nuclear recoil experiments are expected to give us additional informations related to reaction mechanisms such as angular distributions and/or kinetic energies of products nuclei. Reported here is our applications of the recoil technique to photonuclear reactions and their results of analyses.

The recoil properties of 26 nuclides, varying from ^{24}Na to ^{64}Cu, produced in the photonuclear reactions on ^{nat}Cu (nat: natural isotopic abundance) at bremsstrahlung end-point energies (E_0) of 250 to 1000MeV have been investigated using the thick-target thick-catcher method. Kinematic properties of the product nuclei were calculated by the two-step vector velocity model. The obtained mean ranges smoothly increase with increase of the mass difference (ΔA) between products and target, and show E_0-independence at $E_0 \geqq 600$MeV, reflecting the limiting behavior above (3,3) resonance region. The forward-to-backward ratios (F/B) of the all obtained nuclides are about 2-3. The calculated mean kinetic energies of spallation products increase with increase of ΔA, showing the following three components; (1) (γ, xn) products by giant-resonance and/or quasi-deuteron resonance absorptions, (2) (γ, xnyp) products by mainly (3,3) resonance absorption initiated in the surface region of the nucleus ($\Delta A \leqq 15$), (3) in the deep region of the nucleus ($\Delta A > 15$). The obtained mean kinetic energies at $E_0 \geqq 600$MeV were well reproduced by a calculation performed by PICA (Photon-Induced Intranuclear Cascade Analysis) code by Gabriel and Alsmiller at E_0=400MeV, except for (γ, xn) products by giant-resonance, which is not included in PICA model.

The recoil properties from the additional targets of ^{27}Al, ^{nat}Ag, ^{nat}Ta, and ^{197}Au are now being measured in our group, and the preliminary results show the same trend as ^{nat}Cu. The radionuclides of $A_p = 1/2\text{-}1/3 \times A_t$ are identified in the catcher foils of ^{nat}Ta, and ^{197}Au targets, and their recoil properties exhibit those of fission reaction, clearly distinguished from spallation reaction. These results will be discussed by referring to the previous literature values including hadron-induced reactions, and to the reaction mechanism and the nuclear model on which the PICA is based.

Fax: +81-76-264-5742, E-mail: haba@kenroku.ipc.kanazawa-u.ac.jp

B01
s.21

A CORRELATION BETWEEN ISOMER SHIFTS OF ^{237}Np MÖSSBAUER SPECTRA AND COORDINATION NUMBERS OF Np ATOMS IN NEPTUNYL(V) COMPOUNDS

M. SAEKI[1], M. NAKADA[1], T. NAKAMOTO[1], T. YAMASHITA[2], N. M. MASAKI[1] and N. N. KROT[3], [1]*Advanced Science Research Center and* [2]*Department of Chemistry and Fuel research, Japan Atomic Energy Research Institute, Tokai, Ibaraki, 319-11, Japan,* [3]*Institute of Physical Chemistry, Russian Academy of Science, Moscow, Russia*

Summary: A correlation between isomer shifts of ^{237}Np Mössbauer spectra and the coordination numbers (CN) of Np atoms in neptunyl(V) compounds was established using six compounds in which the CN of Np atoms are known.

Key words: coordination number of Np, isomer shift, Mössbauer effect, neptunyl(V) compound

Abstract: The nature of neptunium makes its chemistry full of variety and attractive, which neptunium possesses five oxidation states of 3+, 4+, 5+, 6+, and 7+, and all of them form complexes. Among the oxidation states, the studies on Np(V) are less than those on other states, especially for the Mössbauer work. In this paper, we will report the ^{237}Np Mössbauer spectroscopic study on a correlation between the isomer shifts and the coordination numbers of Np atoms in neptunyl(V) compounds. Several compounds, which were not studied by Mössbauer spectroscopy, were synthesized from nitric acid solution of freshly prepared neptunyl(V) hydroxide. The concentration of neptunium in the solution was in the range of 10^{-1} M. The formed compounds were identified by means of X-ray diffraction method. The Mössbauer spectra were measured in a cryostat equipped with a driving system (Wissel Co. System MS II). An assembled ^{241}Am metal source was used.

The structures of the malonate ($(NpO_2)_2C_3H_2O_4 \cdot 4H_2O$, I), the formate ($NpO_2OOCH \cdot H_2O$, II), the double formate ($NH_4NpO_2(OOCH)_2$, III) and the glycolate ($NpO_2OOCCH_2OH \cdot H_2O$, IV) are known by X-ray crystallography. Those of the double malonate ($NH_4NpO_2C_3H_2O_4$, V) and the phthalate ($(NpO_2)_2(OOC)_2C_6H_4 \cdot nH_2O$, VI) are unknown, however, the CN of the Np atoms has been confirmed on the basis of electron absorption data. The CN of Np atoms in I, II, IV and VI is 7, that is, pentagonal bipyramid. On the other hand, that in III and V is 8, hexagonal bipyramid. The isomer shifts (δ) of the Mössbauer spectra for the compounds with CN of 7 were spreaded in a small range around -19 mm/s. For the compounds with CN of 8, the larger values were obtained as the δ. This difference between the δ's is explained by the change of electron densities at the nuclei with the CN of Np.

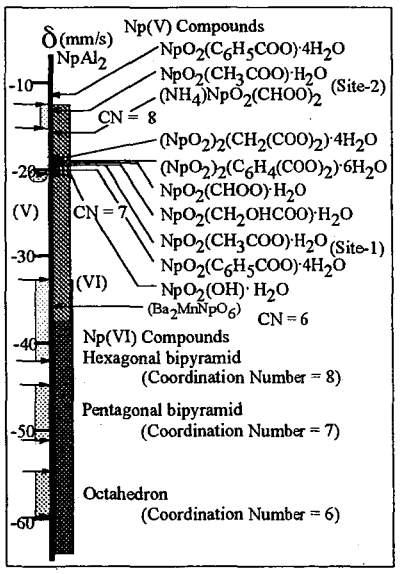

Fig. Summary of isomer shifts in Np Compounds

Fax: 029-282-5927, E-mail: saeki@analchem.tokai.jaeri.go.jp

B02
s.21

SYNTHESIS AND ^{151}Eu- AND ^{57}Fe-MÖSSBAUER SPECTROSCOPIC STUDIES OF NEW EUROPIUM-IRON COMPLEXES

M. KATADA, T. Nawa, H. Kumagai,[1)] S. Kawata,[1)] and S. Kitagawa[1)]

Radioisotope Research Center, Tokyo Metropolitan University, Minami-ohsawa 1-1, Hachioji, Tokyo 192-03, Japan

[1]Department of Chemistry, Graduate School of Science, Tokyo Metropolitan Universiity, Minami-ohsawa 1-1, Hachioji, Tokyo 192-03, Japan

Sammary: New lanthanoid-iron complexes having phenanthlorine as the chelating ligand were synthesized and characterized by Mössbauer spectroscopy. The crystal structure of Eu cmplex was determined by X-ray analysis. The complex consists of one dimensional zig-zag polymer.
Key words: Lanthanoid(III)-iron(III) complex, Polymer complex, Mössbauer spectroscopy

Mössbauer spectroscopy provides very valuable information on the intermolecular interaction in a solid as well as the nature of chemical bonding. However there have been a few studies of lattice dynamics with Mössbauer spectroscopy. In the present work, ^{151}Eu- and ^{57}Fe-Mössbauer spectroscopic studies were carried out to elucidate the lattice dynamics and the electronic state of europium and/or iron atoms in new lanthanoid-iron complexes. The complexes were prepared by mixing 5 mmole of $LnCl_3 \cdot nH_2O$ (Ln = lanthanoids) and 15 mmole of 1,10-phenanthroline (phen) in 25 ml of H_2O and 5 mmole of $K_3Fe(CN)_6$ in 25 ml of H_2O. ^{151}Eu-Mössbauer spectra observed exhibit a single broad line with unresolved hyperfine sturucture. The temperature dependence of areal intensity of ^{151}Eu-Mössbauer spectra falls in the range of the one-dimensional polymers. In the Ln-phen-iron series, the europium complex can be prepared as a single crystal. The crystal structure determined by X-ray analysis consists of one dimensional zig-zag polymer structure. The Eu atom is eight-coordinated to four N atoms of two phenanthrolines, two cyano N atoms and two water molecules in a distorted dodecahedral arrangement. The Fe atom is six-coordinated to cyano C atoms in an octahedral arrangement, FeC_6 group. The phenanthroline molecules involved form stacking structure in the solid. The stack contains two coordinated and two uncoordinated phenanthrolin ligands. The bonding force of inter-molecular is expected to be weak due to the formation of this type of stack. While ^{57}Fe-Mössbauer spectra of lanthanoide-iron complexes consist of a well resolved quadrupole doublet at room temperature. The values of quadrupole spliting (QS) of ^{57}Fe-Mössbauer spectra for Ln-phen-iron powder complexes fairly depend on the ionic radii of lanthanoid ions except for Gd, Yb and Lu ions. The value of QS of powder sample of Eu-complex is similar to those of the powder Ln-phen-iron complexes (Ln = La-Sm, Tb-Tm). However the QS value of the sigle crystal Eu-complex is different from powder complexes and is larger than those of powder ones. This value is similar to that of Gd-complex (powder). We will discuss a correlation between structure and Mössbauer parameters.

B03
s.22

POSITRONIUM AS ACTIVE PROBE OF VACANCIES IN INSULATING MATERIALS

ITO Yasuo

Research Center for Nuclear Science and Technology,
The University of Tokyo, Tokai, Ibaraki 319-11, Japan

Summary: Examples are given to show that Ps can create and/or make larger the holes; the "bubble-like" Ps in low molecular weight organic solids and in plasticized by sorption polymers. However, this active nature of Ps can be turned into usefulness.

Key Words: Positronium, nanometer size vacancies, sorption, polymers, organic solids

Positronium is supposed to be an excellent probe of molecular size holes in insulating materials, but there is a question whether it is reflecting the native vacancies correctly. Due to the very large zero-point energy it is quite probable that Ps can "dig" holes as it does make "bubbles" in liquids. Furthermore when many holes are connected as in polymers, Ps will seek the largest holes where the zero-point energy is the least. In either case the vacancy information brought forth by Ps leads to an overestimation.

Formerly we reported that Ps can take two states in many low molecular weight organic solids. The lifetime of one of them, the longer lived one, is smoothly connected from the "Ps bubble" state as if it were in a super-cooled liquid. This was a puzzle at the time of its finding, but now we are almost sure that Ps is creating holes in these solids. *(Y. Ito, H.F.M. Mohamed and M. Shiotani, J. Phys. Chem., 100, 14161 (1996))*

In polymers, however, such drastic evidence for Ps creating holes had not been observed. Recently we performed the positron annihilation experiments of sorption of CO_2 gas into polymers and the result was as follow. The lifetime τ_3 and intensity I_3 of o-Ps showed a V-shaped dependence on the CO_2 pressure. Their decrease at low CO_2 pressures was attributed to the Langmuir-type sorption, and the increase at large pressures is due to the Henry-type sorption. The rise of τ_3 and I_3 due to the Henry-type sorption was so conspicuous that they could exceed their initial values before the sorption. For detailed examination we measured the amount of the sorbed CO_2 and the change of the overall volume. The free volume, estimated from these measurements decreased or remained unchanged at the high CO_2 pressures where τ_3 and I_3 Increased. Apparently Ps is digging holes in these states where the movements of the polymer chains are becoming easier, or plasticized, due to the sorption.

Whether "vacancy spectroscopy" using Ps can be realized or not would depend on how we deal with the active nature of Ps interaction with holes. There is some hope that the active nature is turned into usefulness instead of regarding as a shortage.

FAX: 81-29283-2374 E-mail: tsu01314@koryu.statci.go.jp

B06
s.21

Sb–121 AND Fe–57 MÖSSBAUER SPECTRA OF ANTIMONY–CONTAINING IRON CARBONYL COMPLEXES: $[HSb\{Fe(CO)_4\}_3]^{2-}$ AND $[Sb\{Fe(CO)_4\}_4]^{3-}$

M. Maeda, M. Takahashi* and M. Takeda

Department of Chemistry, Faculty of Science, Toho University, Funabashi, Chiba 274, Japan

Summary: ^{121}Sb Mössbauer spectra for the title complexes, whose isomer shifts are intermediate between the organoantimony(III) and organoantimony(V) compounds, suggest that the considerable electrons are donated from hydrido ligand and $\{Fe(CO)_4\}$ fragments to antimony atom.

Key words: ^{121}SbMössbauer Spectra, ^{57}Fe Mössbauer Spectra, Intermetallic Bond

Recent studies on the complexes having the bonds between d–block and heavy p–block elements have led to a number of exciting molecules with novel molecular structure and bonding. We have studied the ^{121}Sb and ^{57}Fe Mössbauer spectra for $A_2[HSb\{Fe(CO)_4\}_3]$ (A = Et_4N, PPh_4, PPN) and $A_3[Sb\{Fe(CO)_4\}_4]$, having a tetrahedral $HSbFe_3$ and $SbFe_4$ core, respectively, to elucidate the Sb–Fe bond. Interestingly the ^{121}Sb Mössbauer spectra at 20 K for these clusters are almost symmetrical absorption peaked at *ca.* 8 mm s^{-1} relative to source, being the intermediate region between the typical organoantimony(III) and organoantimony(V) compounds. The ^{121}Sb Mössbauer spectra for $A_2[HSb\{Fe(CO)_4\}_3]$ (isomer shift (δ) = 0.99 mm s^{-1} relative to InSb, quadrupole coupling constant (e^2qQ) = –2.0 mm s^{-1} for PPh_4 and Et_4N salt) indicate almost spherical electron distribution around the antimony atom and suggest that considerable amount of electrons are donated from the $\{Fe(CO)_4\}$ fragment to the antimony 5p orbitals; since the e^2qQ values are extremely small, the degree of the electron donation is almost the same as to that of the hydrido ligand. The ^{121}Sb Mössbauer parameters for $(Et_4N)_3[Sb\{Fe(CO)_4\}_4]$ (δ = 0.00, e^2qQ = 0.0 mm s^{-1} (experimentally)) are close to those of $[HSb\{Fe(CO)_4\}_3]^{2-}$ salts, supporting the above considerations. The slightly smaller δ value, corresponding to the increased s electron density at the antimony nucleus, for $(Et_4N)_2[Sb\{Fe(CO)_4\}_4]$ is due to increased 5p electron population of Sb atom through the shielding effect.

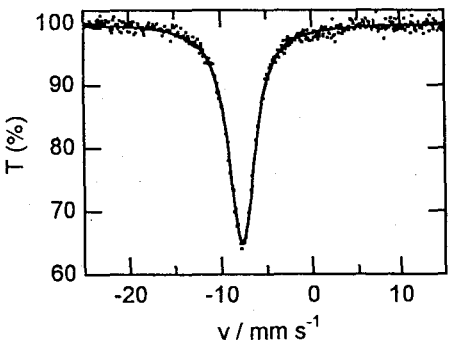

Fig. 1 ^{121}Sb Mössbauer spectrum for $(Et_4N)_2[HSb\{Fe(CO)_4\}_3]$ at 20 K.

The ^{57}Fe Mössbauer parameters at 80 K for $(Et_4N)_2[HSb\{Fe(CO)_4\}_3]$ (δ = –0.07 mm s^{-1} relative to α–iron foil, quadrupole splitting (QS) = 2.57 mm s^{-1}) are close to those of $Fe(CO)_5$. The smaller QS value for $(Et_4N)_2[HSb\{Fe(CO)_4\}_3]$ may indicate that the electrons are donated to antimony 5p orbitals.

fax +81-474-75-1855 e-mail takahasi@ns2.toho-u.ac.jp

B07
s.21

APPLICATION OF THE '*Tg*−Δ RULE' TO THE LOCAL STRUCTURAL STUDY OF FERRATE GLASSES

T. NISHIDA, S. KUBUKI, and Y. MAEDA
Department of Chemistry, Faculty of Science, Kyushu University
Hakozaki, Higashiku, Fukuoka 812-81, Japan

Summary: Mössbauer and DTA study of aluminoferrate and galloferrate glasses revealed that the glass transition temperature (*Tg*) is in proportion to the quadrupole splitting (Δ) of Fe(III). The slopes of the straight line (650~680) indicate that Fe(III) substitutes Al(III) and Ga(III).
Key words: ferrate glass, '*Tg*−Δ rule', distortion of FeO_4, Mössbauer, DTA

A linear relationship named the '***Tg*−Δ rule** [1]' exists between the glass transition temperature (*Tg*) of inorganic glasses and the quadrupole splitting (Δ) of Fe(III), which occupies the sites of either the network former (NWF) or the network modifier (NWM). The '***Tg*−Δ rule**' implies that the *Tg* of oxide glass is primarily determined by the distortion of NWF−oxygen polyhedra. The iron (III) occupies tetrahedral NWF sites, *e.g.* Si(IV) and B(III) sites, in several oxide glasses [1,2]. In this case, a large slope of 680 $^{o}C/(mm{\cdot}s^{-1})$ is obtained from the straight line of the *Tg vs.* Δ plot. By contrast, the slope becomes 260 when the Fe(III) occupies octahedral NWF sites, as recently observed in tungstate glasses [3]. In the case of phosphate, sulfate, and fluoride glasses in which Fe(III) is weakly bonded to anions at NWM sites, much smaller slope of 35 is obtained [1].

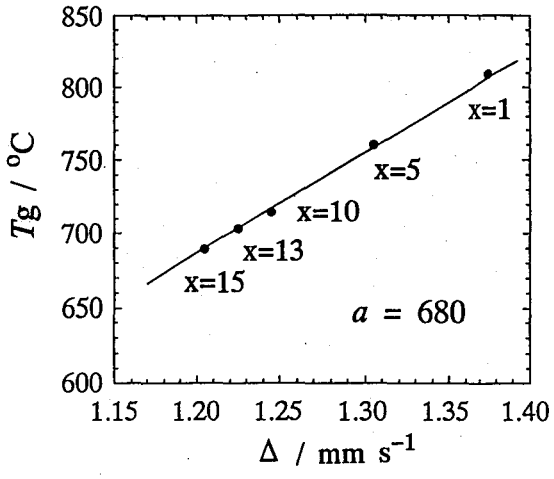

Fig. 1. The *Tg vs.* Δ plot for $60CaO{\cdot}(40-x)Al_2O_3{\cdot}xFe_2O_3$ glasses

Figure 1 illustrates the *Tg vs.* Δ plot obtained for $60CaO{\cdot}(40-x)Al_2O_3{\cdot}xFe_2O_3$ glasses. The slope of the straight line was estimated to be 680. In the case of $60CaO{\cdot}(40-x)Ga_2O_3{\cdot}xFe_2O_3$, $50CaO{\cdot}(50-x)Ga_2O_3{\cdot}xFe_2O_3$, and $40CaO{\cdot}(60-x)Ga_2O_3{\cdot}xFe_2O_3$ glasses, the slopes of the straight lines were estimated to be 650, 670, and 660, respectively. These values indicate that the distorted FeO_4 tetrahedra substitute distorted AlO_4 or GaO_4 tetrahedra. The large slopes of 650~680 are ascribed to the small change of Δ, because the tetrahedral NWF undergoes a smaller structural change than the octahedral NWF or NWM.

References:

1) T. Nishida, H. Ide, and Y. Takashima, *Bull. Chem. Soc. Jpn.*, **63**, 548 (1990).
2) T. Nishida, *Z. Naturforsch.* **51a**, 620 (1996).
3) T. Nishida, M. Suzuki, S. Kubuki, M. Katada, and Y. Maeda, *J. Non-Cryst. Solids.*, **194**, 23 (1996).

Tel/Fax: +81-92-642-2591. E-mail: glassscc@mbox.nc.kyushu-u.ac.jp

B08
s.21

MOSSBAUER SPECTROSCOPY OF NANOCLUSTER SYSTEMS.

I. P. Suzdalev
N. N. Semenov Institute of Chemical Physics, Russian Academy of Sciences, Russia.

"Summary":The paper deals with dynamic and magnetic phase transitions in nanocluster systems including ironoxide nanocluster and polymer systems.The properties of these systems depends on intercluster interactions and can be changed by the action of hydration, surfactants,freezing, pressure.

"Key words":nanocluster systems,Mossbauer spectroscopy,thermodynamics,phase transitions.

For nanocluster region of the matter there appear new properties compared to that in the atomic dispersions and in the massive materials.Two groups of size effects are considered for iron oxide cluster systems: intracluster dynamics connected with melting of the cluster and magnetic phase transitions in clusters. The following cluster systems were under study: (1) ferrihydrite clusters isolated in pores of polysorbes, (2) oxyhydroxide clusters isolated in pores of sulphonated exchange resin. (3) gamma iron oxide clusters non-modified by carbon inclusions and (4) gamma iron oxide clusters modified by carbon inclusions.

For nanoclusters (1) and (4), an increase in intracluster atomic mobility was observed upon reaching critical size of clusters (d ~ 2 - 3 nm). This effect was discussed by thermodynamic approaches taking into account quantum effects of fluctuation between solid and liquid states, change of cluster surface energy, change in chemical potential and drop in melting point typical of small clusters. Intracluster atomic mobility was shown to increase by the action of surfactants.

Ordinarily the isolated magnetic clusters lose the magnetic ordering by second order magnetic phase transitions or by superparamagnetic behavior when the magnetic moment of a cluster fluctuates as a whole.Besides the second order magnetic phase transitions in nanoclusters, the first order magnetic phase transitions were observed in nanocluster systems (1), and (4). This phenomenon was interpreted by thermodynamic approaches in terms of the first order magnetic phase transition in nanoclusters or the jump-like magnetic transition (JMT). The JMT was shown to be very sensitive to the surface energy, cluster-cluster, cluster-support interactions, magnetostriction and cluster compressibility. There were predicted the appearance of new properties of the matter at the point of association of isolated nanoclusters into a nanocluster system. The new properties may also arise under the action on clusters of external pressure and hydration of the matrix.

The thermodynamic approach introduces the critical parameters of the system suffering the effect of JMT: critical size (d_{CR}) of a cluster and temperature (T_{CC}) at which the cluster system loses magnetic ordering by the jump. For nanocluster systems (1) and (4) the following critical parameters were obtained by Mössbauer spectroscopy: d_{CR} ~ 3 nm, T_{CC} ~ 7 - 10K and d_{CR} ~ 12 nm, T_{CC} ~ 200 - 300K, respectively. These values are in a rather good agreement with the thermodynamic predictions.

For clusters (2), the hydration of polymeric matrix was shown to shift the critical temperature of magnetic phase transition by ca. 3 - 4K. This effect was interpreted in terms of variation of the extent of cluster-support interaction changing surface energy of the cluster. For relatively large clusters (4) with d ~ 12 nm, the shift of the critical temperature for magnetic phase transition was treated in terms of the lattice strain (pressure) induced by carbon inclusions.

e-mail suzdal@glasnet.ru

B09
s.21

MOSSBAUER SPECTRA OF $(Fe_{0.5}Zn_{0.5})PS_3$ AND ITS INTERCALATION COMPOUNDS

H. Sakai *, T. Yamazaki , N. Machida , T. Shigematsu, and S. Nakashima[1)]

Department of Chemistry, Faculty of Science, Konan University
Okamoto 8-9-1, Higashinada-ku , Kobe 658 , Japan
[1)] Radioisotope Center, Hiroshima University
Kagamiyama 1-4-2, Higashi-Hiroshima 739 , Japan

$(Fe_{0.5}Zn_{0.5})PS_3$, isomorphous with $FePS_3$, ordered antiferromagnetically at 100K. Mossbauer spectra of the compound, similar to that of $FePS_3$ at room temperature, indicated no magnetic hyperfine interaction at 80K.
Key words : Mossbauer Spectroscopy, Magnetic Susceptibility, Layer Structure

It is known that $FePS_3$ and $ZnPS_3$ form a complete series of solid solutions by isomorphous replacement of iron by zinc. In the present work Mossbauer spectra and magnetic susceptibilities of $(Fe_{0.5}Zn_{0.5})PS_3$ are measured and compared with those of $FePS_3$. The temperature dependence of magnetization revealed that $(Fe_{0.5}Zn_{0.5})PS_3$ ordered antiferromagnetically at about 100K, though observed at 126K for pure $FePS_3$. The Neel points were shifted to lower temperatures as the content of zinc increased. Mossbauer spectra of $(Fe_{0.5}Zn_{0.5})PS_3$ indicated a paramagnetic quadrupole doublet at room temperature and 80K, while $FePS_3$ showed the magnetic hyperfine pattern with internal magnetic field of 90kOe at 80K.

We succeeded in preparing $(Fe_{0.5}Zn_{0.5})PS_3$ intercalated with pyridine. In the XRD pattern of the intercalation compound the diffraction peaks corresponding to $(Fe_{0.5}Zn_{0.5})PS_3$ were completely missing, suggesting that the intercalation were performed completely with pyridine. The Mossbauer spectra are changed significantly by the intercalation, suggesting the charge transfer from guest molecules to the host matrix. The spectra consist of three quadrupole doublets, corresponding to a low spin Fe^{2+} state and two kinds of high spin Fe^{2+} states, indicating that pyridine is intercalated ununiformly in the host crystal. The Mossbauer spectra are quite similar to those of $FePS_3$ intercalated with pyridine.

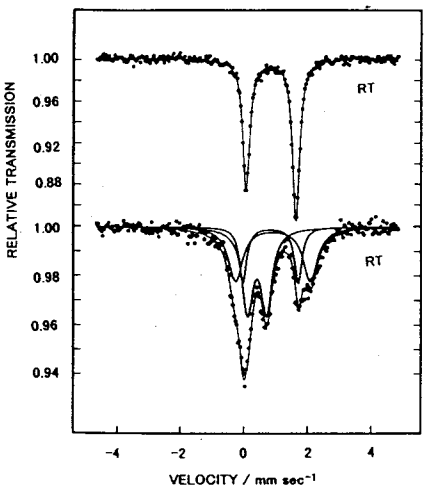

Mossbauer spectra of $(Fe_{0.5}Zn_{0.5})PS_3$ and $(Fe_{0.5}Zn_{0.5})PS_3$ intercalated with pyridine at RT.

H.Sakai Fax: +81-78-435-2539, E-mail: hisakai@center.konan-u.ac.jp

B10
s.21

MÖSSBAUER SPECTROSCOPIC STUDIES OF MOLECULE-BASED MAGNETS: $NBu_4[Fe(II)_xMn(II)_{1-x}Cr(III)(ox)_3]$ AND $NBu_4[Fe(II)_xNi(II)_{1-x}Fe(III)(ox)_3]$

S. Iijima, S. Koner and F. Mizutani

National Institute of Bioscience and Human-Technology, Higashi 1-1, Tsukuba, Ibaraki 305, Japan

Summary: The variation of the direction of internal magnetic field at ^{57}Fe nucleus was investigated for $NBu_4[Fe(II)_xMn(II)_{1-x}Cr(III)(ox)_3]$ and $NBu_4[Fe(II)_xNi(II)_{1-x}Fe(III)(ox)_3]$ by using Mössbauer spectroscopy.
Key words: Mössbauer spectroscopy, easy axis of magnetization, metal oxalates

A series of mixed-metal assemblies $NBu_4[M(II)M(III)'(ox)_3]$ are known to exhibit bulk magnetism, where NBu_4^+ = tetra(*n*-butyl)ammonium ion, ox^{2-} = oxalate ion. Mössbauer spectroscopy provides significant information regarding their electronic and magnetic structures [1,2]. In the present work, particular attention has been paid to the directions of the internal field ($\boldsymbol{H}_n$) derived from the magnetically-split ^{57}Fe Mössbauer spectra of these complexes.

The angle (Θ) between $\boldsymbol{H}_n$ and the principal axis of V_{zz} was estimated to be *ca.* 90° for $NBu_4[Fe(II)Cr(III)(ox)_3]$ [1] from the Mössbauer absorption of Fe(II), where V_{zz} is the principal component of the electric field gradient tensor; this means that the $\boldsymbol{H}_n$ is approximately parallel to the honeycomb layers consisting of an alternate array of the bivalent and tervalent ions through ox^{2-} ligands. The mixed crystals $NBu_4[Fe(II)_xMn(II)_{1-x}Cr(III)(ox)_3]$ showed a variation of the Θ with x (Fig. 1a). When x was lowered below 0.5, the Θ began to decrease gradually first and then approached 0° rapidly. This results indicate that the easy axis of magnetization in $NBu_4[Mn(II)Cr(III)(ox)_3]$ is perpendicular to the honeycomb layers. It was suggested that the strong magnetic anisotropy of high-spin Fe(II) governs the Θ - x profile.

Similar kind of the variation of Θ was observed for the Fe(III) in $NBu_4[Fe(II)_xNi(II)_{1-x}Fe(III)(ox)_3]$ (Fig. 1b). The Θ values at x = 1 and 0 were estimated to be 81(10)° and 28(5)°, respectively [2]. When x was between 0.5 and 0.0, the mixed crystals showed intermediate Θ values. As for both $NBu_4[Fe(II)_xMn(II)_{1-x}Cr(III)(ox)_3]$ and $NBu_4[Fe(II)_xNi(II)_{1-x}Fe(III)(ox)_3]$, it was confirmed from the plots of the quadrupole splitting *vs.* x that the sign of V_{zz} was not changed by x.

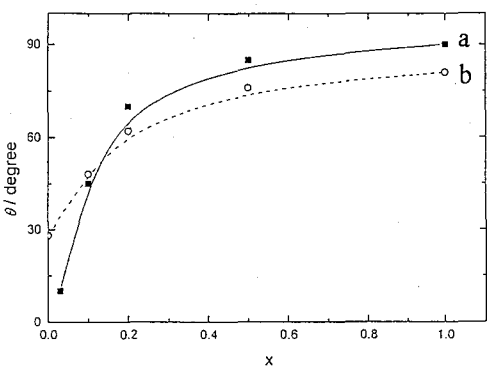

Fig. 1. The variations of Θ with x.

It seems interesting that such a wide variation of Θ was observed, while $NBu_4[M(II)M(III)'(ox)_3]$ assemblies and their mixed crystals essentially exhibit a common molecular structure. In addition, the above results suggest that the direction of the easy axis of magnetization in this metal oxalate system can be controlled freely by the method of mixed crystallization.

1. S. Iijima, et al., *Mol. Cryst. Liq. Cryst.*, **233**, 263 (1993).
2. S. Iijima, et al., *Inorg. Chim. Acta*, **253**, 47 (1996).

B11
s.20

STRUCTURAL STUDIES OF THE LANTHANIDE (III) IONS IN THE AQUEOUS NITRATE AND CHLORIDE SOLUTIONS

Tsuyoshi YAITA, Hirokazu NARITA, Shinichi SUZUKI and Shoichi TACHIMORI

Department of Chemistry and Fuel Research, Japan Atomic Energy Research Institute
Tokai-mura, Naka-gun, Ibaraki, 319-11 Japan

Summary: Structural parameters of the trivalent lanthanide ions in the aqueous nitrate and chloride solutions were measured by the extended x-ray absorption fine structure (EXAFS). We discussed the differences in coordination properties of nitrate, chloride ions and water.
Key words: Lanthanide, EXAFS, Aqueous solution, Nitrate ion, Chloride ion, Water

Abstract

Structural studies for lanthanides (III) in the aqueous chloride and perchlorate solutions have been studied by many researches, but unexpectedly those in the nitrate ones are little. Aqueous nitrate solutions are often used for the separations of the lanthanides such as solvent extraction and ion exchange. Since nitrate ions have the relatively high stability constants with lanthanides in the fundamental anions. Structural informations are useful for understanding the separation behavior of lanthanides. Accordingly, we studied the solvation structures of lanthanide ions in the aqueous nitrate solutions by the EXAFS, and also in the chloride ones as a comparison. Sample solutions were prepared by the dissolution of lanthanum nitrate and chloride salts into waters and acid solutions. These samples were sealed with the polyethylene film including teflon spacer. The EXAFS spectra around LIII-edge of lanthanides were measured in the transmission mode at the BL-27B station of KEK. Figure 1 shows that the representative radial structural function (RSF) by the Fourier transformed EXAFS. The RSF appeared to be mainly characterized by the coordinative oxygens of water (a~d) and of nitrate ion (a,b): the peaks around 200 pm and the non-coordinative oxygens of nitrate ion (a,b): the peaks around 380 pm. From these results, nitrate ions form inner-sphere complexes with lanthanide ions. In contrast, we did not observe chloride ions around lanthanides in Fig. 1, therefore, chloride ions do not form inner-sphere complexes. The quantitative analyses of EXAFS data have revealed that the coordination numbers of the lanthanides ranged from about 8 to about 9 in all the samples. The bond distances were from about 230 to 250 pm for Ln - OH_2 and from about 240 to 260 pm for Ln - O_2NO. The nitrate ions coordinate to the lanthanides about 10 pm longer in bond distance than waters.

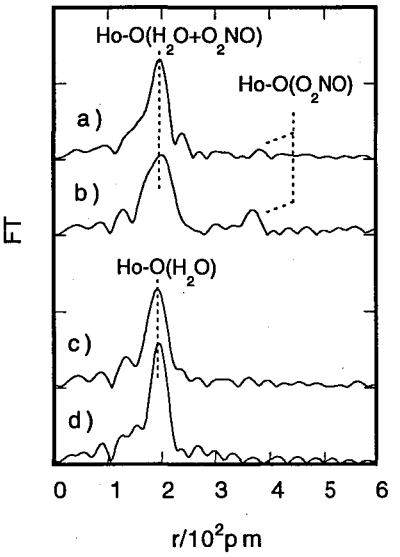

Figure 1. Radial structural function in the aqueous Ho^{3+}- NO_3^- and Cl^- solutions. a)1M Ho(NO3)3-H2O, b)1M Ho(NO3)3-6M HNO3-H2O, c)1M HoCl3-H2O,d)1M HoCl3-6 M HCl-H2O

Fax: +81-29-282-6723, E-mail: yaita@mummy.tokai.jaeri.go.jp

C01
s.51

UPTAKE KINETICS OF DEUTERIATED WATER VAPOR BY PLANTS: EXPERIMENTS OF D_2O RELEASE IN A VINYL HOUSE AS A SUBSTITUTE FOR TRITIATED WATER

N. Momoshima[1], H. Kakiuchi[1], T. Okai[2], S. Yokoyama[3], H. Noguchi[3], M. Atarashi[4], H. Amano[4], S. Hisamatsu[5], M. Ichimasa[6], Y. Ichimasa[6], Y. Maeda[1]

[1]*Dep. of Chem. Fac. of Sci., Kyushu Univ., Hakozaki, Higashiku, Fukuoka, Japan.*
[2]*Dep.of Nucl. Eng., Fac.of Eng., Kyushu Univ., Higashiku, Fukuoka, Japan.*
[3]*Dep. of Health Phy., JAERI, Tokaimura, Naka, Ibaraki 319-11, Japan.*
[4]*Dep. of Enviro. Safety Res., JAERI, Tokaimura, Naka, Ibaraki 319-11, Japan.*
[5]*Depa. of Public Health, Akita University School of Medicine, Hondo, Akita, Japan.*
[6]*Fac. of Sci., Ibaraki University, Mito, Ibaraki, 310 Japan*

Summary: D_2O vapor release experiments were carried out in a vinyl house to examine uptake of D2O by plants. The D_2O level in leaf reached an equilibrium with that in air within a few hours, suggesting rapid uptake from leaf surface.
Key Words: Tritium, D_2O, uptake, plants

Tritium inventory in ITER, a nuclear fusion ractor under planing, would be comparable to that of natural tritium. Plants around the facility would be exposed to tritium from the facility. To examine uptake of tritium by plants, we carried out release experiments using deuteriated ,water (D_2O) as a substitution for tritium.

D_2O release experiments were carried out in a vinyl house in autumn 1995 and summer 1996 in which different kinds of plants cultivated in pots were placed and exposed to D_2O vapor. A typical result of 1995 experiment was shown in Fig. 1. The concentration of D_2O in air increased rapidly after starting the release and reached constant level at 4 h. The D_2O concentration in air decreased rapidly after taking off the vinyl sheet of the house. The D_2O concentration in Komatsuna followed that in the air but increase and decrease patterns showed time delay and the equilibrium concentration was apparently lower than that in the air. The D_2O in pot soil was highest at the surface and decreased gradually toward deep layer, but their concentrations were clearly lower compared to that in air and the leaf. This fact suggests that the uptake of D_2O was mainly occurred at stoma in leaf, small contribution from soil water. However, after removing the vinyl sheet the D_2O concentrations showed higher level than that of general air, suggesting contribution of soil water to leaf. The decrease of D_2O concentrations in soil was slow. The present results suggests that uptake by leaf surface is a major pass way to plant during the tritium paff is passing and soil water becomes a source after the paff passed.

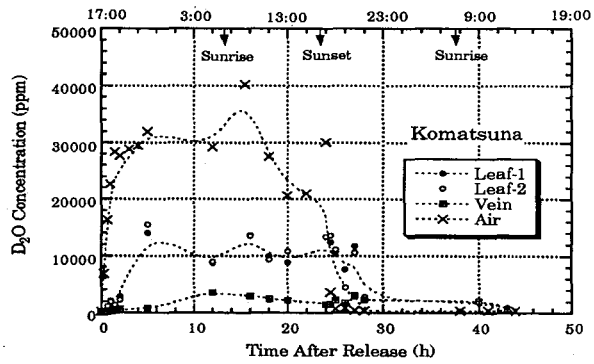

Fig. 1 D_2O concentrations in air and Komatsuna

Fax: +81-92-642-2607, E-mail:momoscc@mbox.nc.kyushu-u.ac.jp

C02
s.52

VALIDATION OF PROGRAM SYSTEMS FOR INSTRUMENTAL NEUTRON ACTIVATION ANALYSIS

K. Heydorn

Isotope Division, Risø National Laboratory, DK-4000 Roskilde, DENMARK

Summary: Reliable results by neutron activation analysis depend not only upon validated software for γ-spectrometry; validation of the entire program system may now be carried out by the T-test, which ascertains statistical control of all sources of variability.
Key words: Validation, Neutron Activation Analysis, T-test, Statistical Control, γ-spectrometry

Validation of software for γ-spectrometry has attracted considerable attention over a number of years, and most recently the International Atomic Energy Agency has taken the initiative to produce γ-spectra suitable for testing and validating commercial software for processing of spectra with up to 8 K channels, obtained by actual counting of γ-sources with a germanium semiconductor detector.

The availability of validated software for γ-spectrometry opens the possibility of validating the entire program system used to arrive at the final analytical results by instrumental neutron activation analysis. Replicate results should remain in statistical control, regardless of differences with respect to neutron flux density, irradiation, decay, and counting times, counting equipment, counting geometry, dead time, pile-up, peak widths, as well as sample size, matrix, etc. etc.

An experimental design is presented that incorporates these variables, as well as many of the factors mentioned, in a manner that checks the absence of influence under practical conditions of analysis. Verification of statistical control is carried out by means of the statistic **T**, which closely follows a χ^2-distribution, and which is very sensitive to deviations even at relatively small numbers of degrees of freedom.

In the actual investigation it is essential to use materials of unquestionable homogeneity, and therefore we have chosen a series of environmental reference materials produced by the SM&T Programme of the European Union. These materials offer a variety of trace elements at concentrations varying by many orders of magnitude, and therefore suitable for testing the validity of our method over the entire range of experimental conditions.

It was found that with carefully implemented procedures of analysis in combination with a suitably validated program for processing of γ-spectra, statistical control could be maintained under all practical conditions. When the experimental investigations are carried out with certified reference materials that are relevant to the intended application of the method, validation of the entire analytical method is simultaneously achieved.

Fax: +45-4677-5347, E-mail: heydorn@risoe.dk

C03
s.51

EVALUATION OF ENVIRONMENTAL TRITIUM LEVEL IN PREOPERATIONAL PERIOD OF CERNAVODA CANDU NUCLEAR POWER PLANT

N. PAUNESCU, M. COTARLEA, D. GALERIU, R. MARGINEANU, N. MOCANU

National Institute of Research and Development for Nuclear Physics and Engineering-Horia Hulubei, Bucharest-Magurele, P. O. Box MG-6, Romania

Summary: The paper presents the concentration of environmental tritium in air, water, soil and vegetable in the area of a new heavy water reactor and the evaluation of some tritium environmental transfer parameters (from atmosphere to forage, from irrigation water to land and vegetable).

Key words: Tritium, environment, transfer parameters, heavy water reactor, preoperational level.

In Romania, a CANDU nuclear power plant with five reactors of 600 MWe is under construction. The first unit reached its criticality in April 1996 and became operational at full power in December 1996. The nuclear power plant is placed in Cernavoda area, in the S-E of Romania, between the Danube River and the Danube-Black Sea Canal. The prevalent lacal climate is continental and the agricultural land starting in the immediate vicinity of nuclear power plant is of intensive type.

The routine atmosphereic tritium releases from the 3 GWe nuclear power plant are expected to be about 460TBq $(aGWe)^{-1}$ and the aqueous releases are estimated to 350TBq $(aGWe)^{-1}$.

The aim of this study was to evaluate the environmental tritium reference level before starting of the nuclear power plant. Representative samples for Cernavoda area were analysed: air humidity; water from Danube River, Danube-Black Sea Canal, lakes; drinking and ground water, rain (snow) water; soil at different depths; tissue free water tritium in vegetal and animal foodstuff relevant for human diet: cereals (wheat, maize, barley), vegetables (potato, tomato, cabbage, onion, bean), fruits, grapes, wine and milk; organically bound tritium in wheat and maize grains.

Equipment and methods: Liquid scintillation analyzer tip TRICARB 1900 TR; scintillation cocktails type Instagel and Pico Fluor LLT; sampling system for trapping the atmospheric tritium on molecular sieves; furnace; vacuum line and freeze trap (-60 ℃); equipment for simple, fractionating and azeotropic distillation.

Results and discussion: The background level of tritium concentration was determined in environmental samples in Cernavoda area, in preoperational stage of nuclear power plant. The mean values determined during 1994-beginning of 1996 are: (7.4 ± 5.5) Bq/L in air humidity, (3.1 ± 0.7) Bq/L in tissue water from vegetable and (0.6 ± 0.2) Bq/L in tissue water from cereals (grains). The values of tritium concentration in air, water, soil and plants are low, as for an area without contamination sources. The presence of tritium in these samples is due to common fallout. Steady-state conditions are achieved for environmental transfer of tritium in the absence of local tritium source. Considering the environmental transfer model from Canadian standard [CAN/CSA-N288.1-M87, 1987], we calculated the transfer parameters for deposition from atmosphere on forage and crops (P_{14}), and the contamination of land and vegetation by spray irrigation water, (P_{24}) The default values comparing with our values are presented in the following table:

	P_{14} (m^3 kg^{-1})	G_w (kg L^{-1})	f_v	P_{24} (L kg^{-1})
Default values	50	1.05	0.85	0.81
Cernavoda area	29-49	1.2±0.4	0.96±0.30	0.90±0.27

Fax: (401)420-91-01, E-mail: paun@carmen.ifa.ro

C06
s.51

DETERMINATION OF FALLOUT Pu IN THE VOLCANIC SOIL OF KOREA

M. H. LEE, C. W. LEE AND J. H. LEE

Korea Atomic Energy Research Institute, P. O. Box 105, Yusung, Taejon, Korea

Summary :
Key words:

The Pu contamination level in the terrestrial environment due to atmospheric fallout is highly variable with time and geographic location. Their behaviors are very complicated, and are largely dependent on the physico-chemical properties of soil, the chemical forms of these nuclides, and the biological and physicochemical processes in a given environment. In this study, the concentration of $^{239,240}Pu$, ^{238}Pu and ^{241}Pu and their isotopic ratio in the volcanic soil were investigated to estimate the contribution of atmospheric nuclear tests and Chernobyl accident to Korea in these time.

Soil samples were colleted from 5 sites in Cheju island in 1996. Sampling points of soil were selected on a flat area, if possible, in order to exclude precipitation run-off. In each site, 5 to 10 soil samples were taken with a core sampler (4.5 cm in diameter) within an area of about 50 m × 50 m to a depth of about 5 cm. The samples were dried at 110℃ for 48 h after pebbles and fragment of plant root were removed and then sieved through a 1.0 mm screen. Radiochemical analysis of $^{239,240}Pu$, ^{238}Pu and ^{241}Pu were carried out on aliquots of 100 g soil. The purified Pu fraction was divided into two nearly equal parts: one part was subjected to beta (^{241}Pu) by a low background liquid scintillation counter (QUANTULUS 1220 WALLAC), and the other part was used for the measurement of other Pu isotopes ($^{239,240}Pu$, ^{238}Pu) by means of alpha-ray spectrometry (EG&G ORTEC).

The results of the mean values with standard deviation in the volcanic soil was 84.9 ± 16.9 (individual data ranged from 62.8 to 110.7) Bq/m^2 for $^{239,240}Pu$, 3.48 ± 1.93 (2.19 to 4.51) Bq/m^2 for ^{238}Pu, and 313.6 ± 120.8 (432.7 to 186.6) Bq/m^2 for ^{241}Pu. The concentration of fallout Pu are higher than that in other forest site. This result is explained by geological and geographical location of sampling and the characteristic of the volcanic soil. Cheju island has more precipitation than any other area. When rain falls on the volcanic soil which has the porosity and permeability of the lavas, it easily percolate on the volcanic soil. The loss of nuclides by rainwater rolling off on the volcanic soil is smaller than that on other soil. Also the organic matter (more than 40%) forms complexes with fallout radionuclides such as plutonium compound and fix fallout radionuclides in the soil.

The activity ratio of $^{238}Pu/^{239,240}Pu$ and $^{241}Pu/^{239,240}Pu$ varies according to the source and can be utilized to identify the different sources of release. The mean activity ratio of $^{238}Pu/^{239,240}Pu$ in soils was calculated to be 0.042, a little higher than the value of 0.037 which is characteristic of fallout from nuclear weapon testings. The small difference in the value of activity ratio can be explained by insufficient purification of the Pu-fraction from other alpha-emitters like ^{238}Th. But, the mean activity ratio of $^{238}Pu/^{239,240}Pu$ is not very different from the typical value of worldwide fallout. The mean activity ratio of $^{241}Pu/^{239,240}Pu$ in the volcanic soil was found to be 3.72, which corresponds to that observed in the cumulative deposit from the global fall-out of nuclear weapon testing. Therefore, the contribution of the Chernobyl-derived plutonium to Korea was negligible relative to their concentrations from weapon testings, considering that the reporting value of $^{238}Pu/^{239,240}Pu$ was 0.47 in the Chernobyl fallout over Sweden and that of $^{241}Pu/^{239,240}Pu$ was 85 in the Chernobyl fallout over Finland.

Fax: +82-42-863-1289, E-mail: cwlee@nanum.kaeri.re.kr

C07
s.52

FLUORINE DETERMINATION BY 2.5 MeV NEUTRON ACTIVATION ANALYSIS

M. N. Al-Haddad, A. Aksoy and F. Z. Khiari

Energy Research Laboratory, King Fahd University of Petroleum and Minerals, Dhahran 31261, Saudi Arabia

Summary: Fluorine was determined using 2.5 MeV neutrons from D(d,n) reaction. The induced activity of ^{16}N was used as an indicator for fluorine in Teflon samples. Measurements were done with cyclic activation. Minimum detection limit was around 1 g for 1 cycle and 0.5 g for 3 cycles.

Key words: Fluorine, fast neutrons, rabbit system, cyclic activation, minimum detectable limit.

Fluorine is important as a trace element in water supplies, as a significant constituent of minerals in the earth's crust, as a constituent of synthetic polymers. The purpose of this study is to investigate the capability of the KFUPM 350 kV light ion accelerator in determining the fluorine content using the 2.5 MeV D(d,n) neutron activation analysis technique. Fluorine detection is based on the $^{19}F(n,\alpha)^{16}N$ reaction, with a threshold neutron energy of 1.6 MeV. The ^{16}N decays to ^{16}O with a half-life of 7.13 seconds resulting in γ-rays of 7.12 MeV and 6.13 MeV energies. Polytetrafluorethylene (PTFE: C_2F_4) samples were imvestigated for their fluorine content. Two PTFE samples with masses of 2.2 g and 8.5 g were transferred in polyethylene capsules between the counting and irradiation stations using an automatic fast sample transfer (Rabbit) system with 4 sec transfer time. The γ-rays from ^{16}N were counted with a shielded pair of 5" x 5" NaI(Tl) detectors placed face-to-face and connected to a PC-based data acquisition and analysis system. The energies below 4.1 MeV were rejected by the lower level of SCA. Data was acquired in pulse height mode using an ADCAM multichannel buffer (MCB) with 4096 channels. The total number of counts was also registered in a counter-timer. The identification of the element ^{19}F was carried out by verifying the 7.13 sec half-life from the data acquired using a multichannel scaling (MCS) unit with a 1 sec dwell time. The attached figure shows the decay curves of ^{16}N for three cycles. Optimization of the experimental setup such as energy threshold of the SCA, irradiation, delay and counting times has been carried out.

The minimum detection limit of fluorine improved with the number of irradiation cycles and it was found to be about 400 mg for three cycles. The time was set on the system to automatically transfer the samples in 4 sec back to the counting station after 60 sec irradiation for a counting period of (40 - 60) sec. This cycle of 60 sec irradiation, 4 sec decay and (40 - 60) sec counting times was repeated a few times to study the variation of the sensitivity of the detection system. Results and details of the experiment along with supporting drawings, figures and tables will be presented.

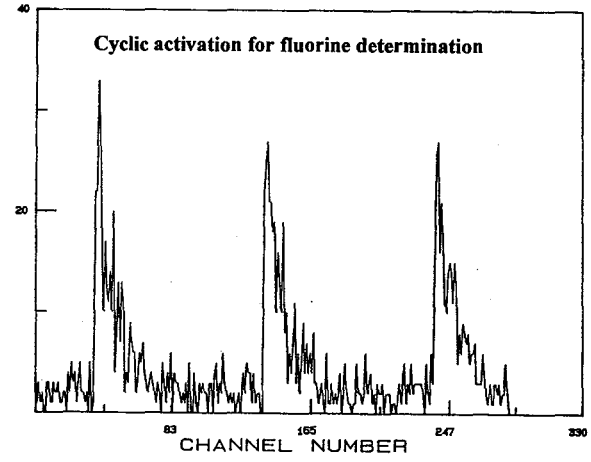

Fax: +00 966 3 860 42 81, E-mail:meyassar@dpc.kfupm.edu.sa

C08
s.52

DETERMINATION OF BORON IN JAPANESE GEOCHEMICAL REFERENCE SAMPLES BY NEUTRON-INDUCED PROMPT GAMMA-RAY ANALYSIS

C. YONEZAWA, P. P. RUSKA, H. MATSUE, M. MAGARA and T. ADACHI
Japan Atomic Energy Research Institute, Tokai-mura, Naka-gun, Ibaraki-ken 319-11, Japan

Summary: Determination of traces of B in the Japanese geochemical reference samples has been performed by neutron-induced prompt γ-ray analysis using cold and thermal guided neutron beams of the JRR-3M. Accuracy of the results were evaluated by comparing with those of the other methods.
Key words: Neutron-induced prompt γ-ray analysis, B, Japanese geochemical reference sample

A neutron-induced prompt γ-ray analysis (PGA) is one of the highest sensitive analytical methods for B, and can determine ppb levels of B nondestructively. Although the destructive analytical methods such as inductively coupled plasma-atomic emission spectrometry and spectrophotometry have serious problems of contamination and evaporation loss of B in the course of chemical treatment, PGA has less possibility for such problems and can give accurate determination. Owing to the Doppler broadened γ-ray line for B 478 keV, 11 elements including Na, Ni, Cl showed spectral interference in the determination of B. However, serious interference was given practically by Na. In the present work, we have examined the spectral interference correction by the following three methods: 1) computer fitting, 2) reference peak method, and 3) subtraction of the Na 472 keV peak area predicted from the Na concentration. In the first method, the interfered peak shape was decomposed by fitting B peak as an integrated Gaussian function, whereas for the other interfering peaks like Na as a normal Gaussian function. In the second method, Na interference was corrected using 92 and 869 keV peaks as reference peaks. In the third method, interfered B peak area was subtracted with Na 472 keV peak area which was predicted from the Na content determined by PGA. Determination of B contents in 21 Japanese geochemical reference samples has been performed by the three interference correction methods.

The determination was carried out by using a PGA system at the cold and thermal neutron beam guide of 20 MW reactor JRR-3M with a neutron flux at the sample position of 1.4×10^8 (cold) and 2.4×10^7 (thermal) n cm^{-2} s^{-1}, respectively. Twenty-one of igneous and sediment rocks reference samples distributed by Geological Survey of Japan (GSJ) were analyzed. After being dried at 105 °C for 7 h, the samples (100-250 mg) were heat-sealed in 25 μm thick fluorinated ethylene propylene resin (FEP) film. Standard B samples (B 4.86-102 μg) were prepared by evaporating portions of a standard B solution onto a filter paper of 13×13 mm^2, then heat-sealed in the FEP film. The Compton suppression spectra of the samples and standard B samples were measured for 15000-50000 s and 1000-5000 s, respectively, in He atmosphere with both the cold and thermal neutron beams. The B peak area was determined by computer fitting and covell's methods, setting the region of interest at 466-490 keV. The background counts of B were evaluated by measuring 7 pieces of the FEP films and were corrected in the determination.

For almost all samples, variations of the analytical results were less than 10% except for the samples of low B content (B <3 ppm), where the variations were 1.6-20%. The analytical results among the three correction methods were agreed within 10% except for low B content samples such as JDo-1, JF-1 and JG-3. The accuracy of the analytical results was confirmed by comparing with the other values. The analytical results obtained by the fitting method agreed within 20% to the compiled values of 1994, except for JF-1, JF-2, JGb-1, JG-1a and JP-1, of which analytical values were deviated 22-97% from the compiled values. The analytical results obtained by the present methods tended to give relatively higher values comparing with the compiled values. Because the fitting method can correct the interference not only from Na but also from Cl, Ni and others simultaneously, it seemed that the fitting method presented most reliable results among the correction methods investigated. Sodium contents in the reference rock samples were also reported.

FAX: 81-29-282-6097, E-mail: yonezawa@analchem.tokai.jaeri.go.jp

C09
s.52

COMBINATON OF ACTIVATION ANALYSIS AND SOME OTHER MODERN ANALYTICAL TECHNIQUES - NEW POSSIBILITIES FOR STUDY OF ENVIRONMENT

I. V. SHTANGEEVA

Institute of Earth Crust, St. Petersburg University, Universitetskaya nab., 7/9, St. Petersburg 199034, Russia

Summary: INAA and ICP-MS methods were used to study variations in chemical element concentrations of plants. Interactions among different ions (both toxic and biologically essential) during their penetration into the plant tissues was studied.

Key words: INAA, ICP-MS, environmental pollution, trace elements.

Instrumental neutron activation analysis and method ICP-MS were used to study different variations of chemical element behaviour in water, soil and some species of plants in natural environment and experimental conditions. Use both these analytical techniques for elemental analysis allowed to determine in environmental samples concentrations of up to 60 different chemical elements. It is important that INAA enables us to analyse any environmental samples in their natural state. In spite of use of ICP-MS method for analysis of environmental samples requires additionally sufficiently elaborate samples preparation, but in this case we can obtain information about many important and very interesting for environmental study chemical elements, for example, Pb, Li, Mn, Mg, Cu, V, Al, Ti and some others. On the other hand, determination of these last elements by INAA presents some dificulties or may be even impossible. In our work some regularities of chemical elements bioaccumulation were studied. Element redistribution among environment and different parts of plants from polluted areas compared with those from background zones (for example, forests far from any sources of pollution). Influence of increased concentrations of some toxic elements in environment on change in elemental composition of plants (including biologically essential elements) was also studied in experiment: plants were grown in water and soil with additions of Cd, Ag, Cr, Ca and different combinations of these elements. It was found that environmental pollution can cause significant variations in both elemental composition and also physiological functions of the plants.

Fax: (812)218-28-35, E-mail: Irina@ivs.usr.pu.ru

C10
s.51

APPLICATION OF RADIOCHEMICAL METHODS AND DISPERSION MODEL IN THE STUDY OF ENVIRONMENTAL POLLUTION IN BRAZIL

Ieda I. L. Cunha, Rubens C.L.Figueira, Roberto Saito.
Radiochemistry Division - IPEN-CNEN-SP
Caixa Postal 11049 - Pinheiros - São Paulo, Brazil.

Summary: Methodologies for analysis of anthropogenic and natural radionuclides in marine samples were developed and applied in environmental samples. Radioactivity levels obtained represent reference values to Brazil.
Key words: Anthropogenic radionuclide, natural radionuclide, marine sample.

Abstract. In the last years there has been an increasing interest in artificial and natural radionuclides present in the environment and their possible effects on human health.The radionuclides can be transported across long distances from their source of emission, removed from the atmosphere and deposited in the biosphere and hydrosphere and enter to the human population by several pathways and one of them is the marine environment.
Considering these problems and the lack of information concerning our country,monitoring programs are been carried out concerned with investigations on radionuclide levels in marine samples. Radiochemical methods for precise determinations of cesium-137, strontium-90, plutonium-239, lead-210 and polonium-210 in seawater, fish, sediment and seaweed have been already developed. Since 1991, marine samples are been collected at different locations from the brazilian coast.
Results of systematic measurements of these radionuclides have showed that artificial radioactivity levels are in agreement with the values from regions not affected directly by nuclear accidents or nuclear reprocessing plant discharges and are due to the global fallout.The average concentration of Cs-137 is of 1.4 $Bq.m^{-3}$ in seawater, ranged from 13 to 220 $mBq.kg^{-1}$ in fish, and from 0.2 to 1.5 $Bq.kg^{-1}$ for sediments. Levels of Sr-90 in seawater are of 1.8 $Bq.m^{-3}$ and in fish varied from 19 to 75 $mBq.kg^{-1}$. Sediments present concentrations of Sr-90 lower than 0.8 $Bq.kg^{-1}$ and for Pu-239 of 0.05 $Bq.kg^{-1}$. Po-210 levels in fish ranged from 0.5 to 5.3 $Bq.kg^{-1}$.The data generated represent reference values for our country and are used to estimate the intake levels of these radionuclides by consuming of marine products.
A study for Cs-137 radionuclide dispersion in the surface water was also developed.The Ocean Model simulates the surface water contamination caused by routine or accidental releases.For the model simulation, it was applied in the North Sea, based on the published transfer coefficient data.Results obtained show that the model provides a good response to evaluate the radionuclide dispersion in the marine environment.
This work is part of a research programme that aims at providing technology for reliable assessment of radionuclide contamination, at ensuring the capability of our laboratory to perform radionuclide analysis present in low concentration in environmental samples and at maintaing a data base of radionuclide levels.

FAX: 5511-816-9188; e-mail: marmelin@ih0.ipen.br

C11
s.62

DEVELOPMENT OF PULSE TIME INTERVAL ANALYSIS (TIA) COMBINED WITH PSD-LIQUID SCINTILLATION COUNTING FOR THE DETERMINATION OF ENVIRONMENTAL α-NUCLIDES

T. Hashimoto, Y. Yoneyama, K. Sato, Y. Komatsu

Department of Chemistry, Faculty of Science, Niigata University 950-21, Japan

Summary: Time interval analysis (TIA), which has been verified to be suitable for the selective extraction of correlated successive α–decay events within liquid scintillator, was further developed by combining the pulse shape descrimination technique and simple chemical analysis.

Key words: time interval analysis, liquid scintillation counting, environmental α-emitters

The recent development of electronics and scintillation chemicals make us possible to discriminate conveniently pulse shapes derived from scintillator between α- and β-decay events as known a pulse shape discrimination (PSD) as well as prominent improvement of energy spectrum resolution in the liquid scintillation counting technique.

In order to enhance the detection sensitivity of α–α successive decay-events, the PSD method associated with high resolution α-counting technique was successfully incorporated into the time interval analysis (TIA) method, which has been preferably available for the selective determination of correlated successive decay events associated with millisecond lives. As a result, the detection efficiency has been enhanced owing to elimination of β-rays in background or random pulse events in Th- and Ac-series in addition to confirmation of β–α correlated decay events in shorter time interval region due to ^{214}Bi(β)-^{214}Po(α)- decay processes in uranium series. The ^{225}Ra, belonging to Np-decay series and β-emitter of 14.9 days half-life, was also detectable to the TIA-technique after the long period cooling in the mixture of radium-extractant added small amounts of HDEHP, which was proved to maintain equilibrium state between Ra and its descendants.

The present counting system has been verified to be applicable to the simultaneous detemination of three (including Th, Ac, and Np) decay series if the chemical purification of radium fraction was applied to the environmental samples using an extractive scintillator (RADEX); the TIA method was practically employed to the simultaneous determination of α–α correlated events due to Th-, Ac-, and Np-decay series as a yield tracer nuclide, in addition to utilization of an α-peak area at lowest energy for the determination of ^{226}Ra itself in uranium decay series.

Finally, this radioanalytical method was practically applied to the determination of natural radionuclides belonging to three decay series in environmental samples and compared with the alpha-spectrometric results using a Si-surface barrier detector.

Fax:+81-25-262-6116 or 6169, E-mail: `thashi@curie.sc.niigata-u.ac.jp

D01
s.02

NUCLEAR DATA LIBRARIES AND ONLINE SERVICES FOR RADIOCHEMISTRY

P.Obložinský, O.Schwerer, D.W.Muir and R.M.Iyer

International Atomic Energy Agency, P.O.Box 100, A-1400 Vienna, Austria

Summary: The IAEA operates the most comprehensive collection of nuclear data libraries worldwide, many of them relevant also to radiochemistry applications. This paper gives an overview of databases available from the IAEA online via the Internet (WWW, Telnet and FTP).

Key words: Nuclear data, cross sections, nuclear decay, databases, Internet, Worldwide Web

The nuclear databases maintained at the IAEA Nuclear Data Center contain data libraries important for all areas of nuclear science and technology including radiochemistry, such as data for nuclear reactions and nuclear decay, nuclear fission, activation analysis and dosimetry. While the IAEA nuclear data services by conventional mail have a long history, we focus here on the rapidly expanding computerized nuclear data online services offered to the nuclear science community. The most important databases available are the following:

Nuclear decay databases, including half-lives, nuclear level schemes and decay properties. The major library is ENSDF (Evaluated Nuclear Structure Data File) covering more than 2500 nuclides; these data are published regularly in the journal "Nuclear Data Sheets" and are available online. The NUDAT database contains the most important decay data, ground and metastable state information as well as related reaction data and is available online. The Nuclear Wallet Cards contain ground- and metastable state information in condensed form and are available as a booklet and online.

Specialized bibliographies: NSR (Nuclear Science References), contains references for low and medium energy nuclear physics from 1910 to present; published in "Nuclear Data Sheets" and available online. CINDA (Computerized Index of Neutron Data), references to microscopic neutron reaction cross sections from 1935 to present, published regularly as a book and available online.

Nuclear reaction databases (all available online): ENDF - recommended nuclear reaction data libraries for general purpose applications, for incident neutrons up to 20 MeV, supplemented by some data for higher energies and/or incident light charged particles. FENDL - comprehensive library of neutron/photon transport and activation/decay data for fusion and other fast-neutron applications. EXFOR - collection of experimental nuclear cross section data for incident neutrons, photons and charged particles. Additional data libraries for special purposes are available off-line and will gradually be included in the online services.

On top of its function as a data distribution center, the IAEA Nuclear Data Section has an active data development program, using research contracts and coordinated research programs, for the creation and improvement of nuclear databases which may be of importance also to radiochemistry.

Fax: +43-1-20607
email: oblozinsky@iaeand.iaea.or.at
Nuclear Data Services URL:
http://www-nds.iaea.or.at/

D02 s.43 DETAILED STUDY OF THE γ-RADIOLYSIS OF NTA IN A SIMULATED, MIXED NUCLEAR WASTE

A. P. Toste
Southwest Missouri State University (SMS), Chemistry Department, 901 So. National Avenue, Springfield, MO 65804-0089 (USA).

Summary: γ-Radiolysis of the chelating agent NTA in a simulated, mixed nuclear waste resulted in total NTA degradation, with the formation of 4 chelator fragment and 2 dicarboxylic acids as degradation products, which accounted for 9.1% of the original organic content.

Key words: NTA radiolysis, simulated mixed nuclear waste, chelator fragments

The management of mixed nuclear wastes is an international issue of major import, filled with numerous challenges for the scientists and engineers charged with the daunting task of managing them. For example, enormous stockpiles of mixed nuclear wastes await permanent disposal at the U.S.A. Department of Energy's Hanford Site.

Past research, begun at the Hanford Site, confirms that the chemistry of mixed nuclear wastes can be quite complex. In addition to myriad inorganics and radionuclides, these wastes often contain complex mixtures of organics, including both hazardous and nonhazardous compounds. One waste, in particular, a complex concentrate waste derived from reprocessing spent fuel at the Hanford site nearly thirty years ago, was found to contain numerous nuclear-related organics. Compounds identified include chelating agents like EDTA, NTA, and HEDTA and complexing agents like citric acid, which have been used extensively in the nuclear industry as decontamination agents, etc. Analysis of this mixed waste also revealed the presence of 38 different, structurally related chelator and complexor fragments, occasionally at relatively high concentrations, presumably formed via organic degradation, suggesting that the organic chemistry of mixed wastes is not static, but very dynamic.

Current research addresses the chemodynamics of organics in mixed wastes by characterizing the degradation of chelating and complexing agents in simulants of the complex concentrate waste. Recent studies confirm that both radiolysis and the waste's harsh chemistry do indeed mediate the degradation of mixtures of chelating and complexing agents. However, in both of these studies, the use of organic mixtures in the simulants precluded elucidating the degradation of each parent organic.

The aim of this study was to study the effect(s) of γ-radiolysis on the stability of the chelating agent nitrilotriacetic acid (NTA) in mixed nuclear wastes. A nonradioactive simulant of Hanford's complex concentrate waste was prepared by adding 11.9 mM NTA to an inorganic matrix, which was formulated based on past analyses of the actual waste. The simulated waste was then irradiated in a ^{60}Co-source (75,000 ± 10% R/hr) for 0, 5, 10, 50 and 100 hours. The parent compound NTA and any degradation products, or chelator fragments, formed were analyzed as methyl esters by gas chromatography (GC) and GC/mass spectrometry (GC/MS).

Analysis of the irradiated samples indicated that NTA degradation began immediately at an exponential rate, with the most pronounced decline occurring in the first 10 hours of irradiation. All of the NTA disappeared by 100 hours of radiolysis, corresponding to a γ-dose of 7.5 x 10^6 R. Four chelator fragments were identified as degradation products: N-[N'-amino(2-iminoethyl)]-iminodiacetic acid (AIEIDA), N-(methylamine)iminodiacetic acid (MAIDA), N-(methyl)-N,N'-(methylamine)-ethylenediamine-N-acetic acid (MeD'MAED'A) and iminodicarboxy acid (ICC). Two dicarboxylic acids, oxalic and hexanoic acids, were also formed. The simulants' total organic content (TOC) decreased with increasing radiation, indicating that the radiolysis of EDTA is dispersive. Only 9.1% of the original TOC remained after 100 hrs of irradiation.

The GC/MS system, Hewlett-Packard's MS Engine, was purchased via a grant from the National Science Foundation's Instrumentation and Laboratory Improvement Program (Grant USE-9051582), along with a contribution from Syntex Corporation and SMS matching funds.

FAX: 001 1 417 836 6934 ; E-mail: apt248f@cnas.smsu.edu

D03
s.51

SEPARATION OF CARRIER FREE ^{95m}Tc FROM NIOBIUM TARGETS IRRADIATED WITH ALPHA PARTICLES

T. Sekine, M. Konishi, H. Kudo, K. Tagami [1] and S. Uchida [1]

Department of Chemistry, Graduate School of Science, Tohoku University, Sendai 980-77, Japan

[1] Environmental and Toxicological Sciences Research Group, National Institute of Radiological Sciences, Ibaraki 311-12, Japan

Summary : Tc-95m produced by the ^{93}Nb(α,2n)^{95m}Tc reaction was quantitatively separated from the α-irradiated niobium targets by a sublimation method, giving a high quality ^{95m}Tc tracer as a chemical yield monitor suitable for the analysis of environmental ^{99}Tc by ICP-MS.
Key words : ^{95m}Tc tracer, Sublimation, ^{93}Nb(α,2n)^{95m}Tc reaction, ICP-MS, ^{99}Tc

Technetium-99 with a long half-life ($T_{1/2}$ = 2.111 x 10^5 y) has been released into the environment as a result of increasing nuclear events, and the migration of ^{99}Tc attracts interest in environmental studies. Inductively coupled plasma mass spectrometry (ICP-MS) allows us to detect ppt or less levels of ^{99}Tc, employing a high isotopic quality of technetium tracer as a chemical yield monitor. Although ^{95m}Tc has a suitable half-life (61 d) and emits preferable γ-rays as the monitor, ICP-MS spectra of commercial ^{95m}Tc solutions show large background peaks at mass numbers of 97, 98 and 99, arising from contamination with other technetium isotopes.

In this paper, we report preparation of a high quality ^{95m}Tc tracer by a sublimation method. Technetium-95m was obtained by the ^{93}Nb(α,2n)^{95m}Tc reaction bombarding niobium metal foils with α particles from a 40 MV AVF cyclotron at the Cyclotron Radioisotope Center, Tohoku University. The irradiated foils were placed in a quartz tube and heated at 1100 °C in an oxygen gas flow. Technetium oxide was sublimated and quantitatively separated from the niobium targets within 2 h. The technetium oxide deposited on the inner wall of the quartz tube was easily removed by washing with a small amount of water, as a pertechnetate solution. An aliquot of this solution was subjected to ICP-MS to examine the contamination with technetium isotopes in the mass region between 93 and 104. There were no peaks at mass numbers 97, 98 and 99. The contamination level at mass 99 was as low as the detection limit (0.02ppt) of ^{99}Tc by ICP-MS. The sublimation method is superior to wet chemical processes and provides a carrier free ^{95m}Tc tracer without any contamination of ruthenium or molybdenum, which interferes the ^{99}Tc measurement by ICP-MS. This tracer is suitable for ICP-MS and has been practically used to determine the concentration of ^{99}Tc in environmental samples.

Fax : 81-22-217-6597, e-mail : tsekine@mail.cc.tohoku.ac.jp

D04
s.32

PREPARATION AND EXPERIMENTAL STUDY OF ^{125}I-Tyr^3-OCTREOTIDE

F. Wang, X.H. Jing, Y.S. Wang and L. Xiao*
China Institute of Atomic Energy, P. O. Box 275(58), Beijing 102413, P. R. China

Summary: ^{125}I-Tyr^3-octreotide was prepared by chloramine-T method. The quality control was perpormed by reverse phase HPLC. The stability in mice blood and urine was determined. Animal experiments show that labeled compound was excreted mainly through liver and gallbladder.
Key words: ^{125}I-Tyr^3-octreotide, somatostatin analoque, HPLC analysis

Radiolabeled octreotide, a somatostatin analogue, is a useful agent to image the somatostatin receptor-bearing tumors. It has been shown previously that ^{125}I-labeled octreotide possess biological activities as natural somatostatin, binds to receptors on cell membranes of these tumors. We report here the preparation and experimental study of ^{125}I-Tyr^3-octreotide. ^{125}I-Tyr^3-octreotide was prepared by chloramine-T method. Excessive peptide was used in order to prevent oxidation of the disulfide bridge of the Tyr^3-octreotide. The quality control was performed by reverse phase HPLC. Iodination gave labeling yield of >80% and a radiochemical purity of >95% was obtained after purification with SEP-PAK (C_{18} reverse extraction cartridge). The stability of ^{125}I-Tyr^3-octreotide in mice blood (in vitro and in vivo) and in urine (in vivo) was determined by HPLC respectively. Free $^{125}I^-$ from decomposition in blood could be found as a percentage of 40% to 60% 3hr postinjection, but a free $^{125}I^-$ content of <3% only was produced at room temperature even 24hr after mixing blood and ^{125}I-Tyr^3-octreotide in vitro, see table 1. Biodistribution study in normal mice showed rapid blood clearance ($T_{1/2}$ = 4min). The tracer was excreted mainly through liver, gallbladder into guts. There was a high adrenal uptake due to plenty of somatostatin receptors in adrenal glands; the %ID reached to the highest value at 1hr after administration, then decreasing after 2hr. Our preliminary data suggest that a 5-fold excessive peptide is optimal to assure a high labeling efficiency. The ^{125}I-Tyr^3-octreotide is stable in vitro, but decomposes to free $^{125}I^-$ in vivo. This compound labeled in our laboratory will be used as a tracer for further biological studies of somatostatin receptor-bearing tumors.

Table 1 Percent Radioactive Content of free $^{125}I^-$ Decomposed in Blood and Urine

	30 min	*3 hr*	*24 hr*
Blood (in vitro)	< 3 %	< 3 %	< 3 %
Blood (in vivo)	40 %	60 %	> 80 %
Urine	40 %	40 %	40 %

FAX: +86-10-69357195, E-mail: wangf@mipsa.ciae.ac.cn

D05
s.32

PRELIMINARY STUDIES ON 1-(5-IODO-5-DEOXY-ß-D-ARABINOFURANOSYL)-2-AMINOIMIDAZOLE (IODOAMINO-IMIDAZOLE ARABINOSIDE: IAIA) AS A POTENTIAL SPECT BRAIN AND TUMOR IMAGING AGENT

H.C. Lee[1], P. Kumar[1], A.J. McEwan[2], L.I. Wiebe[1], and J.R. Mercer[1,2,*]

[1]*Faculty of Pharmacy and Pharmaceutical Sciences, University of Alberta, Edmonton, Alberta, Canada T6G 2N8*
[2]*Department of Radiology and Diagnostic Imaging, University of Alberta, Edmonton, Alberta, Canada T6G 2N8*

Summary: An ^{125}I-labeled arabinofuranosyl 2-aminoimidazole nucleoside was evaluated as a potential SPECT brain and tumor imaging agent. Although this compound did not display any uptake into the brain, it showed significant uptake in tumor tissue at 4 h post injection in mice.
Key words: [^{125}I]Iodoaminoimidazole arabinoside, IAZA, hypoxia, SPECT, nitro-reduction

[^{123}I]Iodoazomycin arabinoside ([^{123}I]IAZA), an arabinofuranose sugar-coupled 2-nitroimidazole hypoxic imaging nucleoside developed at the University of Alberta, has been shown to have selective uptake into hypoxic tissues in both animal studies and preliminary human studies with cancer patients. Recently, it has been under investigation to assess tumor hypoxia in advanced cancer patients and to assess limb hypoxia in patients with diabetes mellitus. A very unexpected observation in the imaging of about one-third of patients from the preliminary studies was the brain uptake of radioactivity in the later images (18-24 h) which was sufficiently intense to provide excellent images of the brain. The time course of this highly unusual uptake was not consistent with perfusion images and has been postulated to represent metabolic trapping of radioactivity in the brains of those patients receiving diagnostic doses of [^{123}I]IAZA.

There is no evidence to suggest that IAZA is actively accumulated in brain and therefore the observed brain uptake of radioactivity may be accounted for by a metabolite. However, the actual species or metabolite has not been determined or identified. The present proposed metabolic route involves the reduction of the nitro group on the imidazole base to the amino group via the nitro-reduction process. This process occurs in all living cells but in hypoxic cells nitro compounds can be further reduced via the nitroso and hydroxylamine intermediates to give amino derivatives. This amino derivative is hypothesized to be the candidate responsible for the observed brain uptake of radioactivity. Iodoaminoimidazole arabinoside (IAIA) was prepared by reduction from IAZA and labeled with ^{125}I. Biodistribution studies were performed with normal and EMT-6 tumor-bearing Balb/c mice. The tissue-to-blood ratios show that very little activity localizes in the brain but there is significant uptake of radioactivity in tumor tissue with a maximum tumor-to-blood ratio of 4.34 at 4 h post injection.

Time (h)	Brain-to-Blood Ratio	Tumor-to-Blood Ratio
0.25	0.05±0.01	0.81±0.05
0.50	0.07±0.02	1.18±0.10
1	0.07±0.01	1.55±0.18
2	0.08±0.01	1.56±0.28
4	0.10±0.01	**4.34±0.80**
8	0.07±0.05	2.07±1.09
24	0.33±0.21	1.39±0.49

The preliminary studies with [^{125}I]IAIA look promising and further studies are currently underway to evaluate the suitability of this IAZA derivative as a potential tumor imaging agent. (Supported by Alberta Cancer Board, Research Initiatives Program, Edmonton, Alberta, Canada).

Fax: 1-403-492-1217, E-mail: jmercer@pharmacy.ualberta.ca